

MASTERARBEIT / MASTER'S THESIS

Titel der Masterarbeit / Title of the Master's Thesis

Function of mTORC2 in mitochondria

verfasst von / submitted by

Lukáš Gulla, BSc

angestrebter akademischer Grad / in partial fulfilment of the requirements for the degree of
Master of Science (MSc)

Wien, 2021 / Vienna 2021

Studienkennzahl lt. Studienblatt /
degree programme code as it appears on
the student record sheet:

A 066 863

Studienrichtung lt. Studienblatt /
degree programme as it appears on
the student record sheet:

Masterstudium Biologische Chemie

Betreut von / Supervisor:

Univ.-Prof. Dr. Robert Konrat

Mitbetreut von / Co-Supervisor:

Dr. Ivan Yudushkin

Acknowledgement

I would like to express my gratitude to Dr. Ivan Yudushkin and Univ.-Prof. Dr. Robert Konrat for the opportunity to perform my master's practical course under their supervision, for their advices and help offered before, during and after the practical course. Further I would like to thank Univ.-Prog. Dipl.-Ing. Dr. Kristina Djinovic-Carugo for allowing me to complete my master's practical course at the Department of Structural and Computational Biology. Also I would like to thank Chiara Trilling, MSc for splitting the cells in my absence and helping with the performance of some western-blots and the At last I would like to thank my family and my friends for supporting me during my studies.

Table of Contents

ABBREVIATIONS	5
INTRODUCTION	7
THEORETICAL BACKGROUND	8
mTOR	8
mTORC1	10
mTORC2	13
mSin1	15
AKT/PKB	17
GOAL	20
METHODS	21
CELL CULTURE - TRYPSINIZING, SPLITTING AND FREEZING THE CELL LINES HeLa AND HL-60	21
<i>HeLa cell line - splitting</i>	21
<i>HeLa cell line - freezing the cells</i>	21
<i>HL-60 cell line - splitting</i>	22
<i>HL-60 cell line - freezing the cells</i>	22
TRANSFECTION	23
PREPARATION OF THE SLIDES FOR CONFOCAL MICROSCOPY	23
CONFOCAL MICROSCOPY	23
SDS-PAGE - WESTERN BLOT	24
<i>Preparation of the gel</i>	24
<i>HeLa - preparation of the samples - characterization of the cell lines</i>	25
<i>HL-60 - preparation of the samples - characterization of the cell lines</i>	26
<i>HeLa and HL-60 - loading of the samples onto the gel, running the gel and transferring proteins onto a nitrocellulose membrane</i>	27
<i>HeLa and HL-60 - blocking and primary/secondary antibody incubation and visualization of the bands</i>	29
HeLa CELLS - GDC-0941 INDUCED DEPHOSPHORYLATION OF AKT - PREPARATION OF THE SAMPLES	31
HeLa CELLS - SERUM CONCENTRATION DEPENDENCY	33
ISOLATION OF MITOCHONDRIAL FRACTION	34
RESULTS AND DISCUSSION	36
CHARACTERIZATION OF mSin1-DEFICIENT HeLa AND HL60 CELL LINES	36
DEVELOPMENT OF MITOCHONDRIAL-LOCALIZED mSin1	52
CHARACTERIZATION OF MITOCHONDRIAL mTORC2	56
CONCLUSION	64
OUTLOOK	66
ABSTRACT	67
ZUSAMMENFASSUNG	68
MATERIALS	69
ANTIBODIES	69
BACTERIA	69
CELL LINES	69
CHEMICALS	70
CONSTRUCTS	70
CONSUMABLES	71
ENZYMES	71
<i>Standard enzymes</i>	71
INHIBITORS	72
INSTRUMENTS	72
KITS	73
MEDIA AND SERUM	73
<i>Liquid media</i>	73

<i>Supplementary</i>	73
<i>Solid media</i>	73
<i>Antibiotics</i>	73
PRIMERS	73
<i>Sequencing primer</i>	73
SOLUTIONS AND BUFFERS	73
<i>Standard solutions</i>	73
<i>Buffer</i>	74
BIBLIOGRAPHY	76
APPENDIX	83

Abbreviations

Abbreviation	Definition
4E-BP1	4E binding protein 1
APS	ammonium persulfate
BSA	bovine serum albumin
DAPI	4', 6'-diamidino-2-phenylindole
DEPTOR	DEP domain-containing mTOR-interacting protein
DMEM	Dulbecco's Modified Eagle Medium
DNA	deoxyribonucleic acid
eIF4B	eukaryotic translation initiation factor 4B
FBS	fetal bovine serum
FoxO	forkhead box transcription factors
FRAP1	FK506-binding protein 12-rapamycin-associated protein 1
GAPDH	glyceraldehyde 3-phosphate dehydrogenase
GFP	green fluorescent protein
GPCR	G protein-coupled receptor
Grb10	growth factor receptor-bound protein 10
Gsk3	glycogen synthase kinase 3
GTP	guanosine triphosphate
HK2	hexokinase 2
HRP	horseradish peroxidase
IGF-1	insulin-like growth factor 1
IP3R	inositol triphosphate receptor
MAM	mitochondria associated membranes
MAPKAP1	mitogen activated protein kinase 2-associated protein 1
mLST8	mammalian lethal with SEC13 protein 8
mSin1	mammalian stress-activated protein kinase interacting protein 1
mTOR	mechanistic target of rapamycin
mTORC1/2	mechanistic target of rapamycin complex 1/2
OptiMEM	optimized minimal essential medium
PACS2	phosphofurin acidic cluster sorting protein 1
PBS	phosphate-buffered saline
PEI	polyethylenimine
PH domain	pleckstrin homology domain
PI3K	phosphoinositide-3-OH kinase
PIP ₂	phosphatidylinositol 4,5-bisphosphate
PIP ₃	phosphatidylinositol 3,4,5-trisphosphate
PKB	protein kinase B
PKC α	protein kinase C α
PRAS40	proline-rich AKT substrate of 40 kDa
Protor	protein observed with Rictor

PVDF	polyvinylidene difluoride
Rag	recombination activation gene
Raptor	regulatory-associated protein of mTOR
Rheb	Rag homolog enriched in brain
Rictor	rapamycin-insensitive companion of mTOR
RPMI/HEPES	Roswell park memorial institute/4-(2-hydroxyethyl)-1-piperazineethanesulfonic acid
RTK	receptor tyrosine kinase
SDS-PAGE	sodium dodecyl sulphate-polyacrylamide gel electrophoresis
SGK1	serum and glucocorticoid regulated kinase 1
SIRT1	sirtuin 1
SLC25A5	solute carrier family 25 (mitochondrial carrier; adenine nucleotide translocator), member 5
TBS	tris-buffered saline
TEMED	tetramethylethylenediamine
TSC	tuberous sclerosis complex
TTBS	Tween20 enriched tris buffered saline

Introduction

mTOR (mechanistic target of rapamycin) is a kinase involved in two large protein complexes named mTORC1 (mechanistic target of rapamycin complex 1) and mTORC2 (mechanistic target of rapamycin complex 2).

Both complexes share some of their components, like mLST8 (mammalian lethal with SEC13 protein 8), mTOR and DEPTOR (DEP domain-containing mTOR-interacting protein), but also contain some unique components. mTORC1 contains Raptor (regulatory-associated protein of mTOR) and PRAS40 (proline-rich AKT substrate of 40 kDa), whereas mTORC2 contains Rictor (rapamycin-insensitive companion of mTOR), mSin1 (or MAPKAP1, mammalian stress-activated protein kinase interacting protein 1) and Protor (protein observed with Rictor). Both complexes localize differently in the cell, with mTORC1 being localized on lysosomes and stress granules and probably on mitochondria and nucleus. mTORC2 is situated mostly on the plasma membrane and is believed to be bound to ER and MAM (mitochondria associated membranes).

The mechanisms leading to activation of the complexes are different as is their working mechanism and site of action. mTORC1 is activated by a relatively complicated mechanism on lysosomes and is important for example for cell growth, protein metabolism and biosynthesis of nucleotides. mTORC2 is a part of the activation mechanism of Akt/PKB (protein kinase B), where it contributes to its full activation, by phosphorylating serin 473 of Akt. The phosphorylation was believed to take place exclusively on the plasma membrane, but some studies show a possible activation of Akt/PKB on endomembranes as well. mTORC2 has been localized to MAM, where it seems to regulate the mitochondrial physiology. There is also a possibility of mTORC2 being localized to the nucleus.

An mTORC2-specific component, mSin1, could be expressed as several isoforms, which are localized in different subcellular compartments, such as the plasma membrane, endosomal vesicles or the nucleus.

Akt/PKB is involved with both of the complexes. By inhibiting TSC (tuberous sclerosis complex) through phosphorylation, it contributes to the activation of mTORC1 at lysosomes. Akt/PKB is fully activated once it's phosphorylated at threonine 308 and serine 473. The latter is phosphorylated by mTORC2. This activation also shows a loop connecting mTORC1 and mTORC2 via Akt/PKB signalling.

Akt/PKB as a protein kinase is involved in multiple processes as an upstream regulator or control mechanism. Akt/PKB increased activity has been observed in cancer cells, bringing focus on this protein kinase as a possible way of treatment.

The following theoretical overview of the mTOR family, shows the differences in what is yet known about mTORC1 and mTORC2. The gaps in the localization and most of all in function of mTORC2 in mitochondria triggered our attention and led us to this project.

Theoretical Background

mTOR

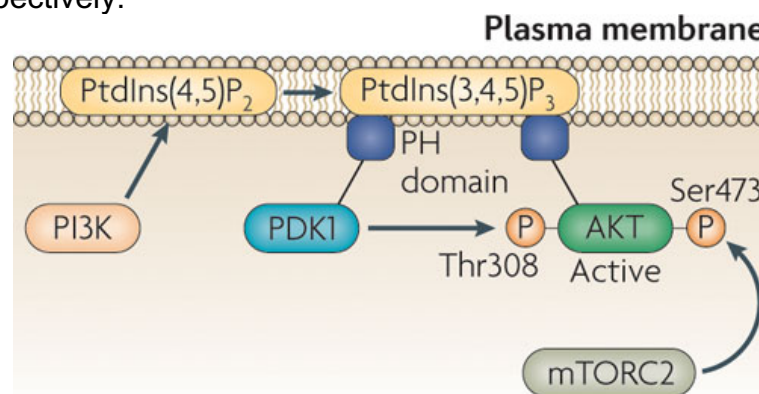
mTOR¹ is a protein kinase and a core subunit of two protein complexes - complex 1 (mTORC1) and complex 2 (mTORC2). These two complexes differ not only in composition, but also in function.

The discovery of TOR was preceded by the discovery of Rapamycin in 1975, a product of a soil bacterium with its name originating from Rapa Nui, or Easter Island.² As shown by Benjamin et al. Rapamycin has antifungal, anticancer and immunosuppressive properties.³ The discovery of TOR⁴ revealed its role in control of cell growth and in human disease.⁵⁻⁷

mTOR, previously known also as mammalian target of rapamycin and also referred to as FRAP1 (FK506-binding protein 12-rapamycin-associated protein 1) belongs to the group of phosphatidylinositol 3-kinases. This 259 kDa large serine/threonine kinase is expressed in eukaryotic cells, including also neural cells.

The activation of mTOR is controlled by the presence of nutrients and by growth factors, such as insulin.⁸ The insulin as growth factor induces the activation of mTOR, which is mediated by PI3K (phosphoinositide-3-OH kinase), showing, that PI3K is an upstream positive regulator of mTOR.⁹

The mTOR activity is also mediated by a downstream effector of PI3K called Akt. Akt is a serine/threonine protein kinase, which is activated by PIP₃ (phosphatidylinositol 3,4,5-triphosphate result of phosphorylation of PIP₂ - phosphatidylinositol 4,5-biphosphate by PI3K¹⁰) binding to its PH domain (pleckstrin homology)¹¹. Akt is then translocated to the plasma membrane, where it is then phosphorylated by 3-phosphoinositide-dependent kinase-1 (PDK1) and by mTORC2 on threonine 308 and serine 473 respectively.¹²



Nature Reviews | Immunology

Figure 1: Mechanism of Akt activation at the plasma membrane. PI3K catalyzes the activation of PtdIns(3,4,5)P₃, which binds to the PH domain of Akt. On such bound Akt, the phosphorylation of threonine 308 by PDK1 and phosphorylation of serine 473 by mTORC2 takes place.¹³

mTOR's functions are included in a lot of cellular processes, such as regulation of cellular growth, proliferation of the cells, survival, protein synthesis, autophagy and transcription.^{8,14}

mTOR as part of the mTORC1 plays a role in the synthesis of myofibrillar muscle protein and skeletal muscle hypertrophy. mTOR in this case is activated by the

presence of specific amino acids or their derivatives. Its activation can also be triggered by exercise. The inactivation of mTORC1 and therefore no signalling leads to the loss of strength and muscle mass in old age and even muscle atrophy.^{15,16}

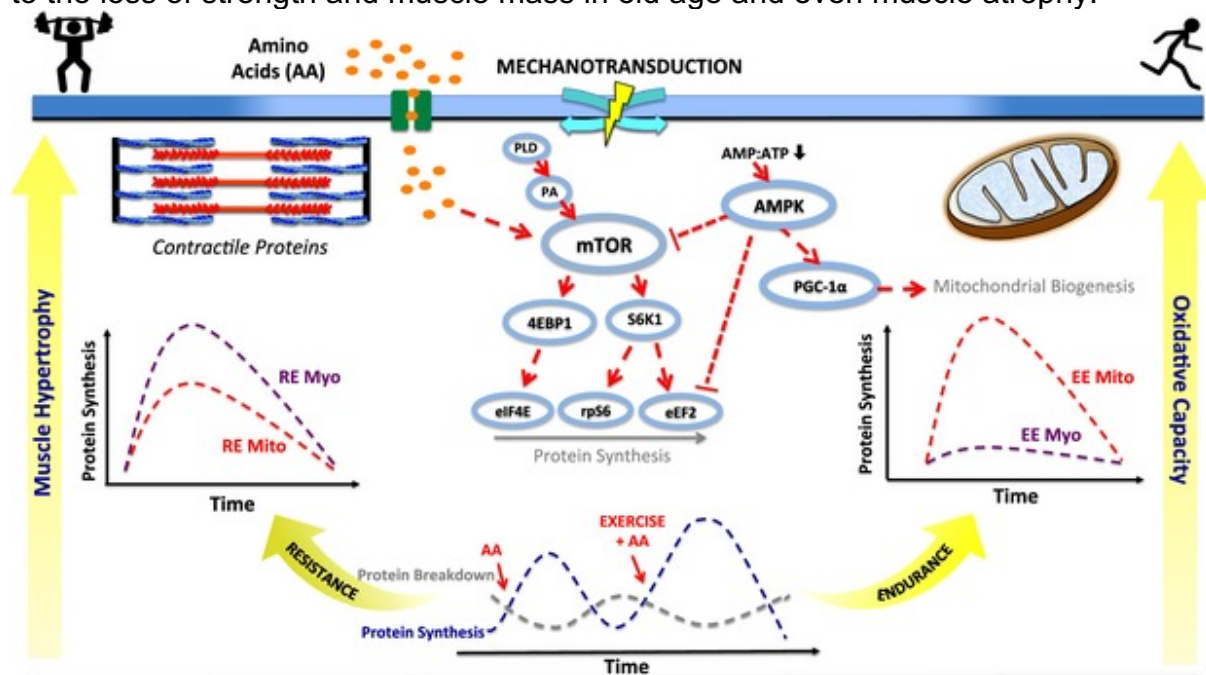


Figure 2: The intake of amino acids stimulates the activation mTORC1 and therefore also its downstream substrates. Resistance exercises (RE) stimulate the muscle protein synthesis via mTORC1 pathway. The endurance exercises stimulate mitochondria protein synthesis.¹⁵

The second complex mTORC2 also seems to be involved in cellular growth once activated. It has a potential role in mediation of neurite outgrowth in neuro2a differentiated mouse cells.¹⁷

Decreasing the activity of TOR in some model organisms seems to increase their life span.^{18,19} It also seems, that decreasing the intake of some amino acids decreases the mTOR activity in yeast and therefore causing an increase of its chronological life span.¹⁸ Feeding Rapamycin, the inhibitor of TOR to mice also led to the extension of their life span.²⁰ This could suggest, that a targeted inhibition of TOR have some positive effects on life expectancy of some organisms.

However, TOR is also included in the development of some human diseases, such as cancer, Alzheimer disease and even obesity.

Inhibiting or reducing TOR activity in *Drosophila Melanogaster* being fed a high fat diet (HFD) prevented higher triglyceride levels and also decreased insulin signalling, meaning that decreasing TOR function has protective effects against obesity induced by HFD.²¹

A higher activity of TOR also plays a role in the development of multiple types of cancer.²²

The reasons for an increase in the activity of TOR is mostly a mutation in the tumor suppressor gene PTEN, which results in increased activity of PI3K, an upstream effector of Akt and TOR. Inhibiting TOR by using rapamycin was therefore seen as one of the possible ways in cancer treatment, but it seems, that TOR has a function not affected by rapamycin, which has a regulatory effect on the survival of cells and which is active in many cancer types.²³

High TOR activity leading to an increased expression of downstream effectors of TOR such as 4E-BP1 (4E binding protein 1), S6K, which participate in mRNA translation.

This overexpression of these downstream effectors has been observed in multiple types of cancer.²⁴

The studies on TOR's role in Alzheimer disease formation or progress are diverse. While some studies show the negative effect of TOR on memory creation, which is one the symptoms of the disease, the others promote its beneficial effects.

Inducing mutation in TSC1 or TSC2 genes, which led to an increase of TOR activity (as TSC1 and TSC2 are TOR's inhibitors) led to deficiency in memory creation. Inhibiting TOR by treatment with rapamycin rescued the behavioural defects and synaptic plasticity.²⁵

On the other hand TOR seems to increase the activity of SIRT1 (Sirtuin 1).²⁶ This cooperation could have positive effects in the treatment of Alzheimer disease, as SIRT1 impacts the amount of A β (amyloid β) and tau proteins (both negatively related to the Alzheimer disease).^{27,28}

mTORC1

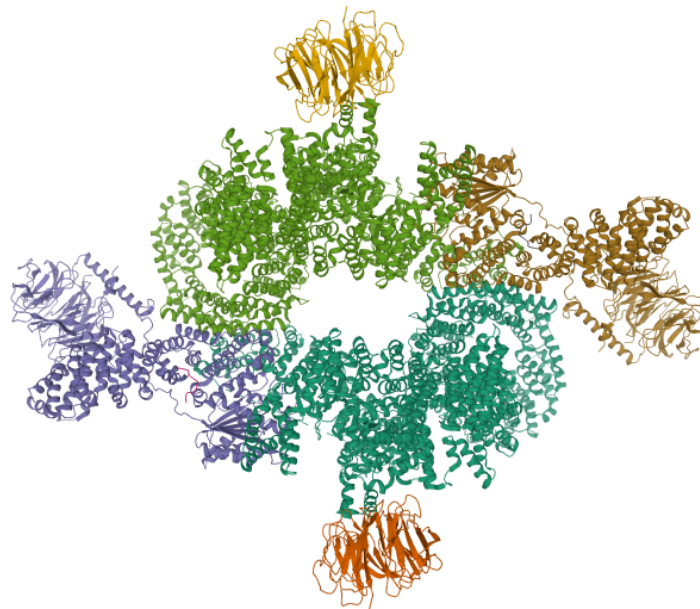


Figure 3: Structure of mTORC1. Orange/red - mLST8, green/turquoise - mTOR, violet/brown -RAPTOR.²⁹

mTORC1 is a protein complex consisting of mTOR, raptor, MLST8, PRAS40 and DEPTOR.³⁰

The function and role of mTORC1 is the regulation of cell growth, which is done by coordinating the protein synthesis in cell^{31,32}, biosynthesis of nucleotides³³, glycolysis, lipogenesis^{34,35} and autophagy³⁶.

In order to perform any action this protein complex first needs to be activated. For the activation of mTORC1 the complex needs to be situated on lysosome, where it can be activated by GTP-binding protein Rheb (guanosine triphosphate-binding protein Ras homolog enriched in brain). The process of translocation to the lysosome is powered by nutrients and the Rags (recombination activating genes). Rheb is not always in the GTP-bound form. The conversion to the GTP-bound form from GDP-bound Rheb is dependent on the presence of growth factors. Rheb is located to the lysosome surface.^{37,38} By growth factor stimulation Akt is phosphorylated, which leads to the

phosphorylation and inhibition of the TSC. The TSC 1 and 2 are parts of GAP heterotrimer, which promotes GTP to GDP conversion and thus inhibits Rheb. The hinderance of the parts of this heterotrimer represses the Rheb inhibitor, which is then activated.³⁹

A heterodimeric GTPase consisting of RagA or B and RagC or D called Rag GTPase and Ragulator ensures the lysosomal localization of mTORC1.^{38,40–42} Amino acids stimulate the guanine exchange in Rag, which activated mTORC1. The stimulation mechanism is yet unknown, however there are multiple studies proposing different explanations, one of them including a proton-assisted amino acid transporter PAT1, located to the lysosome. PAT1 could pump the amino acids out of the lysosome and interact with Rag in order to activate mTORC1.⁴³

The mechanism of recruitment of mTORC1 to the surface of the lysosome is also not determined yet. It was believed, that Rag recruits mTORC1 from the cytoplasm to the lysosome, however it was shown, that Rag is probably fixed to the lysosomal surface.⁴¹ Once on the lysosome mTORC1 forms a complex with 3 other components - v-ATPase (vacuolar-type ATPase), Ragulator and Rag.⁴¹

The activation of mTORC1 at the lysosome seems to be Rheb- and growth factors dependent.⁴¹ Not feeding the cells with amino acids, but stimulating Rheb expression still results in mTORC1 activation, which could possibly be explained by an interplay of mTORC1 and Rheb elsewhere and not on the lysosome.^{44,45}

Once activated mTORC1 phosphorylates multiple substrates at multiple locations such as nucleus, mitochondria, stress granules, cytoplasm or plasma membrane. Phosphorylation of transcription factor TFEB, regulating the autophagy, is performed by mTORC1 at the lysosome.^{46,47} Rheb and Rag are however required for mTORC2 activation at all times. Rheb and TSC (as mTORC1 inhibitor) have been observed at other cellular locations, such as peroxisomes.⁴⁸ mTORC1 is inhibited by reactive oxygen species of peroxisomes, which speaks against its localization on the peroxisomes.

One of the other locations, where mTORC1 components (mTOR, raptor) were detected is the nucleus, where they probably participate in the regulation of the transcription.^{49–51} However these components apparently do not form the whole protein complex.⁵²

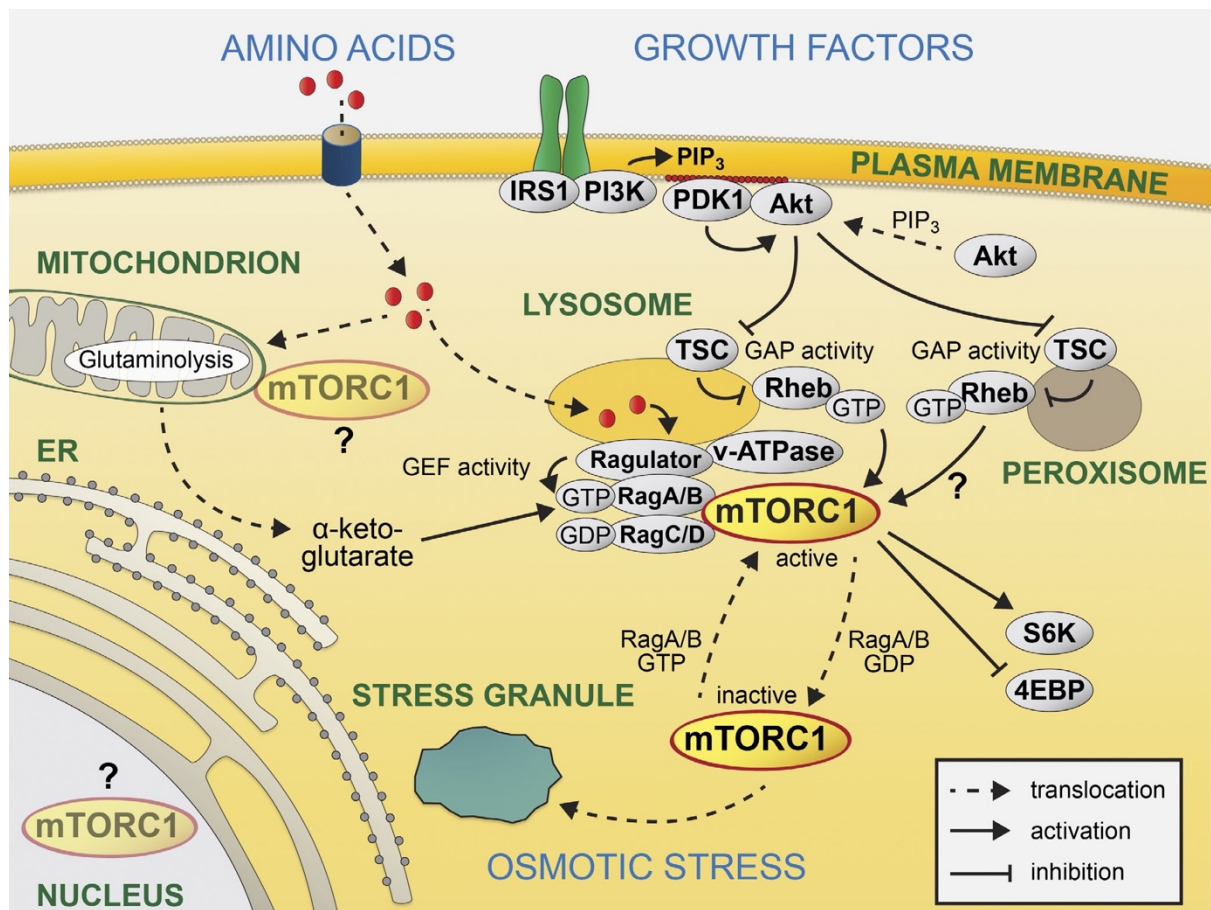


Figure 4 Activation of Akt at the plasma membrane and activation of mTORC1 at the lysosome. mTORC1 forms a complex with RagA/B, RagC/D and v-ATPase and is then phosphorylated/activated by Rheb-GTP, which is not inhibited by TSC. TSC is inhibited by active Akt. There is a possible participation of peroxisome located Rheb-GTP in the activation process. mTORC1 also seems to be located in the nucleus, mitochondria and stress granules, where it is translocated after being activated at the lysosome.³⁹

mTOR as one of the components of mTORC1 and mTORC2 and as the target of rapamycin was found at mitochondria^{53,54} in Jurkat and HEK293 cells, however, it is still unclear whether the whole complex localizes to the mitochondria. The treatment with rapamycin, which inhibits only mTORC1 affects the mitochondrial function. Longer exposure to rapamycin seems to be affecting also mTORC2.⁵⁵ This would point at the mitochondria to be the possible location of mTORC2 instead of mTORC1.

Raptor, as a complex specific mTORC1 component, has the ability to bind a lipid located to the plasma membrane. The lipid PI(3,5)P₂ binds to the WD40 domain of raptor and thanks to this binding mTORC1 localizes to the plasma membrane.⁵⁶ According to the same study this lipid could also help in recruiting mTORC1 to the lysosomes, as it is generated in the plasma membrane and at the lysosome. However, it has not yet been proved, that the complex and the lipid localize to the same locations in the same time.

One of mTORC1 substrates is the p70-S6 Kinase 1 (S6K1). mTORC1 phosphorylates the S6K1, which will then be activated.⁵⁷ The phosphorylation of S6K1 by mTORC1 takes place on two residues - threonine 389 and serine 371.⁵⁷ This activation is followed by another phosphorylation of S6K1 on threonine 229 by PDK1. Such activated S6K1 triggers the protein synthesis by activating the S6 ribosomal subunit.⁵⁸ This is how mTORC1 through a cascade of phosphorylation reactions can initiate the protein synthesis.

Furthermore the activated phosphorylated S6K1 phosphorylates mTOR on serine 2448 as a part of a positive feedback.⁵⁹

Another mTORC1 substrate is the inhibitor of translation 4E-BP1. The phosphorylation of this protein leads to its release from eIF4E (eukaryotic translation initiation factor 4E). Such stripped initiation factor binds other initiation factors (4G and 4A) and forms a complex. The complex targets the 5' cap of mRNA, recruits helicase eukaryotic translation initiation factor A and eIF4B (eukaryotic translation initiation factor 4B).⁶⁰ Once helicase cuts the hairpin loop, protecting the mRNA from an early translation, 40S ribosomal unit is recruited and the translation begins.

mTORC2

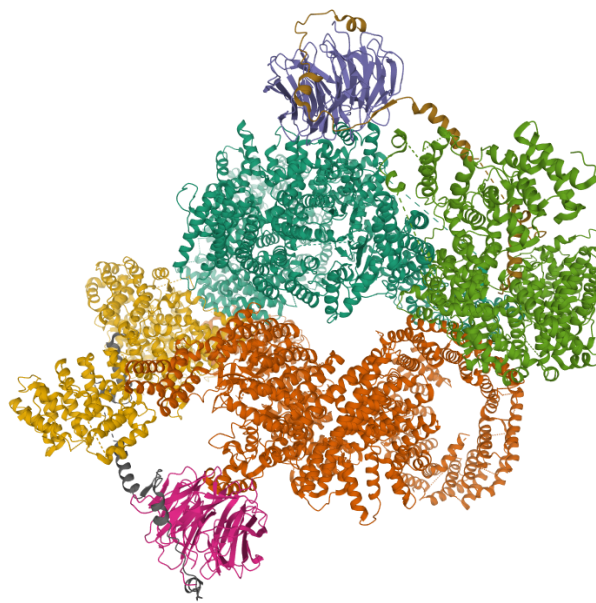


Figure 5: Cryo-EM structure of mTORC2. Red/turquoise - mTOR, orange/green - Rictor, violet/pink - mLST8, brown/grey - mSin1.⁶¹

mTORC2 differs from its fellow complex 1 in several ways. mTORC2 is a protein complex, that is rapamycin insensitive, thus not inhibited by the effects of rapamycin. Another difference is the composition. mTORC2 shares some of its components with mTORC1, such as the kinase mTOR, DEPTOR, mLST8. The unique components of mTORC2 are rictor, mSin1 and protein observed with rictor 1 and 2 Protor 1/2.⁶² The two complexes 1 and 2 do not only differ in composition or in sensitivity towards rapamycin, but also in the mechanisms of their activation, their function and their localization across the cell, however the complex 2 mechanisms are not yet understood and described very well.

Studies show, that mTORC2 localizes to the endoplasmic reticulum.⁶³ Due to mTORC2 substrate Akt localization to the plasma membrane, it was believed, that mTORC2 itself localizes to this cellular compartment. This was indicated by the isolation of lipid rafts, usually localized to the plasma membrane, where mTORC2 and Akt have been indeed confirmed.^{64–66} Such lipid rafts can also be found in the endoplasmic reticulum, forming the so called MAM.⁶⁷ Other studies show, that after fractionation and immunofluorescence rictor, as one of the mTORC2 components, was found only low amounts at the plasma membrane.^{63,68}

Knocking down rictor, and therefore disabling mTORC2, or treating the cells with rapamycin (mTORC2 is sensitive to rapamycin after long exposure⁵⁵) resulted in change of mitochondrial potential, phosphorylation of mitochondrial proteins and respiration.^{53,69} Knocking down rictor led to an increased oxygen consumption and oxidative capacity as well as to higher levels of mTOR-raptor complex, whereas no changes in mitochondrial mass were observed.⁵³ This suggests an existence of a competition between rictor and raptor in binding to mTOR.⁷⁰

Direct substrates of mTORC2, Akt⁷¹⁻⁷⁴ and SGK1 (serum and glucocorticoid regulated kinase 1)^{75,76}, have been localized to mitochondria. This logically leads to the possibility of mTORC2 being localized at mitochondria as well.

The localizations of mTORC2 at the endoplasmic reticulum and the localization of mTORC2 substrate Akt in the endoplasmic reticulum^{63,77} and in mitochondria indicate, that the complex should be localized somewhere in the vicinity of these organelles. mTORC2 has been successfully localized to MAM⁷⁸. MAM is a membrane, which forms an almost synaptic structure of endoplasmic reticulum and mitochondria. It facilitates the transfer of lipids and calcium between mitochondria and endoplasmic reticulum.⁷⁸

A study examining mTORC2 at MAM showed, that the complex is physically associated with MAM and that phosphorylated Akt (by mTORC2) functions as a mediator for the integrity and function of MAM. mTORC2 phosphorylates Akt. Akt is thus active and further phosphorylates MAM proteins (PACS2 - phosphofurin acidic cluster sorting protein 1, IP3R - inositol triphosphate receptor, HK2 - hexokinase 2), which leads to the regulation of calcium flow, energy metabolism and MAM integrity. Disabling mTORC2 results in MAM deficiency (phenotypically).⁷⁸ It was shown, that defecting a MAM tethering factor Mfn2 leads to a higher uptake of calcium by mitochondria.⁷⁹ Knocking out rictor resulted in the same effect.

Akt is believed to be localized at the plasma membrane, where it is phosphorylated by mTORC2 on serine 473 in its hydrophobic motif and by PIP₃ on threonine 308 in its T-loop domain. Such phosphorylation leads to full activation of Akt. As mentioned previously, Akt is not only localized at the plasma membrane, but was found in mitochondria as well.⁷¹⁻⁷⁴ mTORC2 is able to activate Akt on the endoplasmic reticulum.⁶³ In addition endoplasmic reticulum stress leads to inhibition of mTORC2 activity⁸⁰, which suggests a signalling pathway of mTORC2-Akt on endoplasmic reticulum and MAM.⁷⁸

It remains yet to be determined, where exactly is mTORC2 localized and whether it is localized there permanently. Could it be, that mTORC2 is localized mainly at MAM and is deposited at other parts of the cell, such as plasma membrane, when it is needed for phosphorylation of its substrates? This could represent a challenge as it is known, that there are multiple versions of mTORC2, dependent on the isoform of mSin1.⁸¹

The mSin1 component of mTORC2 possesses a phosphoinositide-binding PH domain. This domain ensures the regulation of mTORC2 dependent on insulin. If no insulin is present in the cell, mTORC2 activity diminishes. mTORC2 can also be activated by PIP₃, which binds to the PH domain of Sin1. This binding results in releasing the inhibition of mTOR kinase domain and suppresses the mTOR activity.⁸² Akt can also phosphorylate mSin1, leading to mTORC2 activation, which in return phosphorylates Akt.⁸³

mTORC1 also affects mTORC2. One of mTORC1 substrates, Grb10 (growth factor receptor-bound protein 10), functions as a negative growth factor regulator⁸⁴ and binds

to insulin and IGF-1 (insulin-like growth factor 1).^{84–86} Activation of Grb10 by mTORC1 leads to it binding the IGF-1 and insulin, which leads to inhibition of mTORC2.⁸⁷

As already mentioned, mTORC2, once active, contributes to the full activation of Akt and therefore also contributes to Akt downstream signalling.

Further, mTORC2 is important for normal skeletal growth and bone anabolism. A targeted deletion of rictor led to shortening and narrowing of some parts of the skeleton in embryonic and in post-natal state. The loss of rictor had an impact on the width of long bones and the presence of this mTORC2 subunit is needed for standard osteoblast activity.⁸⁸

mTORC2 does not only play a role in the growth of the body skeleton, but also in the cytoskeleton. Two of mTORC2 components, namely rictor and mTOR, are involved in the regulation of the actin cytoskeleton. This is not done directly, but through the activity of PKC α (protein kinase C α) by an as yet unknown mechanism. Both rictor and PKC α knockdown cells show less cortical actin fibers and an augmented presence of thick actin fibers in the cytoplasm. However in the PKC α knockdown cells, these thick fibers seems to be better organized and to be connected to the rest of the cytoskeleton.⁷⁰

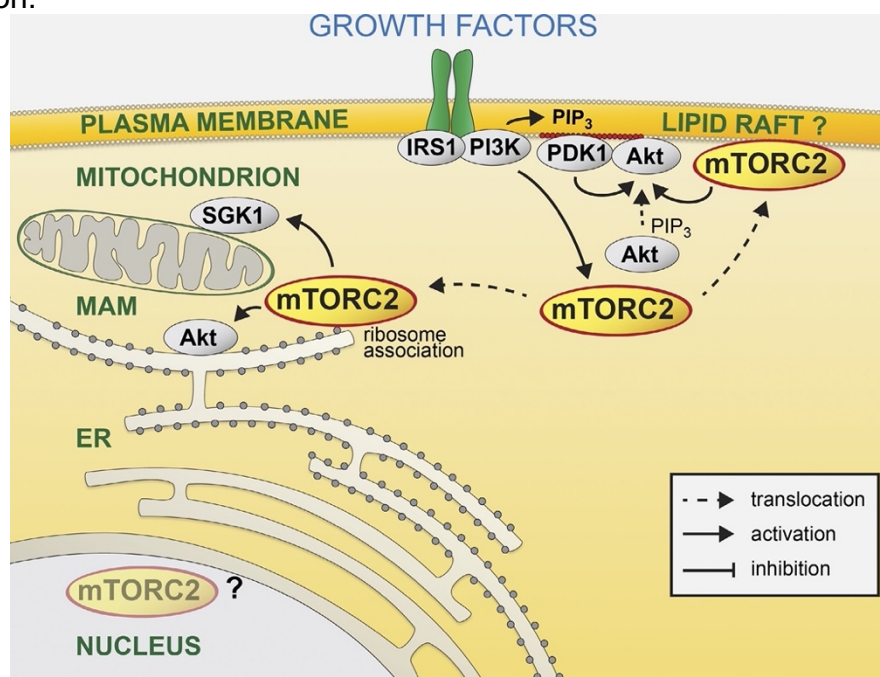


Figure 6: Location of mTORC2 in the cell. mTORC2 localizes at the plasma membrane, where it phosphorylates Akt on serine 473, contributing to its full activation. mTORC2 also localizes to MAM and associates with ribosomes located at the ER. mTORC2 possibly localizes to nucleus.³⁹

mSin1

mSin1, also known as MAPKAP1 (mitogen activated protein kinase 2-associated protein 1), is one of mTORC2's components, which targets mTOR complex 2. mSin1 seems to be a crucial component for the activity of mTORC2, as its deletion resulted in no phosphorylation of serine 473 of Akt. It was also observed, that the missing phosphorylation in the PH domain of Akt didn't have any effect on the phosphorylation in the T-loop of Akt, on threonine 308. This partial phosphorylation of Akt does not seem to have an effect on its activity. The examined substrates of Akt, Gsk3 α and Gsk3 β were still phosphorylated.⁸⁹

The same study showed, that mSin1 is necessary for the interaction of two other mTORC2 components, rictor and mTOR and has no effect on the interaction of mTORC1 components raptor and mTOR.⁸⁹

It was found, that mTOR (length of 2549 amino acids) can bind to mSin1. For this mTOR was fragmented and interestingly the fragments, which were shorter than 2191 amino acids did not show any binding with mSin1. On the other hand the wild type mTOR bounded with mSin1. This led to the conclusion, that amino acids 2148-2300, representing the kinase domain of mTOR, are able to bind mSin1.⁹⁰

For rictor, interestingly, the incubation with TritonX-100 showed, that rictor and mSin1, opposite to mTOR, are able to co-precipitate, leading to the suggestion, that these two are able to form a complex on their own. The interaction between mSin1 and rictor happens on the carboxyl terminus of rictor, more specifically at the amino acids 1181-1708.⁹⁰

It is clear on what parts does mSin1 bind on mTOR and rictor. mSin1 has a length of 522 amino acids, which were again fractioned and examined. Fraction 1-314 and 1-460 are able to bind mTOR/rictor/mLST8. Further examinations reduced this range to 123-314 and then even to a shorter 100-260 fragment, which seems to contain the binding region for both mTOR and for Rictor.⁹⁰

mSin1 does not only interact with mTOR-rictor, but also with mTORC2 substrate Akt/PKB. This was shown by immunoprecipitating mSin1 and Akt under multiple conditions. On the other hand Akt is not interacting with rictor or mTOR.⁸⁹ The site on mSin1, that binds to Akt was narrowed to amino acids 220-260. On Akt the binding region was identified between amino acids 1 and 107, pointing out, that mSin1 binds in the pleckstrin homology domain of Akt.⁹⁰

mTORC2 is able to form three complexes, in dependence of the isoform of mSin1, that is integrated. However, mSin1 forms 6 different isoforms. Just three of these isoforms, 1,2 and 5 are components of mTORC2. These complexes, even though the mSin1 isoforms are not in equal amounts, phosphorylate their substrate Akt at similar level, suggesting, that it is mTOR, which is responsible for the activity of the complex.⁸¹ The three complexes differ not only in the mSin1 isoform they contain, but also in their response on insulin treatment. The complex being formed by isoform 5 of mSin1 seems to be untouched by starvation or by insulin treatment. A possible explanation for this is, that mTORC2 containing isoform 5 regulates the activity of Akt, while depending on other signals.⁸¹

The isoforms of mSin1 localize differently around the cell. Isoforms 1 and 2 localize to the plasma membrane, cytoplasm, nucleoplasm and on the surface of highly dynamic endomembrane vesicles in HeLa, HEK293T and MCF7 cells. Isoform 5 lacks the pleckstrin homology domain, which results in no plasma membrane localization. It localizes in the nucleus and cytoplasm. Stripping the isoform 2 of the PH domain led to the accumulation of mSin1.2 in the nucleus and not on the plasma membrane anymore.⁹¹



Figure 7: Representation of the crystal structure of the C-terminus pleckstrin homology of mSin1 (human orthologue to Avo1 in yeast).⁹²

Isoform 4 does not contribute to the formation of mTORC2, as it does not interact with mTOR or rictor, as shown by no coimmunoprecipitation.⁸¹ Isoform 4 also lacks amino acids 1-192. This fraction overlaps with the fraction of mSin1, which binds to mTOR and rictor⁹⁰, explaining the inability of Isoform 4 to create its own mTORC2, unlike isoforms 1,2 or 5.

The other two isoforms, isoform 3 and isoform 6, also lack sequences. Isoform 3 lacks amino acids 357-403 and amino acids 357-372 and 373-522 are missing from isoform 6.

The missing parts of isoform 6 seem not to have any effect on its interference with other mTORC2 components. Isoform 6 shows a localization to the plasma membrane, along isoforms 1 and 2. In addition isoform 6 formed a cylindric structure in nucleus's proximity, which was observed in interphase cells and disappeared as the cells entered mitosis. The structure reappeared as soon as mitosis was over. This structure surrounded γ -tubulin, which serves as a centriole marker and colocalized with a marker for basal body - acetylated tubulin.⁹³

Akt/PKB

Protein kinase B was identified more than 30 years ago and belongs to the family of AGC protein kinases, which it shares with protein kinase A and C.⁹⁴ Since then three isoforms of Akt/PKB have been identified - Akt1, Akt2 and Akt3 (or PKB α , β and γ respectively).

In order to perform any action PKB first needs to be activated. The activation takes place at the plasma membrane. Crucial for the activation at the plasma membrane is the stimulation of either RTK (receptor tyrosine kinase) or GPCR (G-protein-coupled receptor). The stimulation of these receptors leads to the recruitment of PI3K.⁹⁵ An important role is played by Ras, which regulates PI3K by interacting with it.⁹⁶

Recruited PI3K phosphorylates PIP_2 to PIP_3 , which then interacts with the PH domain of inactive Akt. Inactive Akt has a conformation, which does not allow it to be phosphorylated, thus to be activated. The binding of PIP_3 to its PH domain results in changes of conformation, make its T-loop accessible for PDK1 (phosphoinositide-

dependent protein kinase 1). PDK1 phosphorylates threonine 308 in the T-loop of Akt1.⁹⁷

Such Akt1 is considered activated, but weaker in its actions.⁸⁹ For a full activation the second site (serine 473) in the hydrophobic-motif of Akt needs to be activated. Other studies also confirmed, that the second phosphorylation on S473 helps to stabilize the T308 phosphorylation.⁹⁸ The phosphorylation on S473 is performed by mTORC2. mTORC2 also phosphorylates threonine 450 on Akt. The phosphorylation of this residue is important for proper folding of the nascent AKT polypeptide.^{99,100}

Apart of these and other phosphorylations on Akt, there is also a number of post-translational modifications. One of these, the acetylation on lysine 14, in the PH domain, is believed to be necessary for the interaction between PIP₃ and Akt and to contribute to the membrane localization of Akt.¹⁰¹

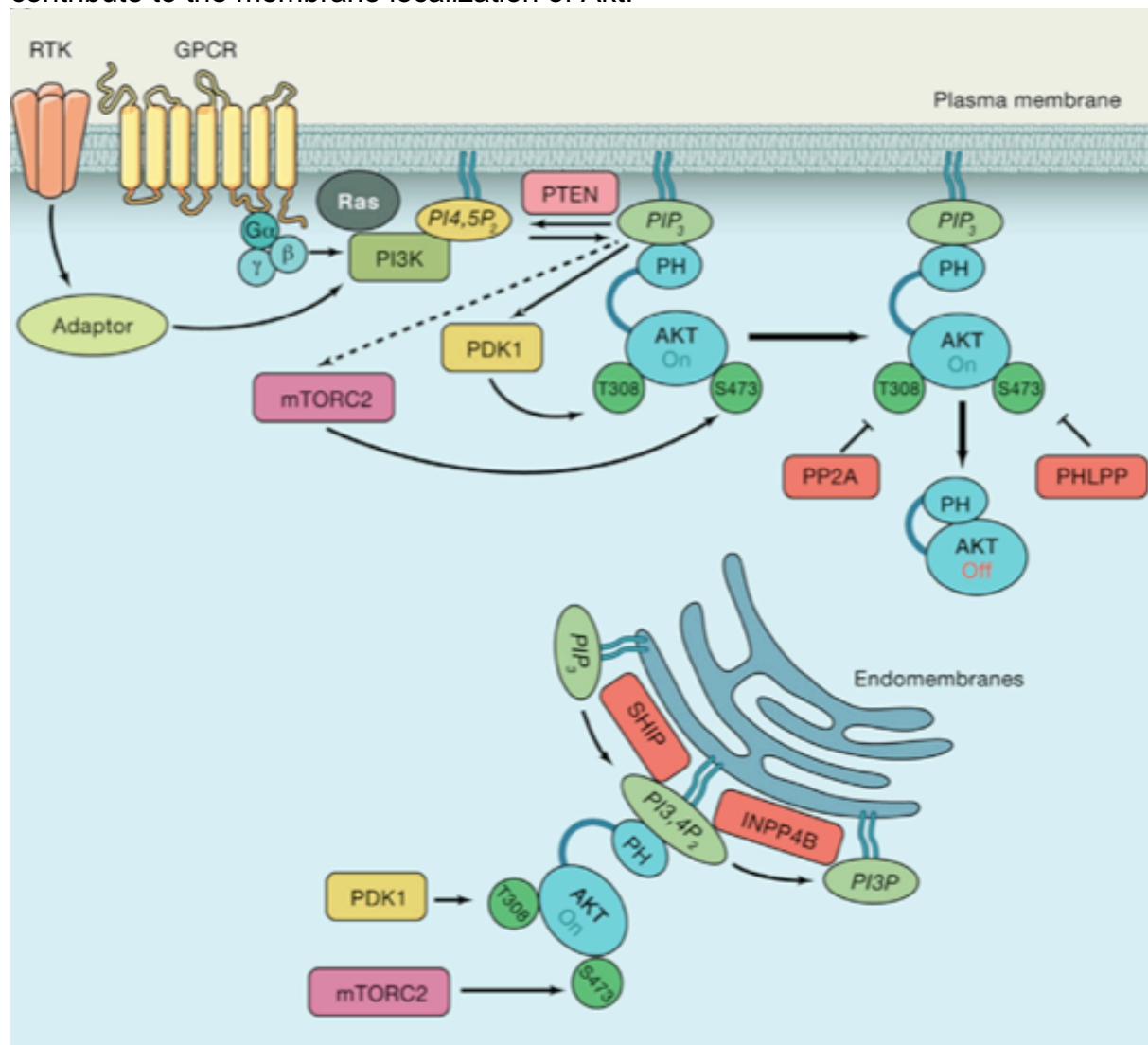


Figure 8: Akt is possibly not activated only at the plasma membrane, but also at other endomembrane systems. The mechanism of Akt activation at endomembranes is very similar to the one at the plasma membrane.¹⁰²

Akt, once active, is able to phosphorylate various other substrates. The first substrate of Akt discovered, is Gsk3 (glycogen synthase kinase 3). Gsk3 forms two isoforms α and β. Akt phosphorylates Gsk3 in its amino-terminal motif (on serine 21 in Gsk3α and on serine 9 in Gsk3β).¹⁰³ This phosphorylation is inhibitory, causing a perturbation in the accessibility of the substrate binding to Gsk3.¹⁰⁴ Phosphorylating and therefore

inhibiting Gsk3 by Akt impacts Gsk3 substrates. The majority of these substrates is inhibited, when Gsk3 is not phosphorylated by Akt.¹⁰⁵

Another Akt target are the FoxO transcription factors (forkhead box transcription factors). The activation of Akt by PI3K causes the FoxO proteins to leave the nucleus, which leads to the cancellation of transcription, regulated by FoxO.^{106,107} Another possibility is, that Akt phosphorylates FoxO, which then loses its transcriptional functions.¹⁰⁸ FoxO controls the expression of genes, that are involved in cell-cycle arrest, tissue-specific metabolic changes, catabolism and growth inhibition and apoptosis.^{109,110}

Additionally, Akt also phosphorylates TSC2. This complex, when not phosphorylated, inhibits mTORC1, by participating in the dephosphorylation of Rheb-GTP to Rheb-GDP. The phosphorylated form of Rheb activates mTORC1. Phosphorylation of TSC2 causes its inhibition and therefore promotes the activation of mTORC1.¹¹¹ Another Akt substrate, coming directly from mTORC1, is one of its components PRAS40. It has been shown, that Akt directly phosphorylates threonine 246 on PRAS40.¹¹² It is known, that PRAS40 inhibits mTORC1, however not anymore once phosphorylated at T246.^{113,114} The direct contribution of Akt to the activation of mTORC1 via PRAS40 phosphorylation has not yet been clearly determined.

The inhibition of Akt would lead to the attenuation of a lot of cellular processes. Such inhibition can be provoked by the removal of nutrients or growth factors from the cell or by the incubation of the cell with some kinase inhibitors. For Akt a drug called A443654 can be used. The treatment with this drug results in the phosphorylation of Akt on serine 473, for which consistent mTORC2 and PI3K activities are required. Several explanations for the accumulated S473 phosphorylation have been proposed. One of them proposes a locked Akt conformation upon binding A443654. This conformation would prohibit a dephosphorylation of the mentioned residue, resulting in accumulation of such phosphorylated, but inactive Akt.¹¹⁵

An increased activity of Akt leading to an increase of its signalling can cause creation of tumors.^{116,117} Therefore a regulation of Akt activity, or even its inhibition, seems to be a logical approach for cancer treatment. The activation of Akt is mostly regulated by PI3K. Inhibiting PI3K would lead to a decrease of Akt activity. One of such inhibitors GDC-0941 shows promising results in the treatment of cancer.¹¹⁷ GDC-0941 inhibits PI3K, which leads to no phosphorylation of Akt substrates PRAS40, FoxO1 and Gsk3 β .¹¹⁸

Goal

Because of mTORC2 being situated to the proximity of mitochondria, to the MAM, and its known effect on mitochondrial physiology⁷⁸, we decided to take a look at its possible effect on the mitochondrial functions like oxidative phosphorylation or oxygen consumption rate or mitochondrial potential.

By creating a mTORC2 defective cell line, which knocks down the expression of mSin1 as one of the mTORC2's unique components, we would like to study the effects of missing mTORC2 on the cell, more specifically on mitochondria. Such cell line would then need to be characterized, by confirming the diminished activity of mTORC2 on phosphorylation of Akt at position serine 473 and the possible effect of not fully activated Akt on one of its substrates Gsk3 β .

In the next step we would take a look at the dephosphorylation rate of Akt's both phosphorylated positions threonine 308 and serine 473 to observe the effect and speed of dephosphorylation of the control and knockdown cells.

The reaction of the cells to different serum concentration and their response to Akt upstream inhibitor GDC-0941 would be the last step in characterization of the knockdown cell line.

For the examination of mTORC2's activity in mitochondria we decided to direct one of its components, mSin1, to mitochondria, by creating constructs of three different mSin1's isoforms, that would locate to mitochondria. We believe that such construct would be able to pull other mTORC2 components to mitochondria, which would lead to the assembly of the whole complex. Then we could study the effect of the present mTORC2 in mitochondria on mitochondrial functions and examine the effect of mTORC2's loss in the cell on mitochondria.

To compare the effects of such targeted mTORC2 with other cell lines, we would characterize a mSin1 knockout cell line HL-60.

Methods

Cell culture - trypsinizing, splitting and freezing the cell lines HeLa and HL-60

HeLa cell line - splitting

To start growing the cell line we thawed the cells (control, mSin1 KD1, mSin1 KD2), that were stored at -80°C. After thawing the cells were transferred from the eppendorf-tube to a 10 cm Petri-dish and filled up to 10 mL with DMEM (Dulbecco's Modified Eagle Medium) containing 10% FBS (fetal bovine serum), 1% Pen/Strep and Glutamine. The cells were grown in an incubator at 37 °C, at 5% CO₂ until they reached a confluence level.

In order to maintain a cell culture, it needs to be split and taken care of regularly. Depending on the speed of multiplying, the splitting needs to be performed to maintain the optimal cell count and to assure the well-being of the cells.

The HeLa cells are adherent, which means they are growing on the bottom of the Petri-dish.

First the DMEM was removed with a pasteur-pipette connected with a tube to a suction pump. The cells were then washed with 2 mL PBS (phosphate-buffered saline), to remove remaining medium, which could possibly prevent the trypsinizing step. To wash the cells sufficiently the Petri-dishes were moved in circular movements. The PBS was removed in the same manner as the medium. To trypsinize the cells, so to collect them from the Petri-dish, Trypsin/DMEM was used. To each plate 1 mL of this solution was added and the Petri-dish immediately transferred to the incubator (37 °C, 5% CO₂) for approximately 3 minutes. Trypsine is an enzyme, that can digest proteins. It digests the proteins, that are connecting the cells to the Petri-dish, so they move to the solution. If the trypsin is left in the Petri-dish too long, it can start digesting the proteins of the cells and therefore destroy them. To get the maximum amount of cells into the solution, the Petri-dish was knocked-on carefully. To stop the reaction with trypsin, 4 mL of DMEM (10% FBS, 1% Pen/Strep/Glutamine) were added and the Petri-dish was washed carefully with the cell suspension in order to collect the maximum possible amount of the cells. Such cell suspension was then transferred to previously marked 15 mL Falcon Tubes. 1,5 mL of such cell suspension were then returned back to the Petri-dish and filled up to 10 mL with the medium DMEM (10 % FBS, 1 % Pen/Strep/Glutamine) and put back to the incubator.

HeLa cell line - freezing the cells

To keep the cells safe and stable for a longer period of time and when they are not being used, the best way to do this is to freeze them. First the cells need to be trypsinized, in the same way as described in the chapter "HeLa cell line - splitting). The gathered cell suspension (in the Falcon Tube) was then centrifuged down at 300 rpm for 5 minutes. In the meantime the freezing solution was prepared. After the centrifugation the medium was removed and the pellet was resuspended in 5 mL of the freezing solution and this amount was split evenly across 1,5 mL cryotubes (1 mL per tube). The cryotubes were put in cell-vial cooler and put in the freezer (-80 °C) for

some time, to ensure a slow freezing of the cell and no creation of ice pieces, that could possibly hurt the cells. Then the cryotubes were removed from the cooler and transferred into liquid nitrogen.

HL-60 cell line - splitting

The HL-60 cells were kindly donated by the group of Dr. Orion Weiner from the University of California, San Francisco, which also provided the necessary protocols. The cells were first thawed at 37 °C only until the last piece of ice melted and resuspended in 20 mL of RPMI/Hepes (Roswell park memorial institute/4-(2-hydroxyethyl)-1-piperazineethanesulfonic acid), containing 10 % FBS and 1% Pen/Strep and Glutamine. Then the cells were spun down at 400 g for 5 minutes and the supernatant was aspirated. The pellet was resuspended in 20 mL prewarmed complete medium and put into T-75 culture flask.

The HL-60 cells are not adherent, they are growing directly in the solution. The process of splitting them is therefore different from the HeLa cells. To split the cells the medium containing the cells was removed from the T-75 culture flask and transferred into a smaller culture flask. Then a sample of 20 µL was taken and transferred into an Eppendorf-tube, to determine the cell count. This was performed at the cell counter, by mixing the cell suspension with 10 µL of Trypan Blue and putting the mix into a counting chamber. The cell counter provided information about the total cell count, amount of live cells and the ratio. The necessary amount to split the cells sufficiently was $0,3 \times 10^6$ cells/mL. This information was provided by the laboratory, where the cells were cultivated. The necessary volume of the cell suspension was calculated as following:

$$V(\text{cell suspension})[\text{mL}] = \frac{\text{desired amount of cells} [\text{cells/mL}] \times \text{total Volume} [\text{mL}]}{\text{actual amount of cells} [\text{cells/mL}]}$$

Equation 1: Calculation of the suspension volume necessary to split the cells to obtain the desired amount.

The calculated volume was then filled up to 20 mL in the culture flask with the medium RPMI/Hepes, containing 10 % FBS and 1% Pen/Strep and Glutamine. The culture flasks with the cells were put into the incubator (37 °C, 5% CO₂). The cells were split once a week, after reaching satisfactory confluency.

HL-60 cell line - freezing the cells

To freeze the cells a similar procedure was used, as in the case of HeLa. First the cells were spun down at 400 g for 5 minutes. The supernatant was carefully removed with a suction pump and the pellet resuspended in 5 mL ice cold freezing medium. The cells were then aliquoted (1 mL) into cryotubes and put into cell-vial cooler for 2 days at -80°C and then transferred into liquid nitrogen.

Transfection

To transfect cells, so to introduce DNA (deoxyribonucleic acid) into the cells, PEI (polyethylenimine) can be used.¹¹⁹ The DNA forms a positively charged complex with PEI, which binds to the negatively charged cellular surface and enters the cells via endocytosis.¹²⁰

In order to transfect the cells for the confocal microscopy cover slips were first put in 95% Ethanol solution and then in wells of a 12 well plate, which was then put into an incubator to dry out at 37 °C and 5% CO₂.

Then the cells were seeded into the wells (1 mL/Well of a 700 µL cell suspension filled up to 14 mL with full medium solution) or on a 6 well plate (2mL/Well of a 700 µL cell suspension filled up to 14 mL with full medium solution).

After reaching confluency the cells were transfected. First the DNA (2 µg/Well) was mixed in a sterile Eppendorf-tube with PEI in 1:3 (DNA:PEI) ratio. This mix was filled up to 100 µL with OptiMEM (optimized minimal essential medium) or serum-free DMEM and left incubating at room temperature for 15 minutes.

Before transfection the medium in the wells was replaced with a 0,9/1,9 mL fresh one and 100 µL of the transfection mix were added. The cells were then incubated for 6-9 hours

(37 °C, 5% CO₂) and then the medium was replaced by a fresh one.

The cells from the 6 well plate were collected using RIPA buffer, sonicated and 10x loading buffer was added. The samples were boiled for 10 minutes at 95 °C and then loaded onto a gel.

The medium from the 12 well plate was removed and the coverslips were removed from the bottom of the wells carefully with forceps.

Preparation of the slides for confocal microscopy

To fix the cells on the coverslips, the coverslip were put on a tissue (the side containing the cells on top) and 500 µL of 4% formaldehyde in PBS were put on the coverslip and left incubated for 15 minutes at room temperature.

The formaldehyde was removed and 500 µL of 1x TBS (tris-buffered saline) were put on the coverslip and left incubated for five minutes at room temperature. The TBS was removed and the cells on the coverslip were washed with 500 µL 1x PBS for five minutes at room temperature.

In order to stain the cell nucleus the coverslips were once again washed with 500 µL 1x PBS containing 1µg/mL DAPI (4', 6'-diamidino-2-phenylindole).

The 1xPBS/DAPI was removed and the coverslips were left to dry. 3 µL of MOVIOL were put on a slide and the coverslips (cells facing the slide) were carefully mounted on the slide evading the formation of any bubbles.

Such slides were left on the bench to dry.

Confocal microscopy

The confocal microscopy bases on pointing the illumination and detection on one single point of the sample, thanks to spatial filters, that are inserted into the paths of the objective and condenser. The final image is produced by scanning all points in the field of view.¹²¹

SDS-PAGE - Western Blot

The first step in the Western blot analysis of samples is the SDS-PAGE (sodium dodecyl sulphate-polyacrylamide gel electrophoresis). Electrophoresis is a phenomenon of the movement of charged particles in a liquid medium in an electric field. The condition for a uniform movement and for a separation according to the size of the sample(s) is a uniform charge of all the samples. This is achieved by SDS, which is added to the sample and cooked for a period of time, in order to denature the proteins and give them a uniform negative charge. Such samples (proteins) can be separated only by their size. Larger proteins move slower in the gel, than small proteins. This migration results in a separation of all the proteins. The gel consists of two parts - stacking and resolving gel. In the stacking gel, there are chloride ions, which move faster than the proteins in the sample. Glycine ions are present in the electrophoresis buffer, which are slower than the proteins in the sample. All of this results in the stacking effect. Chloride ions, proteins and glycine start moving once the current is applied. The fastest chloride ions in the front, followed by proteins from the sample and at the end are the glycine ions. At the border between stacking and resolving gel the pH of the stacking gel (6.8) changes to the pH of the resolving gel (8.8). The higher pH value causes the glycine ions to move faster, which creates the stacking of the sample, because the glycine ions overtake the now slower proteins.¹²² To identify the separated proteins, they are transferred to a nitrocellulose, PVDF (polyvinylidene difluoride) or nylon membrane. A sandwich consisting of a pair of sponges, filter paper, gel and the membrane is put in a tank, filled with transfer buffer. The negatively charged proteins will migrate from the gel to the membrane, once the current is applied. The membranes is then blocked, to avoid nonspecific bindings, probed with the primary antibody, washed and probed with a secondary antibody and washed again. The secondary antibody is tagged with horseradish peroxidase, alkaline phosphatase or fluorophores. Such tagged protein can then be detected.¹²³

Preparation of the gel

The day previous to the experiment or immediately before it, the gels for the western blot were prepared. In a 50 mL beaker first the resolving gel was prepared. TEMED (tetramethylethylenediamine) and APS (ammonium persulfate) were added as last, because they are the polymerase reaction starters. The gel was then poured between two glass plates, held by a BioRad® gel preparation kit, with a plastic pipette until approximately 1 cm below the bottom of the wells (Fig. 1). The top of the gel was covered with Isopropanol to remove bubbles and achieve a straight line. The gel was left to polymerize for 25 minutes and the Isopropanol was removed by simply turning the apparatus upside down. The rest of the isopropanol evaporated while the stacking gel solution was being prepared. For the stacking gel TEMED and APS were again added as last ingredients and the gel was poured onto the resolving gel until it started pouring out. Then the comb was inserted (either 10 or 15 wells) and the gel was left to polymerize for another 25 minutes. The prepared gels were removed from the apparatus and either used directly or stored at 4°C in a wet tissue.

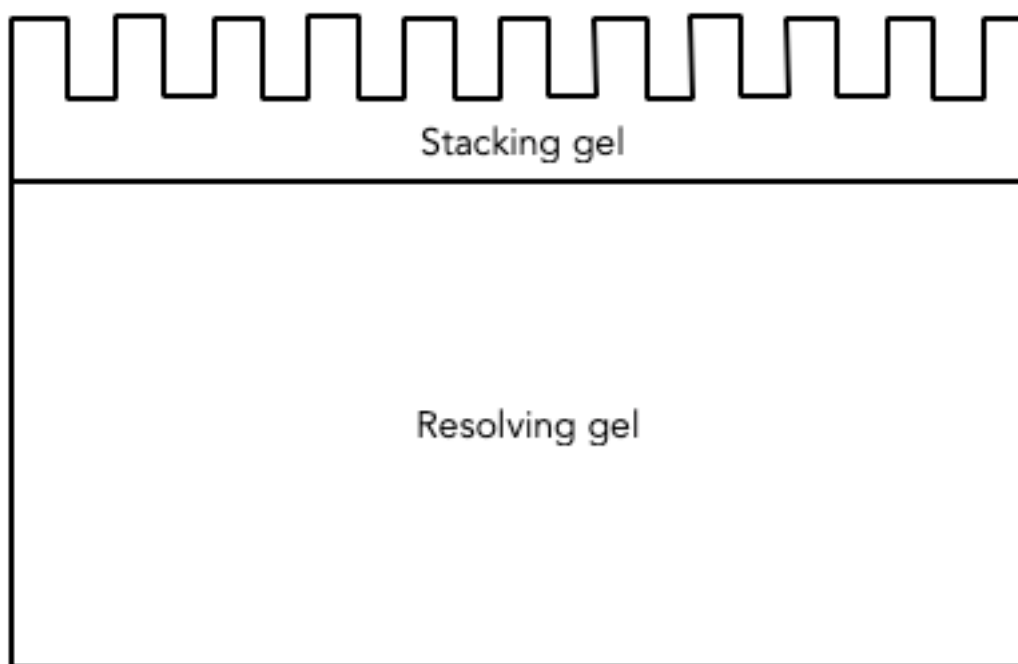


Figure 9: Gel for Western blot. The distance between the bottom of the wells and the border between stacking and resolving gel corresponds to approximately 1 cm, which should be enough for a satisfactory stacking.

HeLa - preparation of the samples - characterization of the cell lines

By introducing short-hairpin RNA against mSin1 into the HeLa cells, we produced two cell lines, that should be producing mSin1 in a lower ratio than the control cell line. Their characterization was performed in multiple steps. The first part was western-blot of the cells, which were pre-treated with different compounds.

At the beginning 1 mL of the cell suspension, gathered while splitting the cells, was transferred into a 12 well plate, 1 mL/well. The cells were let to grow overnight, which was enough to reach confluency. After achieving confluency, the medium was removed and replaced with 900 μ L starving medium (DMEM + 0.5% FBS). Then the cells were left to starve overnight. In the morning of the next day Torin1 and A443654 solutions were prepared. Torin1 solution was diluted 1000 times, by adding 1 μ L of Torin1 stock solution (2.6 mM) to 999 μ L of the serum-free medium, to achieve a concentration of 2.6 μ M. From this solution 100 μ L were added to the wells pre-treated with Torin 1 (Fig. 1). In a similar way, the A443654 stock solution (10 mM) was first diluted 400 times by adding 1 μ L of the A443654 stock solution to 399 μ L of serum-free medium, to obtain the concentration of 25 μ M. From this solution 110 μ L were put into the corresponding wells (Fig. 1). The cells were incubated (37°C, 5% CO₂) like this for 40 minutes. After this time 111 μ L of 1000ng/mL of human recombinant insulin were added and left at 37°C, 5% CO₂ for 5 minutes.

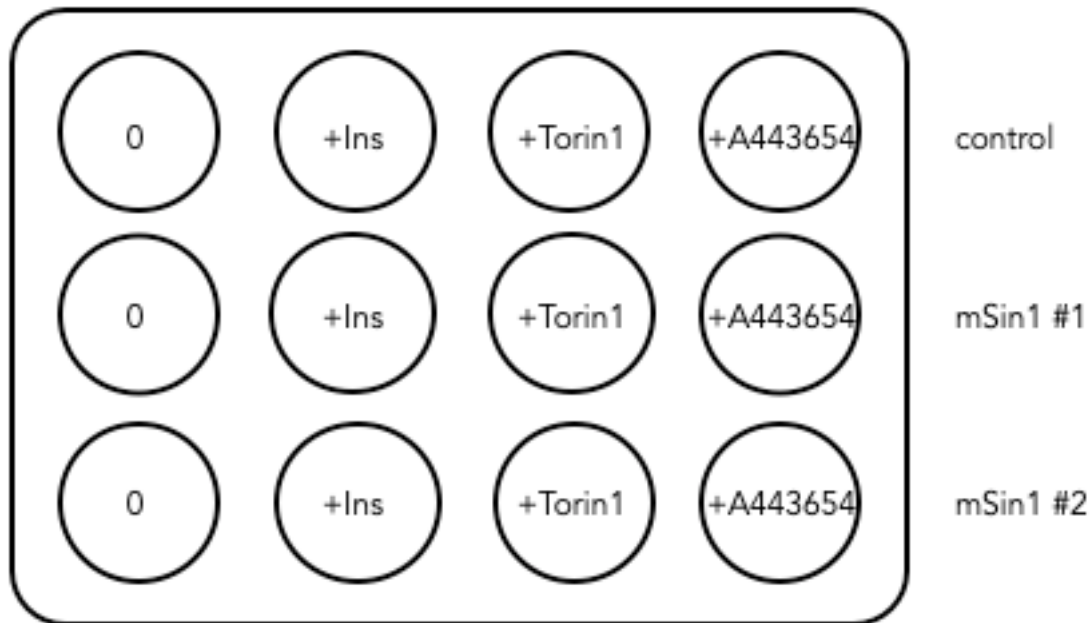


Figure 10: 12 well plate scheme. The cells were first treated with 260 nM Torin1 or 250 nM A443654 for 40 minutes at 37°C. The +ins, +Torin1 and +A443654 marked wells were also treated with 100 ng/mL human recombinant insulin for 5 minutes at 37°C.

After the treatment the medium was removed and 200 μ L of RIPA buffer/Inhibitor were added. To remove all of the cells the bottom of the well was washed multiple times with RIPA buffer/inhibitor and finally transferred into a marked 1.5 mL Eppendorf-tube. In order to break down the DNA of the cells, which could affect the results in a negative way, the samples were sonicated with three impulses (each impuls was one second long). To such samples 22 μ L of 10x sample buffer were added. The samples were put on a heater for 10 minutes, to enhance the function of SDS in the sample buffer and so to ensure the degradation of the protein into its primary form and also to enhance the effect of the reducing agent, to break the disulfide bonds present in the protein. During the boiling step the Eppendorf-tubes have to be opened at least once, to release the pressure built by the boiling.

HL-60 - preparation of the samples - characterization of the cell lines

The cells of the HL-60 cell line are growing in the medium, they are no adherent cells, therefore the handling and their preparation for the experiment is slightly different, than in the case of the HeLa cells. The cells first need to be counted down. From the total amount, the volume containing 1×10^6 cells/mL for the total volume of 10 mL. This volume was put into a T-25 culture flask and the cells were let grow overnight at 37°C and 5 % CO₂. On the next day, the medium and the cells were transferred into a Falcon-tube and span down at 300 g for 5 minutes. The supernatant was removed and replaced with 1 mL of the starving medium (RPMI/HEPES + 0.5 % FBS). The cells were starved in this manner overnight at 37°C and 5 % CO₂ and in the next morning the pre-treatment started. The same reagents were prepared as in the case of HeLa cells and added in the same manner to the HL-60. First the HL-60 were pre-treated with 260 nM Torin1 and 250 nM A443654 for 40 minutes at 37°C and 5 % CO₂. Then 100 ng/mL human recombinant insuline was added for another 5 minutes. After this incubation was over the cells were span down at 300 g for 5 minutes and resuspended in 200 μ L of the RIPA buffer/Inhibitor and transferred into an Eppendorf-tube. The

samples were then sonicated in the same way as HeLa cells and mixed with 22 μ L of the 10x Sample Buffer and boiled for 10 minutes at 95 °C. Such samples were ready to be loaded onto the gels.

HeLa and HL-60 - loading of the samples onto the gel, running the gel and transferring proteins onto a nitrocellulose membrane

The prepared gels were put and secured in the running apparatus and the impermeability was proofed by pouring the running buffer into the apparatus. Once this was secured the gels were put into the running chamber, which was also filled with the running buffer afterwards.

For a good identification of the bands the first and the last well were always loaded with 0.75 μ L of Page RulerPlus Prestained Protein Ladder (Figure 11).

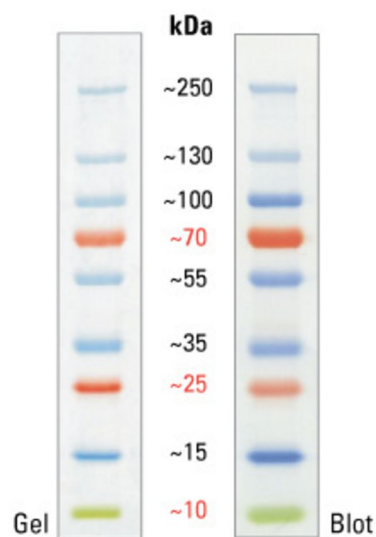


Figure 11: Page RulerPlus Prestained Protein Ladder bands by Thermofisher®.

The samples were always loaded in the same way, starting with the control cells, followed by mSin1 knockdowns #1 and terminating with mSin1 knockdowns #2 (Figure 12). Everytime 2 gels were loaded. The loading volume of the samples corresponded to 7.5 μ L, which was carefully loaded into the wells with a 10 μ L micropipette.

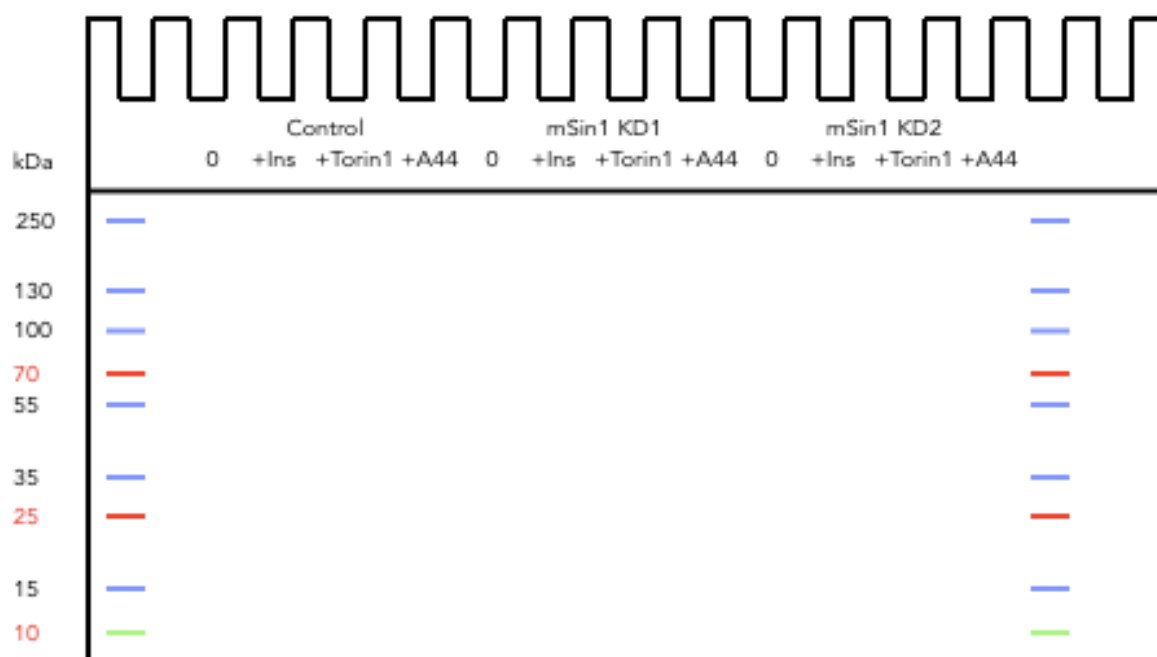


Figure 12: Loading scheme of the 15 wells gel (characterization of knockdown cell lines 1 and 2). The first and the last lane is the Protein Ladder (0.75 μ L), with the corresponding size in kDa. The samples were loaded (7.5 μ L) in this manner for every experiment.

After the loading was completed, the running buffer was filled approximately until 0.5 cm under the top of the bigger glass panel, to avoid overflowing. The apparatus was closed and the voltage was set to 120 V. Thanks to the bromophenol blue in the sample buffer it was possible to follow the running progress in the gel as a blue line. When the blue line was closing the bottom of the gel, the voltage was increased to 150 V, which should guarantee a good separation of smaller sized proteins.

Once the blue line reached the end of the gel, the gels were removed from between the glass panels. Carefully the gel was cut in the corner, to mark the start of the loading and simplifying the identification of the lanes.

For the transfer a so called transfer sandwich was prepared. The transfer sandwich consisted of two sponges, two filter papers and one nitrocellulose membrane, put together as shown on Figure 13.

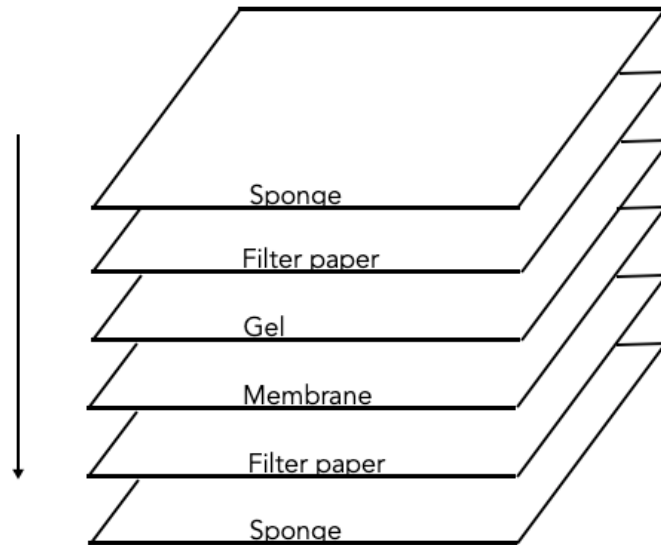


Figure 13: Transfer sandwich for transferring the proteins from the gel onto a nitrocellulose membrane. The membrane is closer to the positive electrode, so the negatively charged proteins migrate from the gel onto the membrane.

The sandwich was put together and secured by a plastic holder and put between the electrodes with the red part facing the anode (+ pole) and the black part facing the cathode (- pole). The nitrocellulose membrane had to be closer to the positive electrode, than the gel, because the negatively charged proteins can then migrate from the gel onto the membrane. The transfer chamber was closed and the voltage set to 80 V for 80 minutes. This time showed to be sufficient for a satisfactory transfer.

HeLa and HL-60 - blocking and primary/secondary antibody incubation and visualization of the bands

After the transfer the membranes need to be blocked, to prevent the antibodies to bind unspecifically to the membrane. The membranes were also marked in the corner, just like the gels, to allow the identification of the loading.

For blocking the membranes were simply put into a plastic box and covered with 25 mL of 5% BSA (bovine serum albumin) in TTBS (Tween20 enriched tris buffered saline). The boxes were put on a shaker for 90 minutes.

Once the blocking was done, the membranes were taken out and cut into smaller pieces (Figure 14 - example of cutting the membrane, the membrane was cut differently depending on the experiment and the sizes of the proteins). The smaller pieces of the membranes, each containing a different protein (corresponding to its size) were put into 50 mL Falcon-tubes with primary antibody. The membranes were marked in the corner with a number corresponding to the primary antibody. The primary antibody binds specifically on the protein on the membrane. The primary antibody solution is the antibody in 5% BSA in TTBS with 0.01% NaN₃. The azide makes it possible to use the primary antibody solution multiple times, by preventing bacterial growth in the solution.

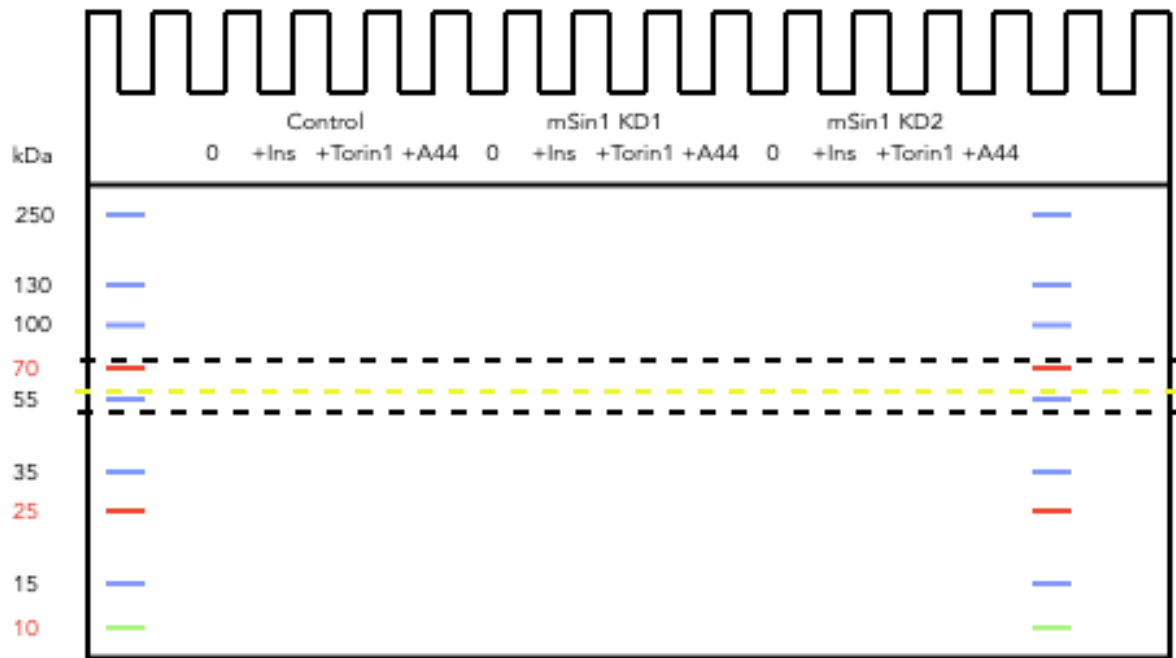


Figure 14: The membranes were cut in 5 smaller pieces, to allow incubation with 5 different primary antibodies. The first membrane was cut into 3 pieces along the black dashed lines, going above 70 kDa and just under 55 kDa. The second membrane was cut into 2 pieces along the yellow dashed line going just above 55 kDa.

We used five different primary antibodies (Table 1). The incubation with primary antibodies was done overnight (or over weekend), at 4°C on a rotator, to increase the binding of the primary antibody on the membrane to the maximum. After the incubation with primary antibodies the membranes were washed in multiple washing steps with TTBS. The TTBS was exchanged after every washing step. At first the membranes were washed for fifteen minutes and then three more times for five minutes. The washing removes rests of the primary antibody, so the secondary antibody binds only to properly attached primary antibody.

Table 1: Primary antibodies used for the primary antibody incubation with the corresponding sizes of proteins for the characterization of the cell lines experiment.

Primary Antibody α	Size [kDa]
mTOR	289
Akt ^{pS473}	56
GAPDH	36
mSin1	59
Gsk3 β ^{pS9}	47

During the washing the secondary antibody solution was prepared. The secondary antibody was used in dilution 1:5000. The secondary antibody should be against the animal in which the primary antibody was developed. We were using secondary antibody against Rabbit and Mouse primary antibodies. Because the secondary antibody binds to the heavy chain of the primary antibody, it doesn't interfere with the bond between primary antibody and the antigen. The membranes were incubated with the secondary antibody for two hours at the room temperature.

After this incubation the membranes were washed again. Once for twenty minutes and then five times for five minutes to remove the rest of the secondary antibody, which could lead to the spoiling of the signal.

The secondary antibody has a HRP (Horseradish Peroxidase) chromogenic agent bound to it. To visualize the bands we used a Immobilon Western Chemiluminescent HRP Substrate, composed out of two solution - HRP Substrate Peroxide solution and HRP Substrate Luminol Reagent. These two solution were mixed together in 1:1 ratio and the whole membrane were covered with the mixture. For visualization the membrane were put in Fusion Fx Vilber Lourmat by Peqlab® and the exposure time was chosen. Multiple shots were taken for different exposure times, until complete saturation was reached.

For quantification the program ImageJ was used. All of the bands were selected and their intensity was measured. The measured data were copied into Microsoft Excel and normalized to the first value over loading control (GAPDH - glyceraldehyde 3-phosphate dehydrogenase), as shown in equation 2.

$$\frac{a' \times b}{b' \times a}$$

Equation 2: Normalization of the quantified data. a - non-treated control, b - non treated loading control of the control cells, a' - sample to be normalized, b' - loading control of the sample.

HeLa cells - GDC-0941 induced dephosphorylation of Akt - preparation of the samples

Another part of the characterization of the HeLa mSin1 knockdowns was the GDC-0941 induced dephosphorylation of Akt^{pT308} and Akt^{pS473}. A similar approach was set, as in the previous characterization step. First 1 mL of the cell suspension obtained after splitting the cells was put into 18 wells of a 24 well plate. These cells were let grow overnight. Then the medium was removed and replaced with 900 µL starving medium (DMEM + 0.5% FBS) and the cells were left starving overnight.

On the next day the the insulin for the cell stimulation was prepared, as well as the GDC-0941. The human recombinant insuline was diluted 100 times (from 100 µg/mL) to 1000 ng/mL. By diluting 4000 times at first to get a concentration of 2500 nM. The loading scheme of the 24 well plate can be seen on figure 7.

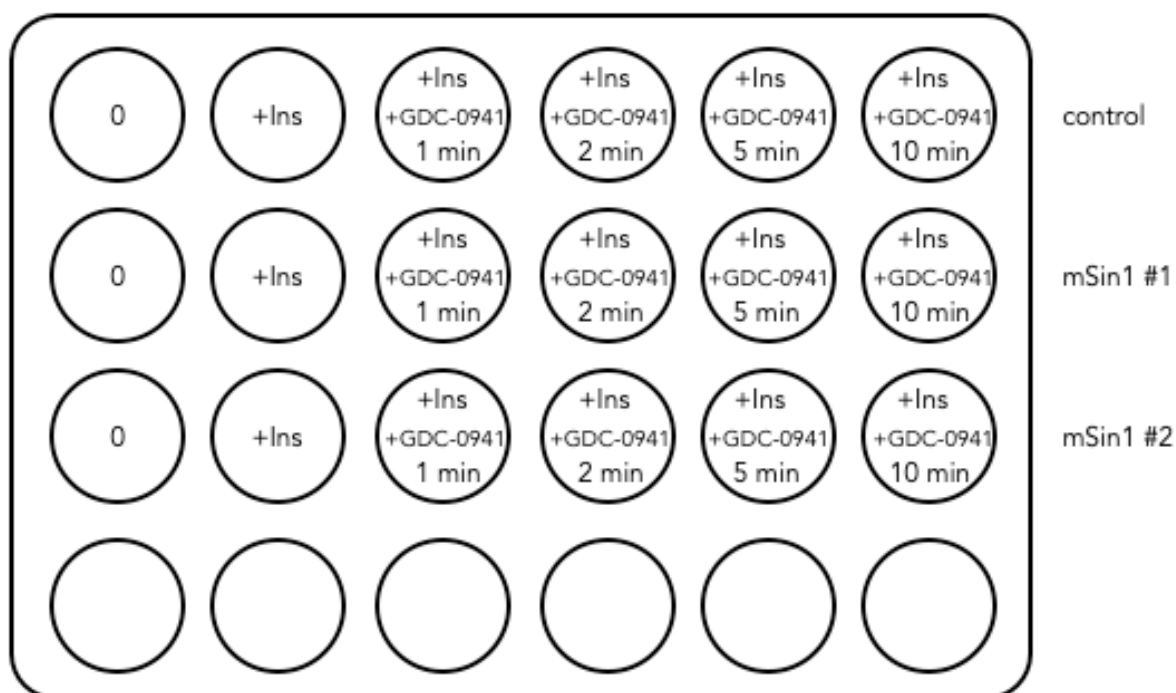


Figure 15: Loading scheme of the 24 well plate with HeLa cells, as well as the stimulation with human recombinant insulin and GDC-0941. The times refer to the length of the treatment with GDC-0941. The bottom 6 wells were unused.

The figure 7 also shows wells, which were treated with GDC-0941 for different times. First 100 μ L of the human recombinant insulin were added, followed by addition of 111 μ L of GDC-0941 as shown in Table 2, to ensure 5 minutes long stimulation with human recombinant insulin alone. The time was followed with a timer.

After stimulating and treating the cells, the medium and the reagents were removed from the wells and the cells were lysed with 200 μ L of RIPA buffer/Inhibitor and the lysates were transferred into 1.5 mL Eppendorf-tubes. The lysates were sonicated (3 impulses, 1 impuls=1 second). Then the 10x SDS sample buffer was added and the samples were boiled for 10 minutes at 95°C.

The samples were then loaded on a gel, treated and analyzed in the same way as described in the previous chapter.

Time	GDC-0941	Insulin
15:00	-	10 min
10:00	10 min	5 min
07:00	-	2 min
06:00	-	1 min
05:00	5 min	Ins
02:00	2 min	-
01:00	1 min	-
00:00	Lysis	

Figure 16: Treatment of the cells for the dephosphorylation experiment. Time corresponds to the time set on a timer. The times in GDC-0941 and Insulin columns correspond to the label on the 24 well plate.

Table 2: Primary antibodies used in the dephosphorylation experiment with the corresponding sizes of the analyzed proteins.

Primary Antibody α	Size [kDa]
Akt ^{pT308}	56
Akt ^{pS473}	56
GAPDH	36

HeLa cells - serum concentration dependency

To further examine the effects of mTORC2 on Akt, or on the phosphorylation of T308 and S473, and as another part of the characterization of the mSin1 knockdown cell line we took a look at the serum concentration dependency and inhibition of Akt by A443654 and GDC-0941.

First the cells were seeded on a 24 well plate. 500 μ L of cell suspension (obtained during the splitting process/after trypsinizing from both control and knockdown #1 cell line) were put into each well (12 wells for control and 12 wells for mSin1 knockdown #1). The cells were let grown until the next day (24 hours, or until the confluency of 70-80% was reached).

Then the medium was replaced with 450 μ L serum free DMEM, 1% FBS DMEM, 2% FBS DMEM, 5% FBS DMEM and incubated overnight at 37°C and 5% CO₂ (figure 9). In the morning of the next day the cells were incubated with 250 nM GDC-0941 for 30 minutes. Following this the cells were incubated for 10 minutes with 250 nM A443654 (figure 9).. The medium and the reagents were then removed from the wells. To collect the cells, they were lyzed with 100 μ L RIPA Buffer containing an inhibitor cocktail and transferred into 1,5 mL Eppendorf-tube.

To shear the cellular DNA the samples were sonicated (2 impulses - each 1 second). Lastly 11 μ L of 10x SDS sample buffer were added and the samples were heated at 95°C for 10 minutes.

Such samples were loaded, treated and analyzed in the same manner as previously described.

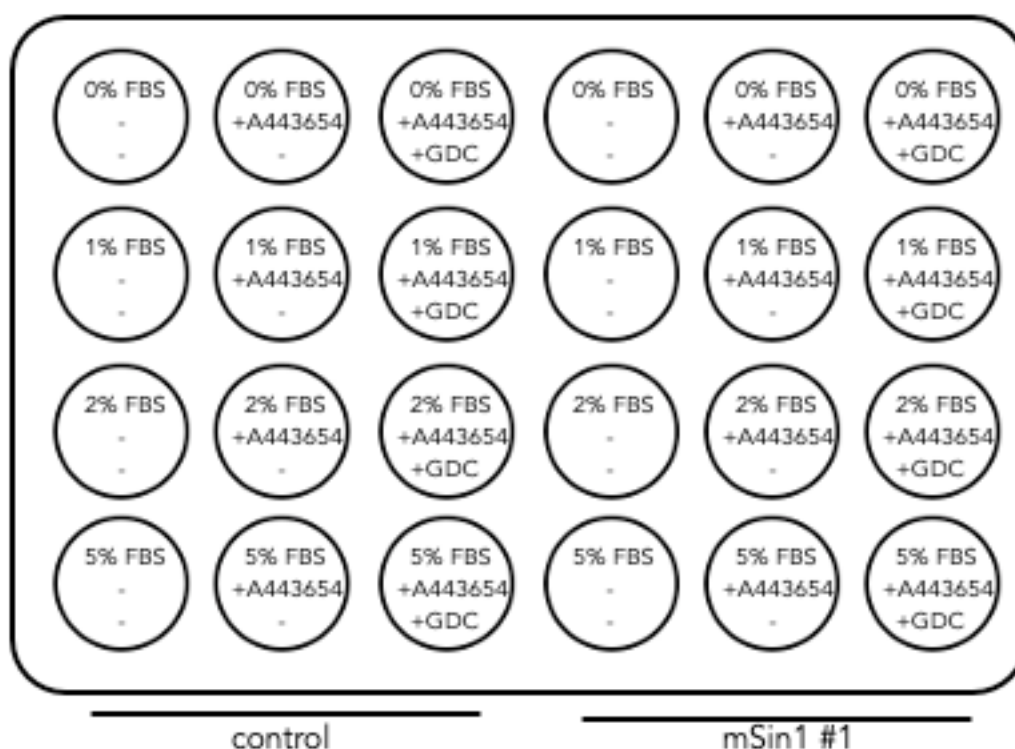


Figure 17: Treatment of the cells for the serum concentration dependency experiment. The cells were incubated with different serum concentrations overnight (0% FBS - serum free DMEM, 1%, 2% and 5% FBS DMEM). On the next day the cells were treated with GDC-0941 (GDC) for 30 minutes, followed by incubation with A443654 for 10 minutes. The cells were then lysed in RIPA buffer containing an inhibitor cocktail.

Table 3: Primary antibodies used in the serum concentration dependency experiment with corresponding sizes.

Primary Antibody α	Size [kDa]
Akt ^{pT308}	56
Akt ^{pS473}	56
GAPDH	36
Gsk3 β ^{pS9}	47

Isolation of mitochondrial fraction

The mitochondrial isolation was performed according to a slightly modified protocol.¹²⁴ To isolate the mitochondrial fraction the same protocol was used for both HeLa and HL-60 cells. The cells were left to grown to reach either confluency (HeLa) or a specific amount of cells was taken (1 million - HL-60). The HeLa cells were first collected via trypsinizing the plate with 1 mL Trypsin/EDTA. The cells were transferred into a 15 mL tube and spun down at 300 g at RT for three minutes.

After the centrifugation the supernatant was removed with a pasteur-pipette and the pellet was washed by resuspending with 3 mL of PBS. The suspension was centrifuged again at 300 g for three minutes at room temperature.

The supernatant was again removed and the remaining pellet was resuspended in 200 μ L PBS. Such suspension was transferred to a 1,5 mL Eppendorf-tube.

The Eppendorf-tubes were held on ice until centrifuged at 600 g for five minutes at 4°C. The PBS supernatant was removed and to the pellet 200 µL ice cold IB_C buffer were added. The pellet was homogenized with a plastic homogenizer. Then another 200 µL of ice cold IB_C buffer were added.

After centrifuging at 4°C and 600 g for ten minutes the supernatant was transferred into another Eppendorf-tube. The pellet was frozen. 50 µL of the supernatant containing the total cell lysate were transferred into another Eppendorf-tube. This fraction was then run in the western-blot as well.

The remaining 350 µL of the supernatant were centrifuged at 7000 g at 4°C for ten minutes. The supernatant was removed and stored in the freezer. The mitochondrial fraction, now contained in the pellet, was resuspended in 200 µL ice cold IB_C buffer, to be washed. The suspension was spun down at 7000 g at 4°C for ten minutes. The supernatant was, just like previously, removed and stored in the freezer. The pellet was carefully resuspended in 100 µL ice cold IB_C buffer.

To both samples, the cell lysate and the mitochondrial fraction, 10x SDS loading buffer was added (6 µL to the cell lysate, 11 µL to the mitochondrial fraction) and the samples were boiled at 95°C for ten minutes.

Such samples were stored in the freezer. Before loading on the gel, the samples were boiled again for ten minutes at 95°C. To ensure an equal loading 3 µL of the cell lysate and 6,9 µL of the mitochondrial fraction were loaded on the gel.

The membranes were incubated with four different antibodies - anti-GAPDH, anti-SLC25A5 (solute carrier family 25 (mitochondrial carrier; adenine nucleotide translocator), member 5), anti-mSin1, anti-mTOR and anti-GFP (only in case of transfected cells, green fluorescent protein).

Table 4: Primary antibodies used in the mitochondrial fraction isolation experiment with corresponding sizes.

Primary Antibody α	Size [Da]
mTOR	289
SLC25A5	33
GAPDH	36
mSin1	59

Results and discussion

Characterization of mSin1-deficient HeLa and HL60 cell lines

By characterizing the mSin1-deficient HeLa and HL60 cell lines we wanted to show, that indeed the cell lines are expressing reduced or no mSin1. By demonstrating this we proceeded to investigate the effects of the reduced mTORC2 activity in the cell in response to various pre-treatments (insulin, Torin1, A443654, GDC0941 or different serum concentrations in the growth medium). More precisely we investigated the effects of mTORC2 activity on Akt S473/T308 phosphorylation as well as on Akt substrate Gsk3 β -S9 phosphorylation. These experiments provided us with effects of mTORC2 activity in the cell and with necessary data on the quality of the cell line needed for further experiments in mitochondria.

To characterize the mSin1-deficient HeLa cell line multiple western-blots were performed. For this two HeLa mSin1-knockdown lines were used, named respectively mSin1 #1 and mSin1 #2. Along with these cell lines, obtained using stable expression of shRNA against mSin1, a control cell line (ctrl) expressing shRNA against GFP was characterized, so we would be able to observe a difference in the levels of mTORC2 components and Akt substrates. The cells were first starved overnight in 0.5% FCS and then pre-treated for 40 minutes with 260 nM Torin1, which is a mTOR inhibitor, and 250 nM A-443654 (Akt-kinase inhibitor), causing Akt hyperphosphorylation on positions S473 and T308. S473 is in the hydrophobic domain of Akt, which is also the position phosphorylated by mTORC2.

The pre-treatment was performed at 37°C. After this the cells were incubated for 5 minutes with 100 ng/mL bovine recombinant insulin. The cells were lysed using RIPA-Buffer containing phosphatase and protease inhibitor cocktail, and the lysates were analyzed using Western blotting with the selected antibodies (Akt^{pS473}, Gsk3 β ^{pS9}, mSin1, mTOR and GAPDH).

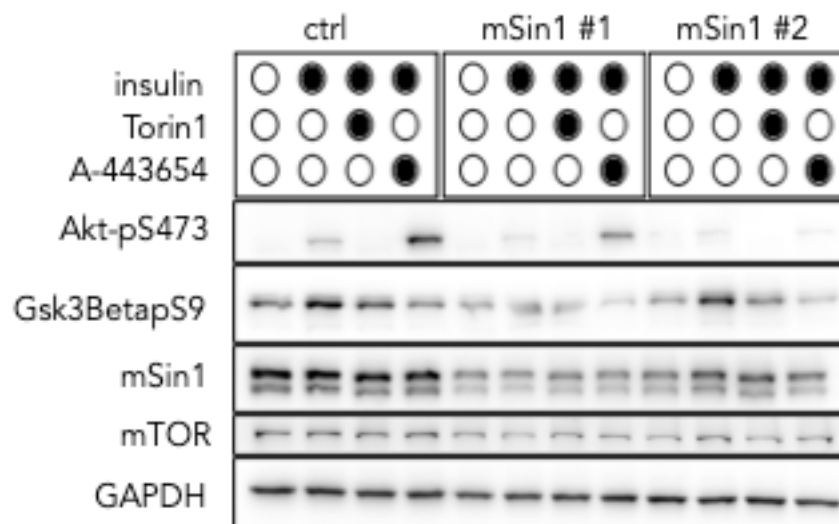


Figure 18: HeLa cells pre-treated with 260 nM Torin1 and 250 nM A-443654 for 40 minutes at 37 °C followed by 5 minutes incubation with 100 ng/mL human Insulin. Lysis in RIPA Buffer.

To characterize the mRictor- and mSin1-knockout (RKO and MKO respectively) cell lines, the same type of characterization experiment was used, also to see if the HL60 suspension cells are reacting to the treatment in the same way.

First the cells were equally seeded (one million cells) in a T25 cell flask and left growing until the next day. In the evening of the next day the cells were spun down and the pellet was resuspended in serum-free medium and the cells were starved overnight. On the next day the cells were incubated with A443654 or Torin1 for 40 minutes and then with bovine recombinant insulin for 5 minutes. The samples were collected with RIPA buffer containing protease and phosphatase inhibitors mix and sonicated and prepared for western blot. The membranes were incubated with anti-mSin1, anti-Akt-pS473/pT308 antibodies.

Firstly the mSin1 presence in the cell lines was analyzed, to test if the knockout cell line indeed is not expressing mSin1.

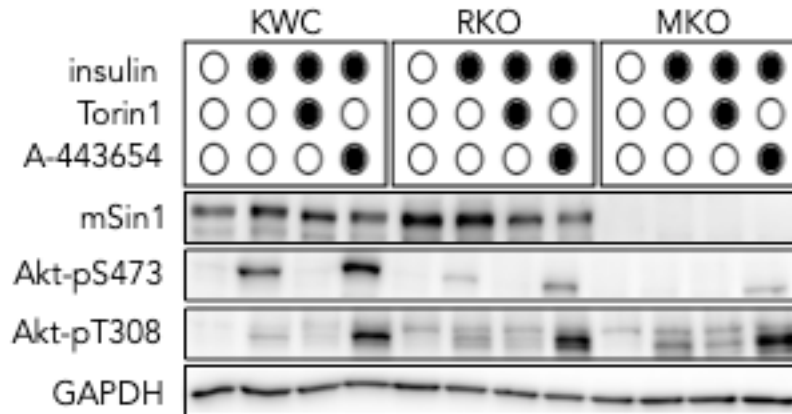


Figure 19: Western blots of the characterization of the knockout cell lines. The cells were pre-treated with Torin 1 (260 nM) and A443654 (250 nM) for 40 minutes and for five minutes with 100 ng/mL bovine recombinant insulin.

The reason for the incubation with GAPDH is to be able to control the loading of the cell lysate into the wells of SDS-PAGE gel. As can be seen on Figure 18 and Figure 19, the loading was successful and the amount of the cell lysate in different wells was more or less constant. The signal of GAPDH was observed at approximately 36 kDa, which corresponds to its true size (36 053 Da). The strength of the signal of mTOR antibody on Figure 18 (observed at 289 kDa, true size 288 892 Da) doesn't vary much. To be able to tell if there is any difference present in its levels, we had to quantify the levels of the protein. The signal of mSin1 (observed at 59 kDa, true size 59 123 Da - Figure 18Figure 19) shows 2 bands, which can be explained by the existence of multiple mSin1 isoforms. In the case of mSin1 we can already see a difference in its expression.

By comparing the mSin1 deficient cell lines with the control cell lines (ctrl, KWC) we can clearly see a difference in the levels of mSin1. The mSin1 #1 cell line shows a reduced level of the endogenous mSin1. The levels of mSin1 in the mSin1 #2 are also reduced, but not in such a high measure, as seen in the mSin1 #1. This can therefore be considered as a first sign of the stability of the cell line, expressing shRNA against mSin1, at least in the case of mSin1 #1.

The HL60 cell line MKO is lacking any mSin1 signal, just as expected. Knocking out Rictor should not have an effect on the mSin1 levels in the cells, which can be observed on Figure 19.

The levels of Akt-pS473 are very low after the overnight starvation. The incubation with insulin partially restores mTORC2-mediated Akt phosphorylation on S473 in HeLa and HL60. The levels are again reduced after mTOR inhibition, as mTOR is a component of mTORC2 and without it, the complex can not act as a kinase to perform the phosphorylation on Akt. The incubation with bovine recombinant insulin and A443654 leads to the hyperphosphorylation of Akt on position S473, just as expected.

The same trend can be seen in the case of mSin1 #1, just to a smaller extent. The reduced expression of endogenous mSin1 causes a reduced level of mTORC2 in the cells, which leads to a lower phosphorylation serine 473 in Akt. The incubation with bovine recombinant insulin leads to a small increase in the signal, but much weaker than it is in the case of the control cells. The pre-treatment with Torin1 and A443654 has the same effect in the control cells, but to a smaller degree. The mSin1 #2 show almost no presence of Akt-pS473 and almost no reaction to the pre-treatment and incubation with A443654 and human recombinant insulin. However during the repetition of this experiment the mSin1 #2 cell line didn't show this effect in a constant manner. We therefore suspected, that the expression of shRNA against mSin1 is not stable in this cell line, which reflects on the variability of the phosphorylation levels of Akt-pS473.

To investigate if the reduction of Akt-pS473 phosphorylation caused by CRISPR-mediated knockout HL-60 would affect the phosphorylation on T308 of Akt we developed the pT308 signal. On Figure 19 we are not able to see any reduction in the phosphorylation of Akt-pT308 in RKO or MKO if compared to KWC.

Then we tested the phosphorylation levels of Gsk3 β ^{pS9}, which is the substrate of Akt-kinase. The Akt-kinase phosphorylates Gsk3 β on Serine on position 9. The reduced levels of Akt activity or its inhibition should lead to a decreased or completely abolish phosphorylation of Gsk3 β ^{pS9}. As can be seen on Figure 18, this is indeed the case. In the case of the control cells (ctrl), the Gsk3 β shows low levels after the night of starvation, being restored after the incubation with human recombinant insulin. The phosphorylation is reduced after mTOR inhibition and therefore no mTORC2 present to activate Akt-kinase. The inhibition of Akt by A443654 also leads to reduction of the phosphorylation of Gsk3 β . In the case of mSin1 #1 the levels of phosphorylated Gsk3 β are constant, but reduced if compared to the control cells (ctrl). This is could be caused by reduced levels of mSin1 and therefore reduced levels of mTORC2 in the cells. The mSin1 #2 show a similar behaviour as the control cells (ctrl), even though the signals seem to be weaker.

We also tested the possible influence of shRNA-mediated knockdown of mSin1 on mTOR, but just as expected we didn't observe any change in the mTOR levels as can be seen on Figure 18

This allows to conclude, that both mSin1 knockdown cell lines are indeed expressing mSin1 at a lower level, but the mSin1 #1 seems to be more stable in the stability of shRNA against mSin1 expression than mSin1 #2, which makes it more suitable for future experiments. CRISPR-mediated mSin1 and mRictor knockout cell line seem to reduce mTORC2 activity as expected, but to test, that this is indeed the case a further quantification was needed.

The quantification of the data was executed with the program ImageJ, by estimating signal intensity as the area of the peak on Western blots. All of the quantifications were performed in the same manner.

The quantified and normalized data were visualized as boxplots. In addition, to examine the statistical significance, the ANOVA test was performed in Origin®.

Figure 20 shows the expression of mSin1 in response to different treatments in the three cell lines. In the non treated cells we observe a statistically significant difference in the expression of mSin1 between the cells of the control cell line and the cells of both knockdown cell lines. The levels of mSin1 are significantly lower in both knockdown cell lines ($p < 0,05$, $n=3$), showing, that the expression of this protein has indeed been lowered by the shRNA against mSin1.

A similar trend can be seen in the cells treated with bovine recombinant insulin, where the levels of mSin1 are again significantly lower ($p < 0,05$, $n=3$) in knockdown cell line 1 than in the control cell line, therefore leading to the same conclusion as before.

After treating the cells with Torin1, the inhibitor of mTOR, we do not observe the same trend. The means in both knockdown cell lines are lower, but have not been evaluated as significantly different by the statistical test.

The last treatment with A443654 resulted in again lower levels of mSin1 in both knockdown cell lines, showing a statistically significant difference. The difference is more significant in the knockdown #1 cell line ($p < 0,01$, $n=3$).

Overall these results show, that we were indeed able to create a knockdown cell line, which expresses mSin1 on a significantly lower level. According to these results we consider the cell line knockdown #1 to be stable in reducing mSin1 and therefore competent for further experiments.

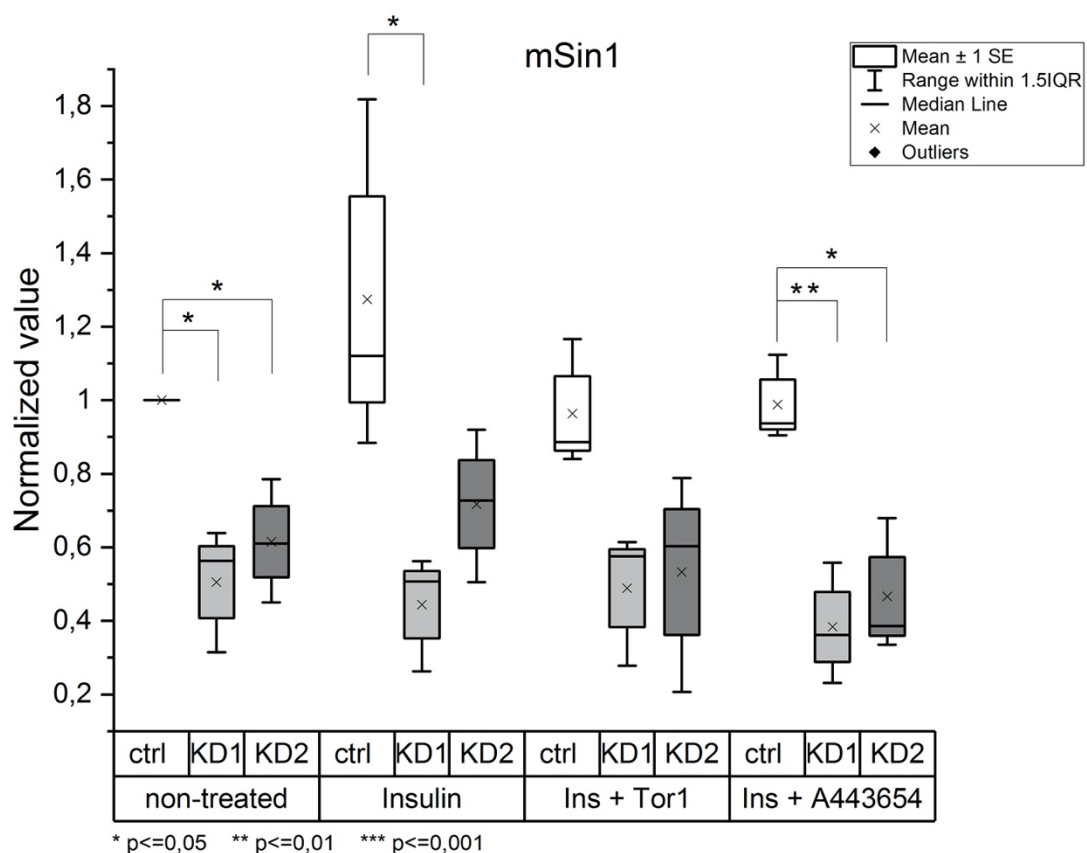


Figure 20: Quantified and normalized levels of mSin1. To examine statistical significance ANOVA test was performed. * - $0.5 \Rightarrow p$ value, ** - $0.01 \Rightarrow p$ value, *** - $0.001 \Rightarrow p$ value, $n=3$. The levels show a dropping trend in the values, when the knockdowns are compared to the control cell line.

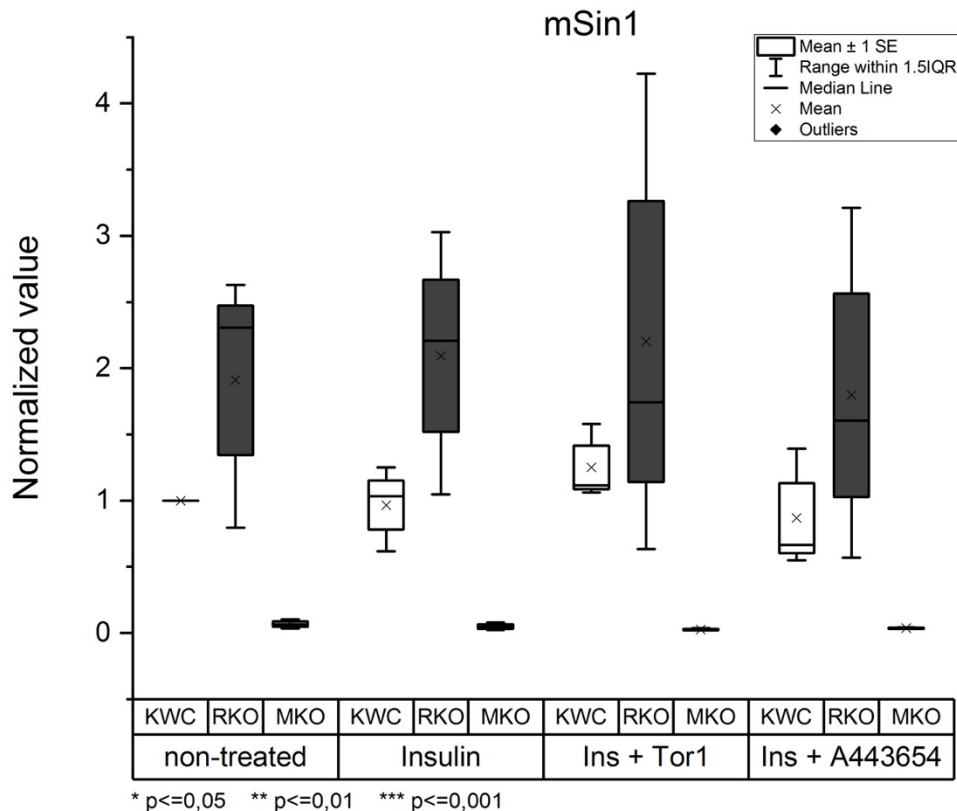


Figure 21: Characterization of KWC, RKO and MKO cell lines. The cells were pre-treated with A443654 (250 nM) or Torin1 (260 nM) for 40 minutes and with for five minutes with 100 ng/mL bovine recombinant insulin. * - 0.5=>p value, ** - 0.01=>p value, *** - 0.001=>p value, n=3.

The quantification of signals on Figure 19 just confirms the observation of the bands intensities. The mSin1 levels in KWC and RKO cell lines remain constant, while the mSin1 levels in MKO cell line remain very close to zero and are quite uniform.

On Figure 22 we see the levels of mTOR in all of the three cell lines (ctrl, mSin1 #1 and #2). mTOR is one of the components of the mTORC2, along with mSin1 and other proteins. The kinase mTORC2 is active only if all of the components are present and only in this case it can phosphorylate its substrate Akt on Serine 473. If only one of the components is missing, the kinase can not perform its role.

In the non-treated cells there is almost no difference between the control cell line and the knockdown #1 cell line. There is a significant drop ($p<0,05$, $n=3$) in the cells of mSin1 #2 cell line. mTOR should be unaffected by knocking down mSin1. However, as we see in the other cells, that were treated with insulin, the levels of mTOR in the knockdown cell lines are lower, as if the cells didn't restore their activity after the treatment with bovine recombinant insulin.

The treatment with mTOR inhibitor Torin1 results in lower levels of mTOR in both knockdown cell lines and leading to a significant drop in the cells of the knockdown #2 cell line ($p<0,05$, $n=3$). On the other hand, we can't observe almost any impact on the cells of the control cell line.

The treatment with A443654 shows again almost no impact on the mTOR levels in the control cell line, but leads to a decrease of mTOR levels in both knockdown cell lines. There is obviously an impact of the expression of mSin1 to the expression of mTOR, another of mTORC2 components. We observed lower levels of mTOR in both of the

knockdown cell lines when compared to the control cell line, which could be indicating, that mSin1 maybe plays a role in the expression of mTOR.

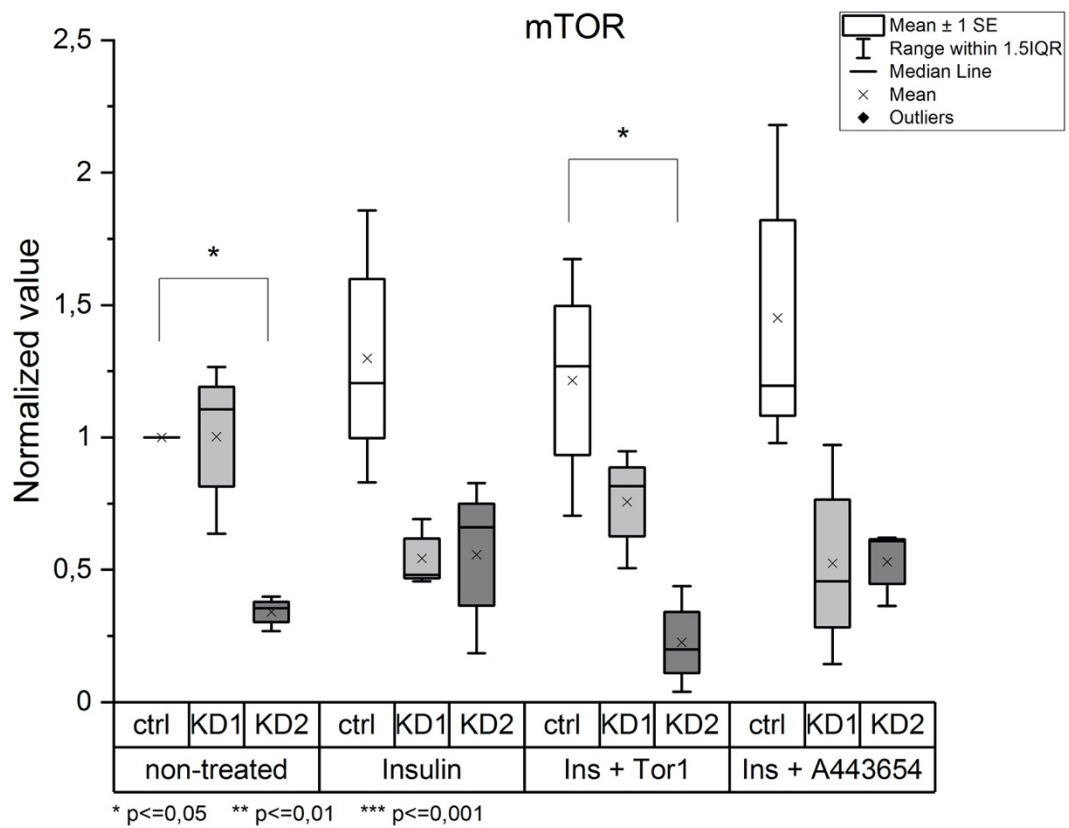


Figure 22: Quantified and normalized levels of mTOR in the control and both knockdown cell lines. To examine statistical significance ANOVA test was performed., * - $0.5 \geq p$ value, ** - $0.01 \geq p$ value, *** - $0.001 \geq p$ value, $n=3$.

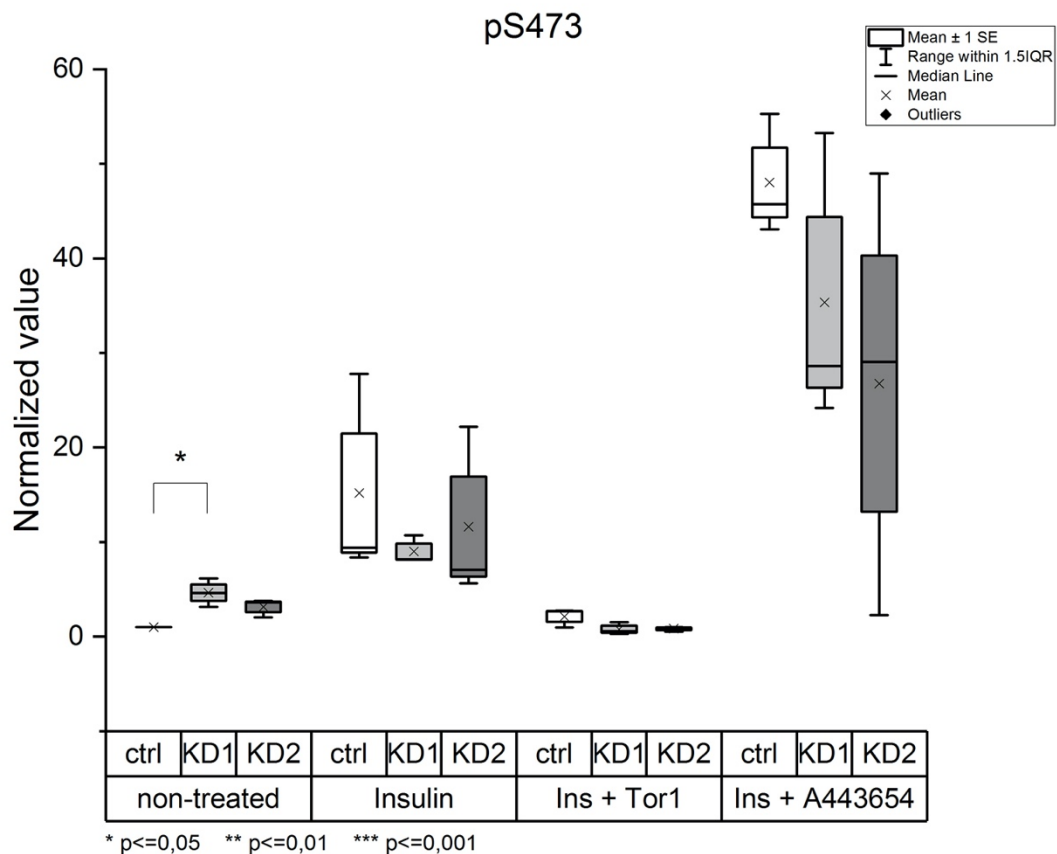


Figure 23: Box plot of quantified and normalized data of Akt-pS473 levels. To investigate statistical significance ANOVA test was performed. * - $0.5 \Rightarrow p$ value, ** - $0.01 \Rightarrow p$ value, *** - $0.001 \Rightarrow p$ value, $n=3$.

To test if the reduced mSin1 levels in shRNA-mediated mSin1 knockdowns and CRISPR-mediated mSin1 knockout we investigated the mTORC2 activity effect on Akt S473. The effects observed in the cell lines are relatively similar. Both insulin and competitive ATP analogue inhibitor of Akt A443654 resulted in the increased phosphorylation of Akt on position 473 (Figure 23). This phosphorylation is lower in both shRNA-mediated mSin1 knockdown cell lines, this reduction is however not significant. In the CRISPR-mediated mSin1 knockout cell lines RKO and MKO treated with A443654 we observed a significant drop in the Akt-pS473 phosphorylation (RKO - $p < 0,01$; $n=3$, MKO - $p < 0,001$; $n=3$)(Figure 24).

By incubating the cells with increasing amounts of serum and in addition with A443654 or GDC-0941 (PI3K inhibitor) we monitored the effect of mTORC2 activity on PI3K-dependent Akt phosphorylation. As we were observed the reduced mTORC2 activity in the mSin1 #1 cell line resulted in lower Akt-pS473 levels for every treatment. These results indicate, that lowered mTORC2 activity (by reduced mSin1) leads to decreased (HeLa, Figure 25; HL60, Figure 24) Akt-pS473 phosphorylation.

The GDC-0941 treatment resulted in reduced phosphorylation of Akt on position S473 in both control and knockdown HeLa cells, demonstrating that the phosphorylation of Akt on S473 is PI3K-dependent.

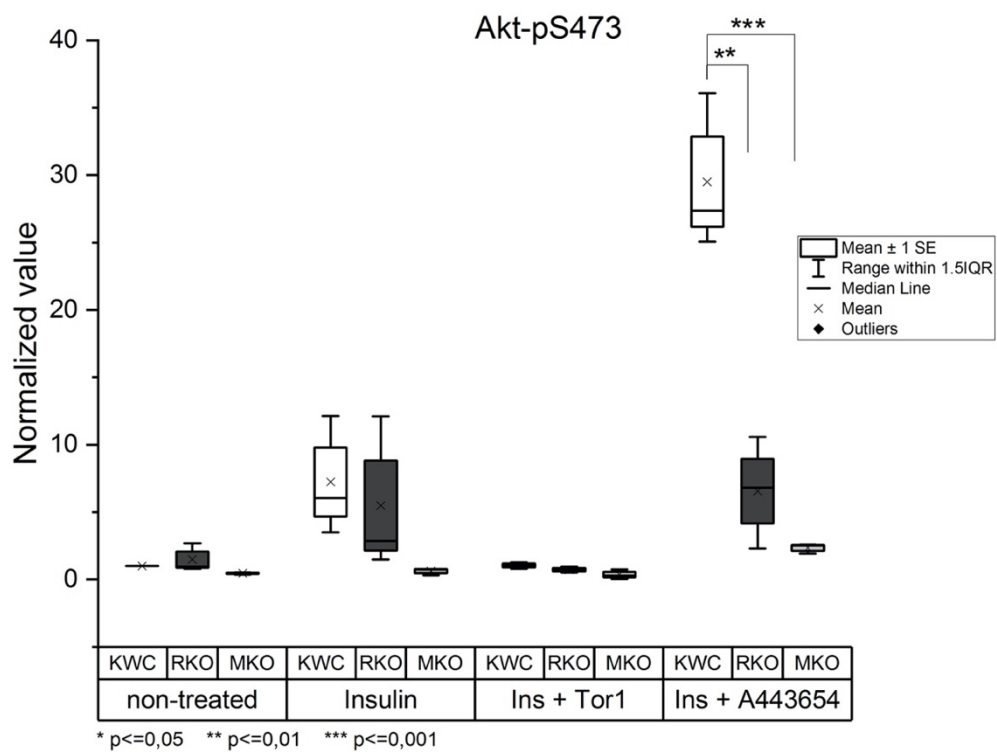


Figure 24: Akt-pS473 levels in KWC, RKO and MKO cell lines. The cells were pre-treated with Torin1 (260 nM) or A444654 (250 nM) for 40 minutes and 100 ng/mL of bovine recombinant insulin for five minutes. * - 0.5=>p value, ** - 0.01=>p value, *** - 0.001=>p value, n=3.

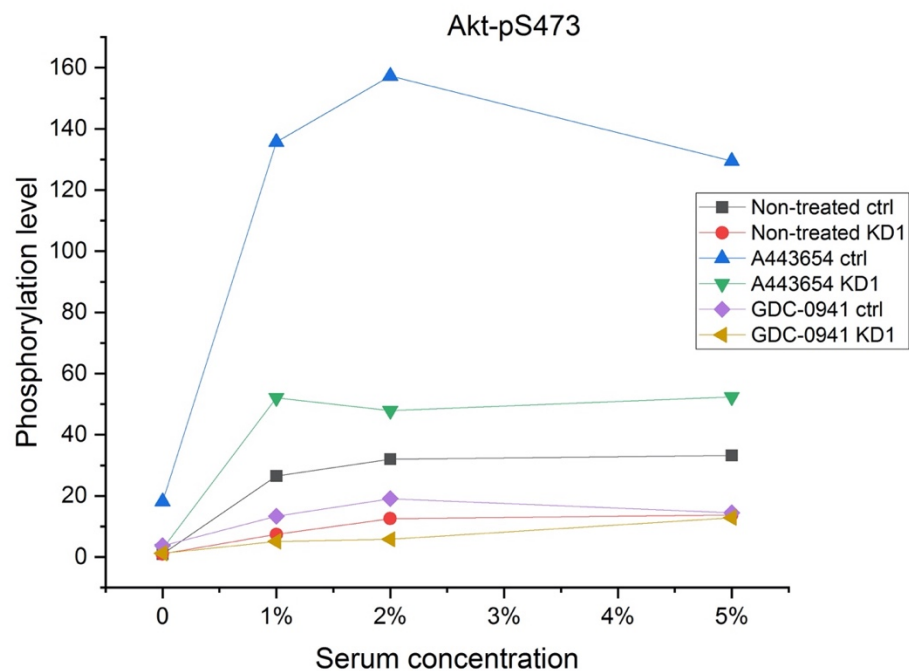


Figure 25: Phosphorylation levels of Akt-pS473 as response to different serum concentration. Plotted are different treatments for both cell lines - ctrl and KD1 (mSin1 #1 knockdown cell line).

To test whether reduced Akt S473 phosphorylation affects Akt T308 phosphorylation and Akt activity we performed the same experiment and determined the phosphorylation levels of Akt T308 in HL60 and the levels of Gsk3 β -ps9 in HeLa. We induced the phosphorylation by incubating the cells with insulin, A443654 and increasing serum concentration. All of these treatments led to an increase of the Akt T308 phosphorylation (hyperphosphorylation in case on A443654) as can be seen on Figure 26. We were not able to observe any reduction in the Akt T308 signal in HL60.

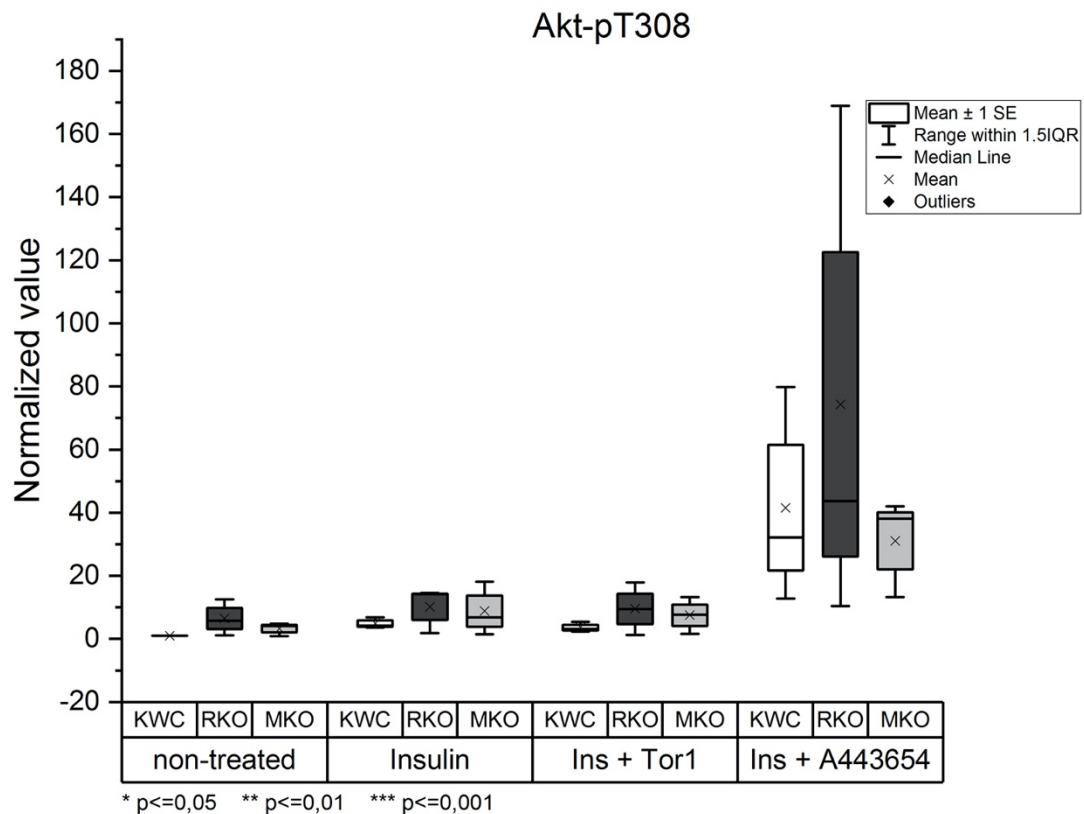


Figure 26: Akt-pT308 quantified levels of KWC, RKO and MKO cell lines, after pre-treatment with Torin1 (260 nM) or A443654 (250 nM) for 40 minutes and 100 ng/ml of bovine recombinant insulin for five minutes. * - $0.5 \Rightarrow p$ value, ** - $0.01 \Rightarrow p$ value, *** - $0.001 \Rightarrow p$ value, $n=3$.

The HeLa cells behave as expected when treated with increasing serum concentrations, A443654 and GDC-0941.

The increasing serum concentration results in increased levels of phosphorylated Akt T308 (Figure 27). The hyperphosphorylation with A443654 and the treatment with GDC-0941 show, that the Akt T308 phosphorylation is, just like Akt S473, PI3K-dependent. Both control and knockdown cells responded to A443654 treatment, however the hyperphosphorylation in the control cells is approximately 2-times higher than in the knockdown cells. Overall the phosphorylation levels of Akt T308 in the control cell line are higher than in the knockdown cell line (Figure 27), which would suggest a connection between Akt S473 and T308 phosphorylation.

However as seen on Figure 26, this behaviour was not observed in the HL60 cells.

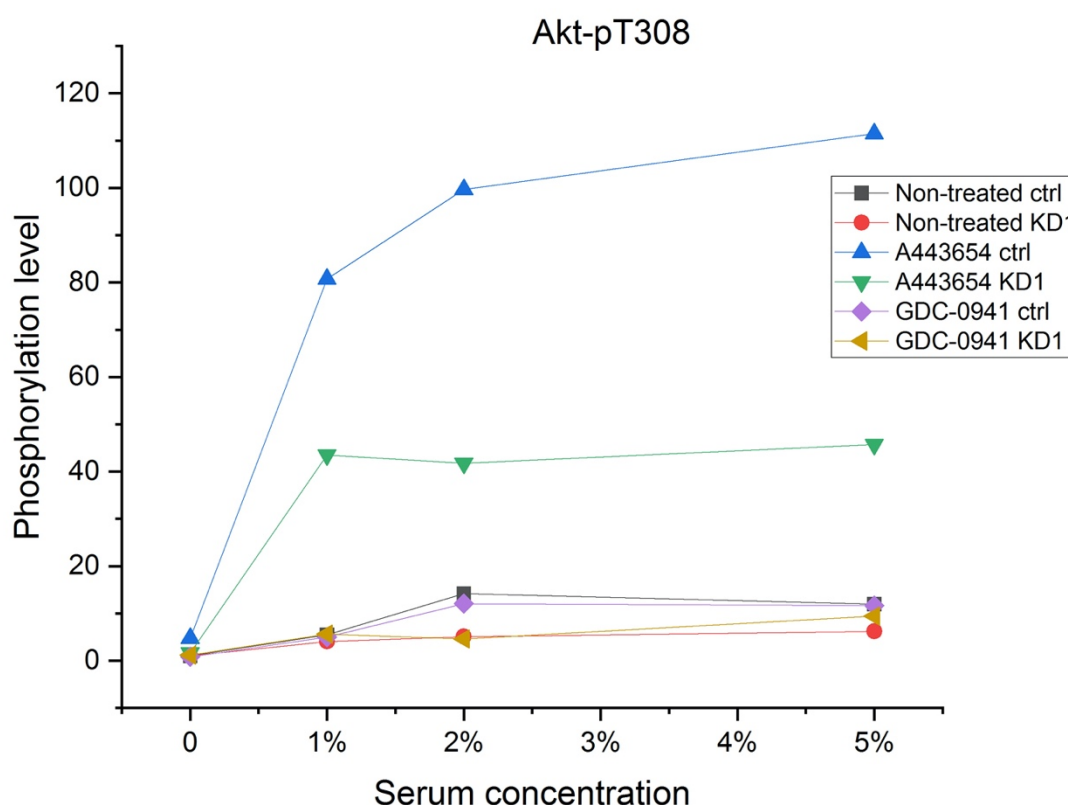


Figure 27: Phosphorylation levels of Akt-pT308 as response to different serum concentration. Plotted are different treatments for both cell lines - ctrl and KD1 (mSin1 #1 knockdown cell line).

We further investigated the effect of reduced Akt S473 phosphorylation on Akt substrate Gsk3 β -ps9. We would expect, that such a reduction would lead to a lower Akt activity, which could mirror on a lower phosphorylation of Gsk3 β on serine 9.

As we observed (Figure 28) the phosphorylation of Gsk3 β -S9 is indeed lower in mSin1 #1 when compared to the control cell line, however not showing any statistical significance. The incubation with insulin led to an increase of Gsk3 β -ps9 levels in the control cell line. Gsk3 β -ps9 levels were reduced after the mTOR treatment as well as after A443654 treatment. The latter inhibits Akt, causing the Akt hyperphosphorylation and leading to no Gsk3 β -S9 phosphorylation.

The treatment with increasing serum concentration corresponded to our expectations. The Gsk3 β -pS9 levels increased with higher serum concentration. The response to the treatments (A443654 and GDC-0941) is also as expected. However the differences between the control and the knockdown cell lines are very small, which indicates, that there is no effect of the phosphorylation of Akt S473 on Gsk3 β -S9 phosphorylation by Akt.

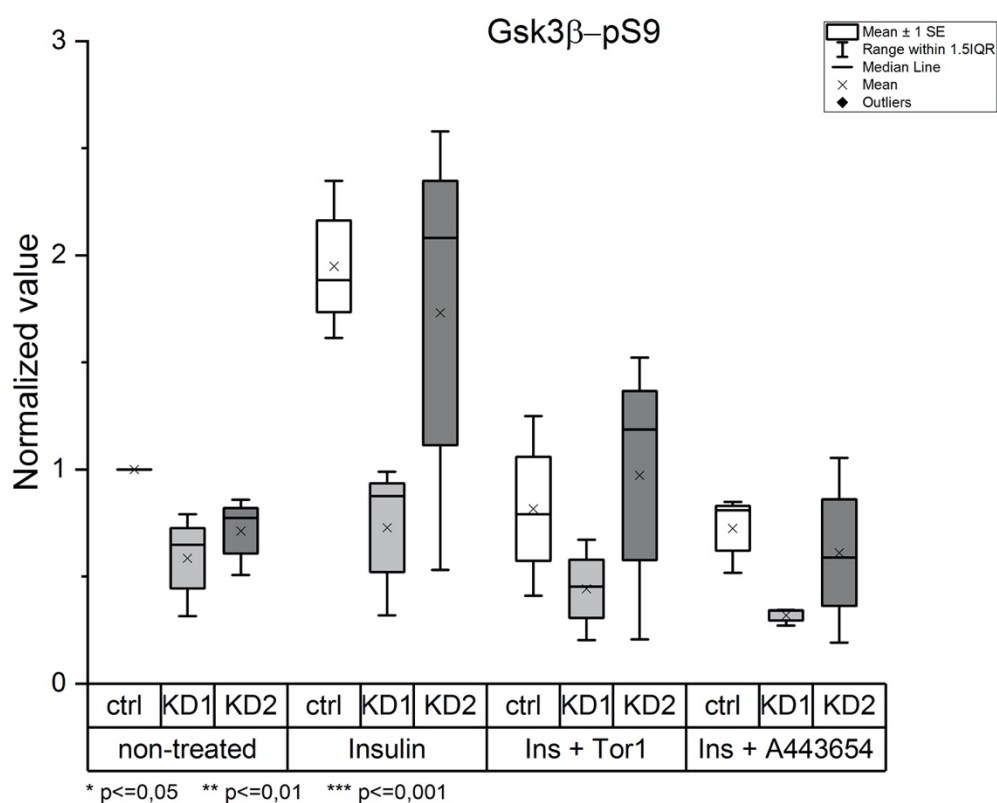


Figure 28: Quantified and normalized levels of Gsk3β-pS9. To examine statistical significance an ANOVA test was performed. * - 0.5=>p value, ** - 0.01=>p value, *** - 0.001=>p value, n=3.

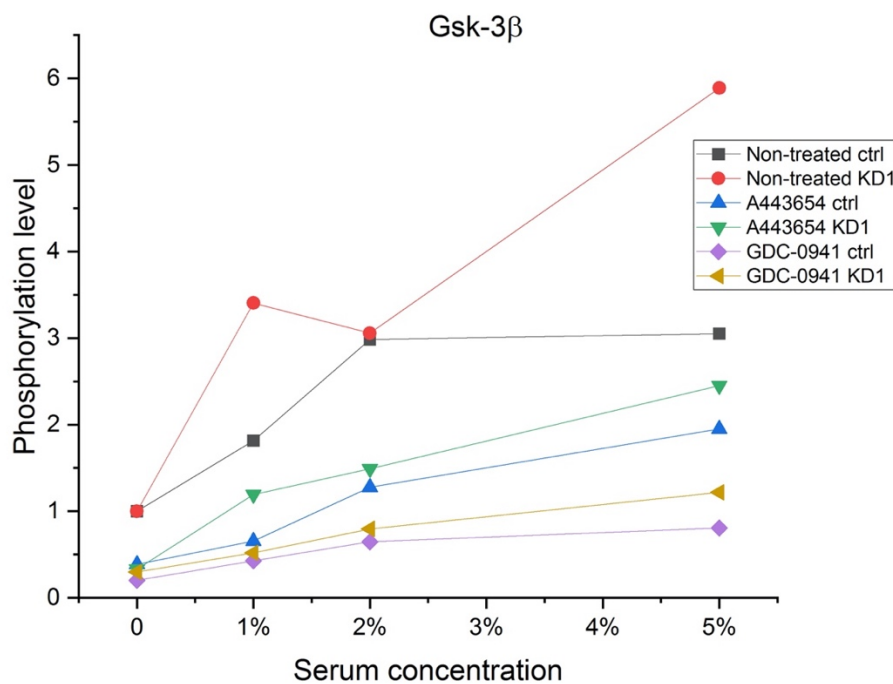


Figure 29: Phosphorylation levels of Gsk3β-pS9 as response to different serum concentration. Plotted are different treatments for both cell lines - ctrl and KD1 (mSin1 #1 knockdown cell line).

To summarize we compared the values from the untreated cells (ctrl, KD1 = mSin1 #1), that were treated with 5% FBS in DMEM (Figure 30).

The differences between the control and knockdown cell line are clearly visible. For Akt-pS473 and pT308 the trend is obviously decreasing, even though not significant. To prove this trend this experiment would have to be repeated more times. The decrease in the Akt S473 phosphorylation seems to cause a very mild decrease in the Akt T308 phosphorylation. The reduction in the Akt S473 phosphorylation does not seem to influence the Akt activity, as it does not seem to affect Gsk3 β -S9 phosphorylation.

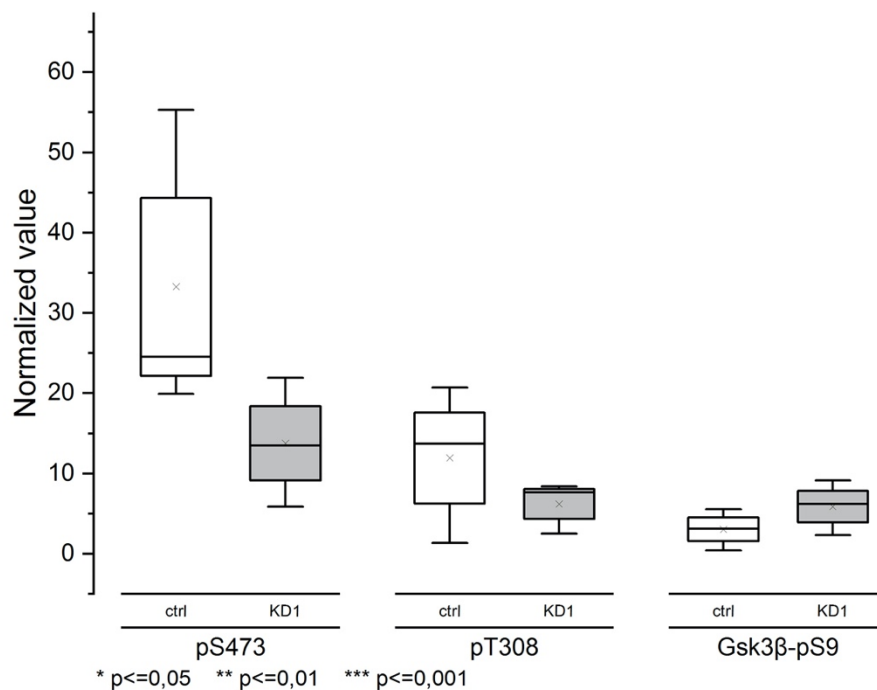


Figure 30: Comparison of the phosphorylation levels of Akt-pS473/pT308 and Gsk3 β -pS9 at 5% serum concentration. The values are from the non-treated cells. * - 0.5=>p value, ** - 0.01=>p value, *** - 0.001=>p value, n=3.

To test if the reduced Akt S473 phosphorylation in the mSin1 #1 cell line affects the dephosphorylation kinetics of Akt-pT308 we pre-incubated the cells with 100 ng/mL bovine recombinant insulin for 5 minutes and 250 nM GDC-0941 for different times, to observe the dephosphorylation effects.

The cells were lysed with a RIPA buffer, containing a cocktail of phosphatase inhibitors. The samples were sonicated and heated with SDS sample buffer to run in a gel.

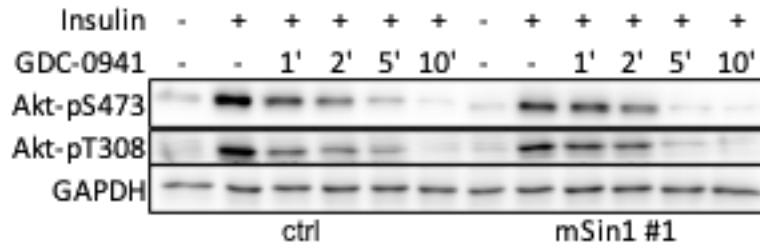


Figure 31: Results of the pre-treatment with human recombinant insulin and PI3K inhibitor GDC-0941. The treatment with insulin was performed for 5 minutes. To follow the dephosphorylation of Akt on positions S473 and T308 the samples were incubated with the corresponding antibodies. GAPDH was used as a loading control.

As we can see on Figure 31 we were able to trigger a dephosphorylation by incubating the cells with GDC-0941. By a closer look at the untreated cells we can see a difference in the phosphorylation of Akt on position S473. The signal is stronger in the control cell lines, than it is in the knockdown 1 cell line, showing, that our knockdown 1 cell line is indeed producing reduced amounts of mSin1 and therefore creating reduced amounts of mTORC2, which is then resulting in reduced S473 phosphorylation on Akt. If we compare the untreated cells phosphorylation levels of T308 we can not see a big difference. This would meet our expectations, as the phosphorylation of T308 should be unaffected by knocking down Sin1.

Furthermore we see, that the longer incubation time with GDC-0941 leads to a higher dephosphorylation on both positions. This means that GDC-0941 inhibits PI3K and therefore activation of Akt, as expected.

To examine the dephosphorylation rate we normalized the values of phosphorylation to the phosphorylation level of insulin-induced Akt. We fitted both datasets to a model with exponential decay and determined dephosphorylation half-time (Figure 32Figure 34). From this equation we were able to determine the halftime of dephosphorylation of Akt-pS473, which is 3,61 minutes and 2,75 minutes for control and knockdown 1 cell line respectively. In case of T308 the dephosphorylation in the control cell line was 4,10 minutes and 2,92 minutes in the knockdown cell line. This could suggest, that reducing Akt-S473 phosphorylation affects the dephosphorylation kinetics of Akt-pT308.

However we observed, that the exponential decay does not fit the data very well. Therefore we plotted the data on a semilogarithmic scale, where we expected the exponential decay to become linear. This is indeed the case for the shRNA-mediated knockdown cell line (Figure 33Figure 35) suggesting, that the knockdown cell line fits a monoexponential decay model. On the other hand the control cell line shows an exponential decay even after plotting in the semilogarithmic scale meaning, that the dephosphorylation of Akt-pS473 and -pT308 follows a biexponential decay.

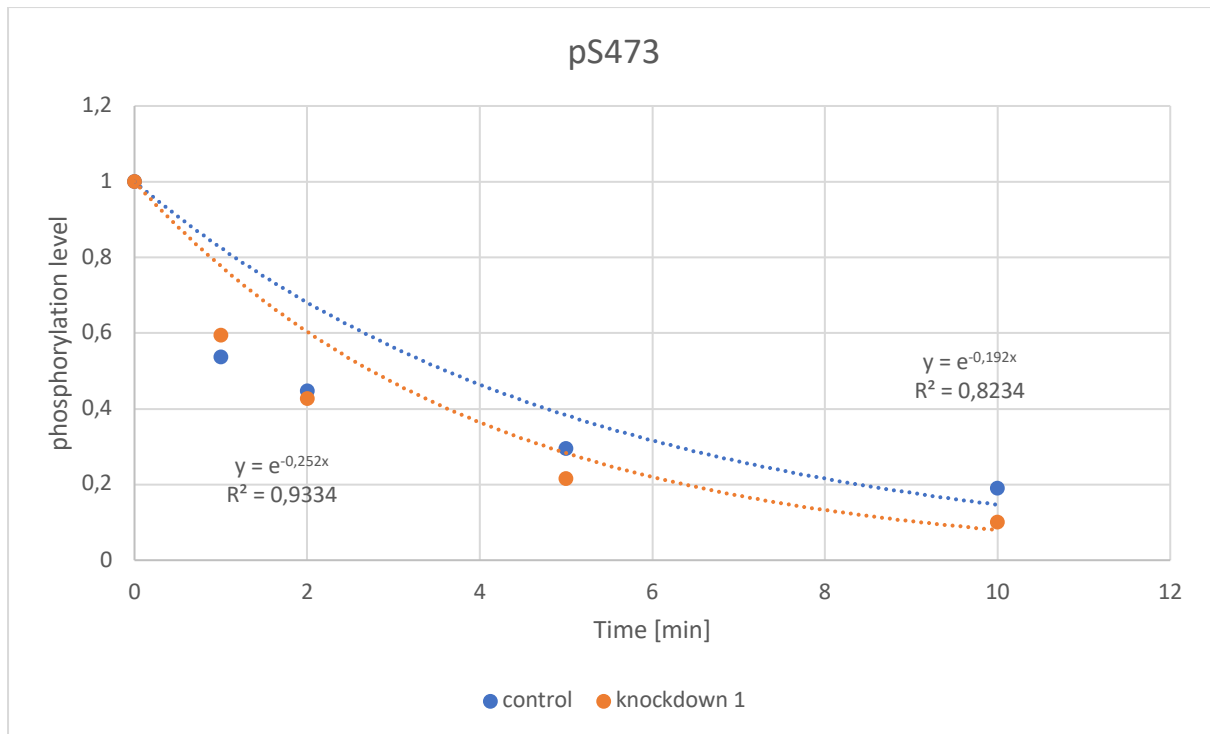


Figure 32: Dephosphorylation of Akt-pS473 after incubation with GDC-0941 for 1, 2, 5 and 10 minutes. Exponential trendlines were added (dashed lines) in order to determine the half time of the dephosphorylation.

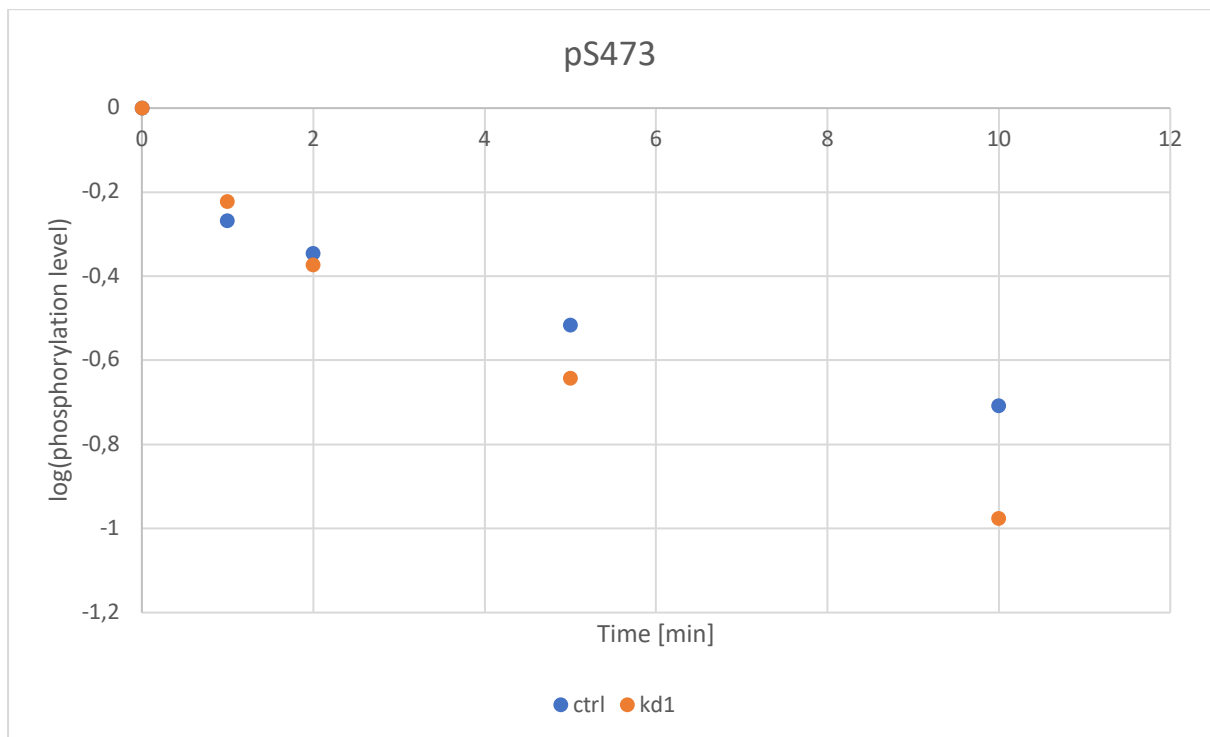


Figure 33: Dephosphorylation of Akt-pS473 after incubation with GDC-0941 for 1, 2, 5 and 10 minutes on a semilogarithmic scale.

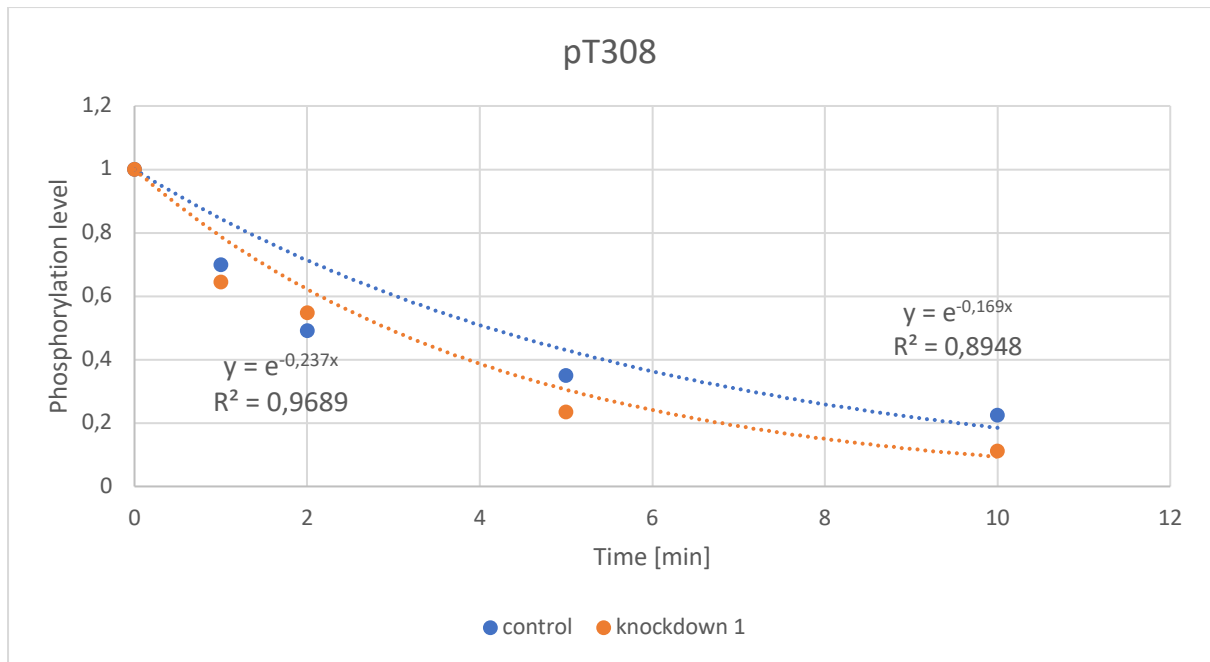


Figure 34: Dephosphorylation of Akt-pT308 after incubation with GDC-0941 for 1, 2, 5 and 10 minutes. Exponential trendlines were added (dashed lines) in order to determine the half time of the dephosphorylation.

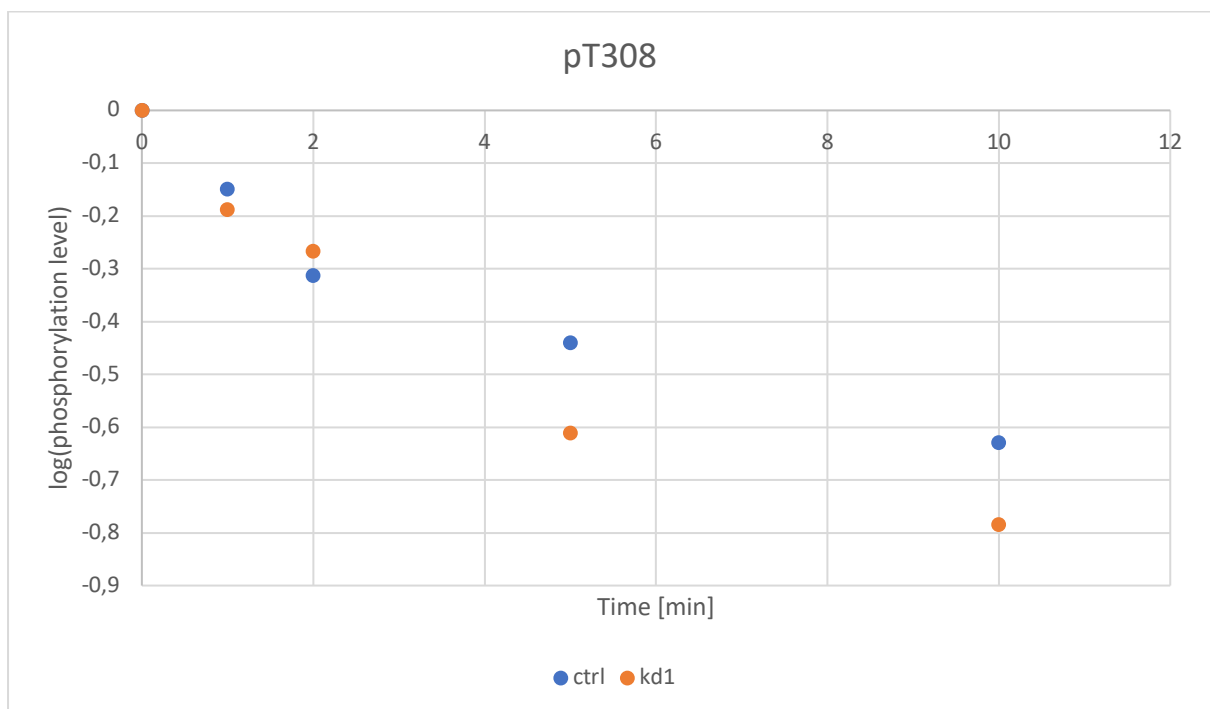


Figure 35: Dephosphorylation of Akt-pT308 after incubation with GDC-0941 for 1, 2, 5 and 10 minutes on a semilogarithmic scale.

We have shown, that the shRNA-mediated HeLa knockdown cell line 1 and the CRISPR-mediated knockout HL60 cell line are indeed expressing reduced (HeLa) to no (HL60) mSin1. This reduction doesn't seem to have an effect on another mTORC2 components (mTOR), but results in lower levels of Akt-pS473 in both cell lines. The effect of reduced Akt-pS473 does not reflect on Akt-pT308 or Akt substrate Gsk3 β . We were able to observe minor decrease in Akt-pT308 in HeLa and HL60, however we can not strictly say, if this is caused by reduced phosphorylation on Akt S473.

Akt S473 phosphorylation seems to have a minor effect on Akt-pT308 dephosphorylation, as seen on the half-times of T308 dephosphorylation.

As these differences are minimal and they vary between the experiments we think it is needed to repeat these experiments multiple times in both cell lines.

We concluded, that cell lines mSin1 #1 and HL60 MKO and RKO indeed express reduced levels of mSin1 and can therefore be used for further experiments concerning the mitochondrial isolation and investigating the effects of mitochondrially targeted mSin1 on other mTORC2 components.

Development of mitochondrial-localized mSin1

As we wanted to investigate the effects of mTORC2 on mitochondria, we decided to create mitochondrially localized mSin1. For this purpose we chose three isoforms of mSin1 - 2, 4 and 5. These three isoforms localize to the endosomes, plasma membrane and nucleus respectively. Therefore to our advantage we were able to verify the translocation from the original organelle to mitochondria by comparing the location of the isoforms and the location of the new constructs. In addition isoform 4 does not come naturally in mTORC2. We targeted the isoforms to mitochondria by cloning the mitochondrial membrane protein Bcl-xL to the isoforms. We further wanted to investigate if the isoforms are able to recruit other mTORC2 components to mitochondria.

mSin1 as one of the crucial components creating mTORC2 exists in form of six different isoforms. These isoforms localize variously around the cell. To pursue and visualize the exact compartments of the cell, to which the isoforms locate, we cloned markers, such as eGFP and mCherry, into the plasmids expressing mSin1 isoforms 2, 4 and 5. These clones can then be visualized with the help of a confocal microscope. First we created the Isoform 2 fused with the red fluorescent protein mCherry. For this purpose the vector N1 was used. For the insertion of the marker the restriction enzymes BsrG1 and Not1 were used. The insert and the vector were separated on an agarose gel, the corresponding bands were cut out and ligated. The resulting vector, expressing the corresponding isoform fused with the corresponding fluorescent protein, were sequenced at Microsynth AG. In this way we obtained isoforms 2, 4 and 6 fused to mCherry (Isoforms 2 and 5) and eGFP (Isoform 4). Such vectors were then transfected into HeLa cells for 24 hours. For visualization the laser scanning confocal microscope LSM700 was used.

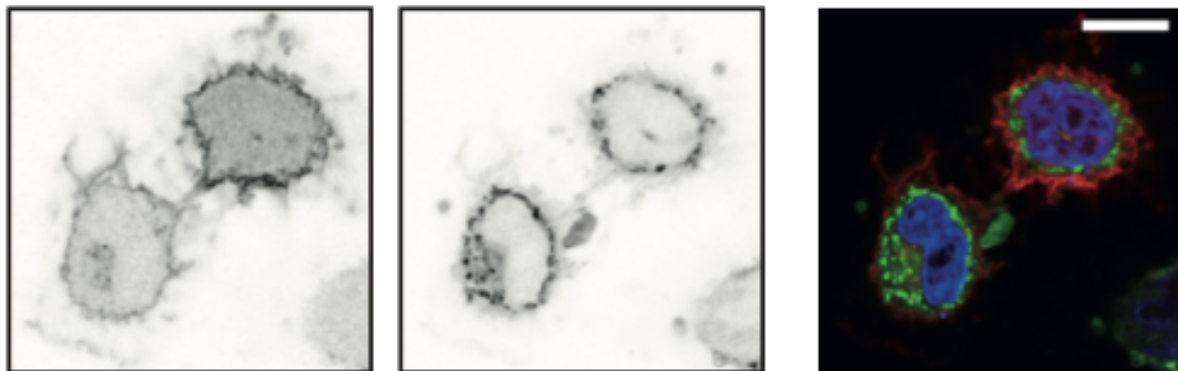


Figure 36: Localization of mSin1 isoform 2 (construct mSin1.2-mCherry). *red* - mSin1.2-mCherry, *blue* - nucleus, *green* - mitoTracker green. The BW pictures show (from left to right) the construct and the mitotracker.

As can be seen on Figure 36, the isoform 2 of mSin1 localizes to the cellular membrane and to some cellular endosomal vesicles. This can be seen as the red colour, coming from the mCherry fluorescent protein. This localization can be also observed on the black and white pictures, taken from the same cells. In addition, the cell nucleus was also stained with DAPI, resulting in blue colour. To visualize mitochondria of the cells, the mitotracker green was used. We can see the mitochondria being located in the proximity of the nucleus and we don't see any overlapping of the mSin1.2-mCherry with the mitochondrial tracker or the nucleus. The Figure 37 represents the localization of another mSin1 isoform, isoform 4. This isoform was fused with eGFP, which results in the green colour. For the visualization

of mitochondria the mitotracker orange was used, to ensure the not overlapping or similarity of the stainings used. The isoform 4 localizes exclusively to the plasma membrane of the cell. There is also no overlapping of the isoform 4 and mitochondria visible on the taken pictures.



Figure 37: Localization of mSin1 isoform 4 (construct mSin1.4-mCherry). *green* - mSin1.4-eGFP, *orange* - mitotracker orange. The BW pictures show (from left to right) the construct and the mitotracker.

The localization of the mSin1 isoform 5 leads us to the cellular nucleus. As can clearly be recognized on Figure 38, the mSin1.5-mCherry localizes in the nucleus, showed as the overlapping of the nuclear DAPI staining and the signal emitted by the isoform 5 resulting in the pink colour. Again, no overlapping with the mitochondria can be observed. The mitochondria localize to the proximity of the cellular nucleus (Figure 38).

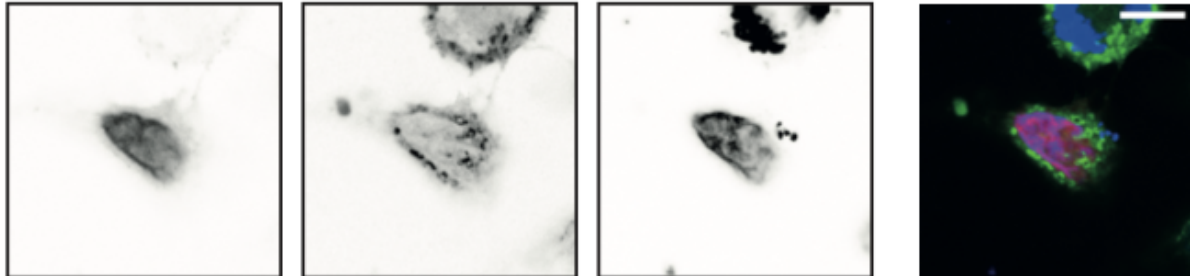


Figure 38: Localization of mSin1 isoform 5 (construct mSin1.5-mCherry). *red* - mSin1.5-mCherry, *blue* - nucleus, *green* - mitotracker green. BW pictures show (from left to right) - the construct, the mitotracker and the nucleus.

Because of our interest in the effect of mTORC2 on mitochondria, we tried to localize the mSin1 isoforms to mitochondria. This was done by fusing the 33 C-terminal amino acids of the mitochondrial membrane protein Bcl-xL to our mSin1 constructs. This, we believed, should help localize the mTORC2 component mSin1 to the mitochondria, which should result in overlapping signals from the constructs and from the mitotrackers, which was indeed the case by all of the three isoforms.

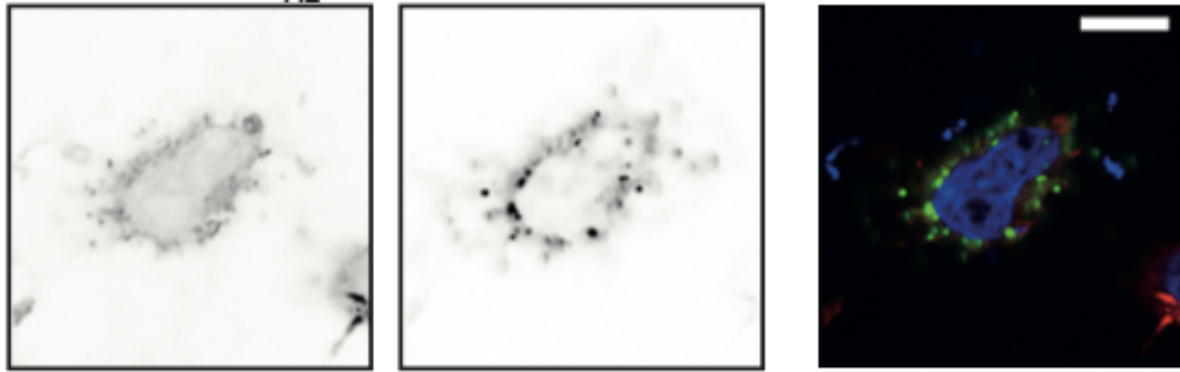


Figure 39: Localization of mSin1 isoform 2 fused with Bcl-xL (construct mSin1.2-mCherry- Bcl-xL). **red** - mSin1.2-mCherry- Bcl-xL, **blue** - nucleus, **green** - mitotracker green. BW pictures (from left to right) - the construct and the mitotracker.

The success of the localizing effect of the Bcl-xL fusion is clearly shown on Figure 39. The fusion of mitochondrial membrane protein Bcl-xL caused a change in the localization of the isoform 2, that is no longer present on the cellular plasma membrane and cellular vesicles, but its signal obviously overlaps with the signal from the mitotracker green, resulting in light green/yellowish colour on Figure 39. The difference between Figure 36 and Figure 39 is obvious.

The same scenario occurred in the case of isoform 4, which was pulled from its initial location on the plasma membrane to the mitochondria. Again, the overlapping signal, in this case formed by the green signal from mSin1.4-eGFP-Bcl-xL and mitotracker orange, resulting in reddish colour in Figure 40. Therefore the relocation of the isoform 4 to the mitochondria, caused by fusion with Bcl-xL, can be considered successful.

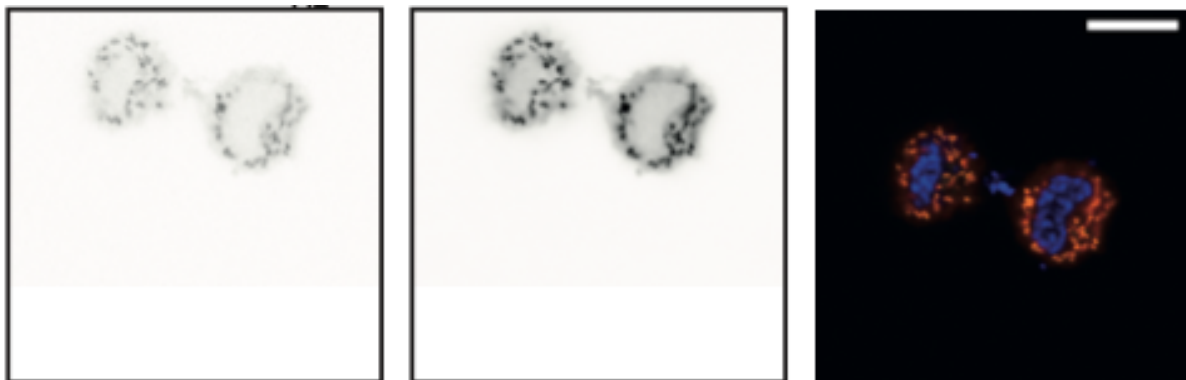


Figure 40: Localization of mSin1 isoform 4 fused with Bcl-xL (construct mSin1.4-eGFP- Bcl-xL). **green** - mSin1.4-eGFP- Bcl-xL, **blue** - nucleus, **orange** - mitotracker orange. BW pictures (from left to right) - the construct and the mitotracker.

The BW pictures also show the localization of the construct as well as the mitotracker. By looking and comparing the two pictures separately, it can be clearly recognized, that both are localized in the same parts of the cell.

Lastly for the isoform 5, the Figure 41 shows, that we were able to translocate it from the nucleus to the mitochondria as well. The attachment of Bcl-xL to the construct results in the overlapping of the mCherry signal of the construct and the green signal of the mitotracker. This is shown as light green/yellowish colour, just like in the case of isoform 2. The vast majority of the isoform 5 relocated from its original location, from the nucleus, to the mitochondria.

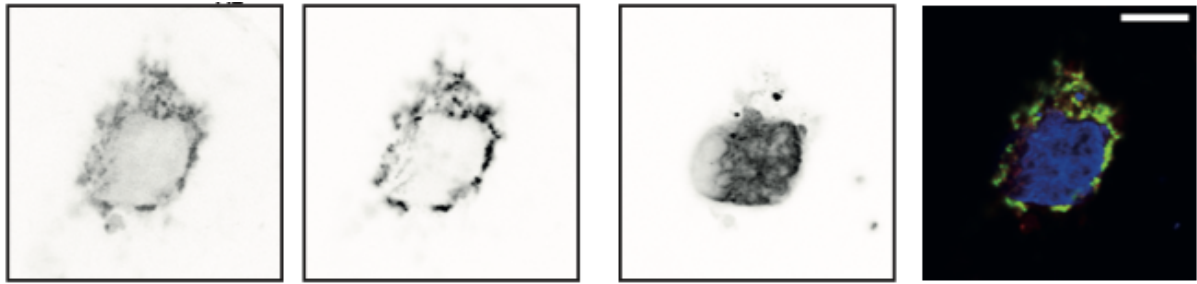


Figure 41: Localization of mSin1 isoform 5 fused with Bcl-xL (construct mSin1.5-mCherry- Bcl-xL). *red* - mSin1.5-mCherry- Bcl-xL, *blue* - nucleus, *green* - mitotracker green. BW pictures (from left to right) - the construct, the mitotracker and the nucleus.

The previously shown Figures prove, that we were able to successfully not only localize the different isoforms of mTORC2 component mSin1, but also to target them to the mitochondria, where we want to study their function and ability to recruit other components of mTORC2 to mitochondria by isolating and characterizing the mitochondria from different cell lines.

Characterization of mitochondrial mTORC2

After successfully creating mSin1 constructs localizing to mitochondria, our next step was to isolate mitochondria from HeLa and HL60 cell lines and compare the possible depletion of mTORC2 components mSin1 and mTOR in the shRNA-mediated knockdown and CRISPR-mediated knockout cell lines and the corresponding control cell lines.

The cellular and mitochondrial fraction were ran on an agarose gel and transferred on a nitrocellulose membrane.

The resulting bands of the western blot can be seen on Figure 42 and Figure 43. The membranes were incubated with four different antibodies - SLC25A, mTOR, mSin1 and GAPDH.

SLC25A5 is a gene coding for ATP/ADP Translocase 2 protein, which works as an antiporter for ADP/ATP exchange between mitochondrial matrix and cytoplasm. The anti-SLC25A5 antibody localizes to mitochondria and is therefore enriched in the mitochondrial fraction.

In order to take a look at the presence of mTORC2 components in mitochondria the membranes were also incubated with mTOR and mSin1. GAPDH was used as a cell lysate marker.

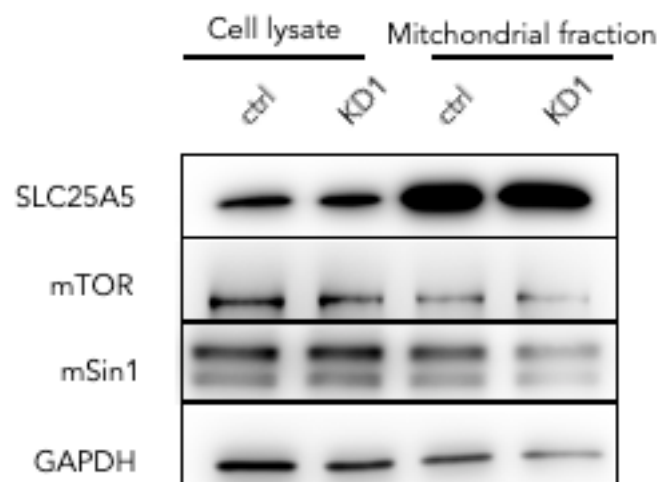


Figure 42: Results of the isolation of mitochondrial fraction of both cell lines, analyzed with western blot.

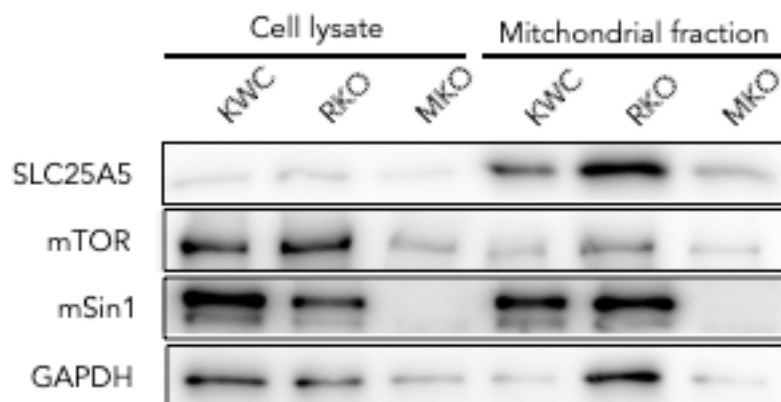


Figure 43: Isolation of the mitochondrial fraction of HL-60 cells.

To verify the mitochondrial enrichment in the mitochondrial fraction we normalized the SLC25A5 signals to GAPDH. Figure 44 and Figure 45 clearly show an enrichment of

SLC25A5 in the mitochondrial fraction for the control cell lines as well as for knockdown (mSin1 #1 = KD1 and both knockout cell lines (RKO, MKO)). These results along with the observations on the membranes (Figure 42, Figure 43) demonstrate, that we were indeed able to isolate mitochondria from the cells of all the cell lines and that the protocol of mitochondrial isolation works for both adherent and suspension cells.

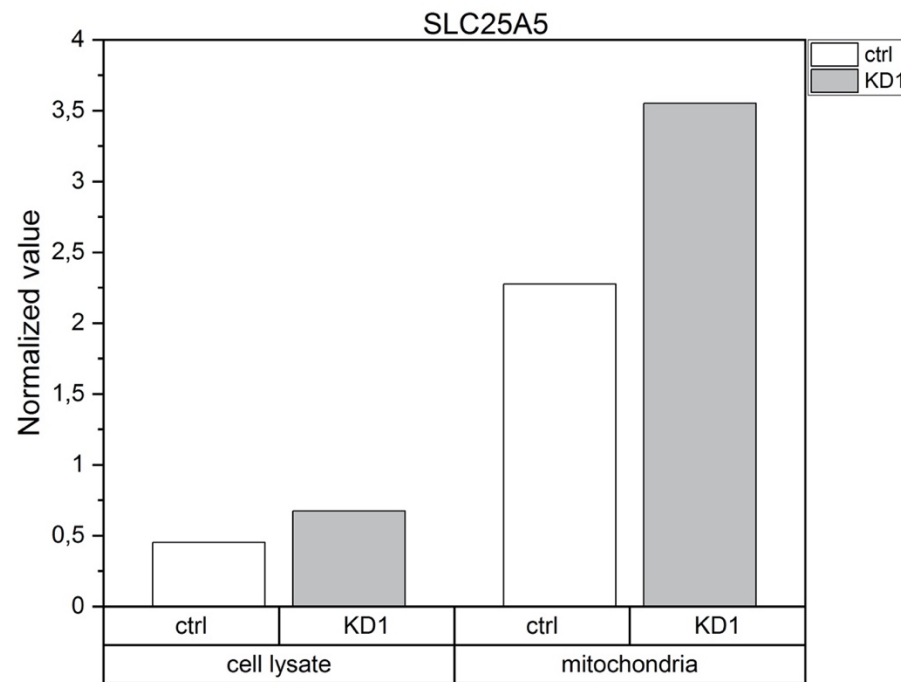


Figure 44: Enrichment of mitochondrial marker SLC25A, normalized to the cell lysate marker GAPDH, in both HeLa cell lines.

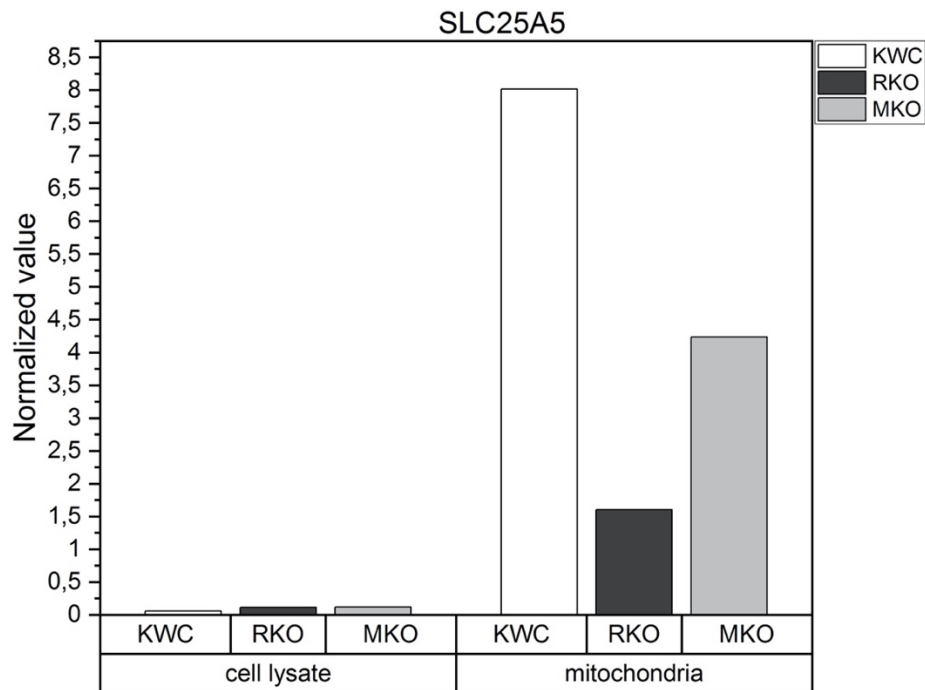


Figure 45: Normalized values of the mitochondrial marker SLC25A5 to GAPDH for KWC, RKO and MKO.

Next we compared the levels of mTORC2 (mSin1, mTOR) components in the mitochondria. The effect of the shRNA on the levels of mSin1 was demonstrated previously, therefore we expected lower to none levels of mSin1 in the mitochondria. As we are able to observe on Figure 42, Figure 43 this is indeed the case.

The quantification of the signals proves the observation. The intensity of the mSin1 bands in the knockdown cell line and RKO in the cell lysate and in the mitochondrial fraction is reduced in comparison to the control cell line and the band disappears completely in MKO (Figure 46Figure 47).

On the other hand the levels of mTOR in the mitochondrial fraction do not correlate with the mSin1 levels. The depletion of mSin1 in mSin1 #1, RKO or MKO cell lines does not reflect in depletion of mTOR. An interesting fact is, that the CRISPR-mediated rictor knockout cell line (RKO) seems to have less mSin1 in the mitochondria. This could possibly mean, that no expression of rictor causes a reduction in the expression of mSin1.

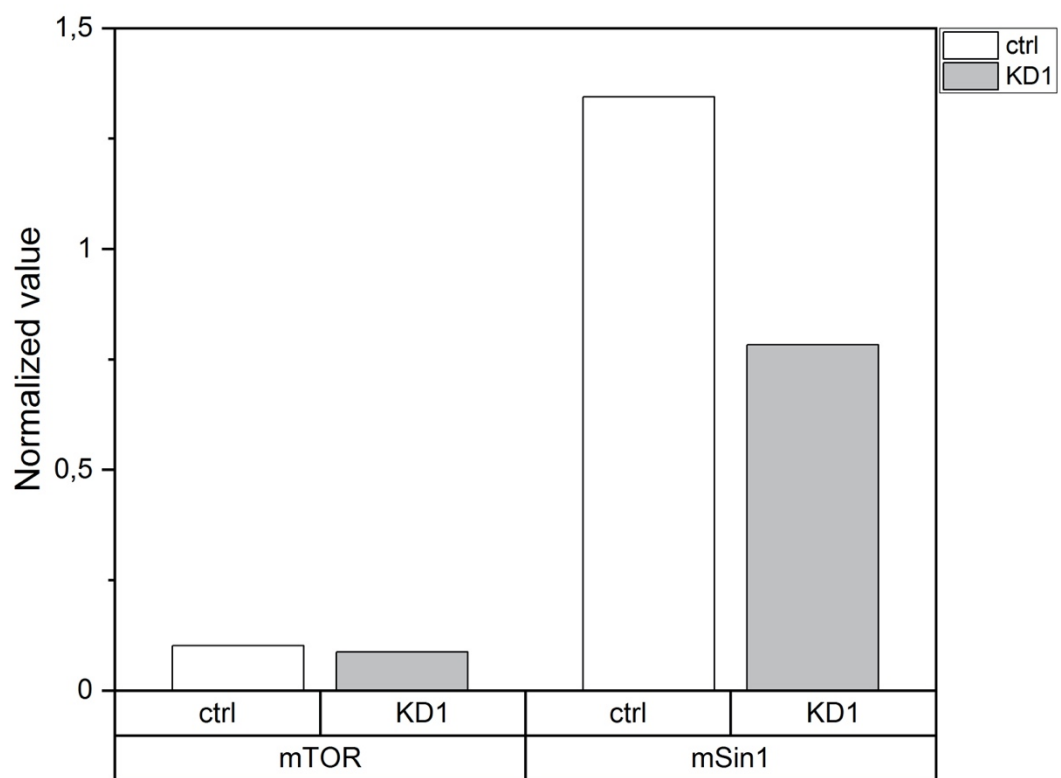


Figure 46: Comparison of mTORC2 components in the mitochondrial fraction of HeLa cells. .

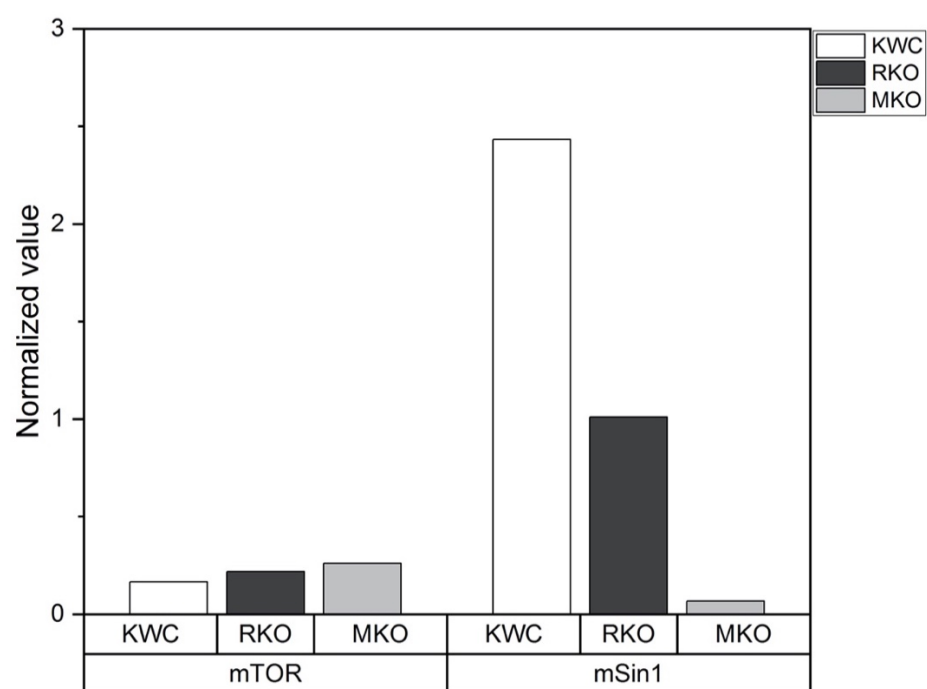


Figure 47: Normalized values of mTORC2 components in the mitochondrial fraction of HL60.

Overall the protocol, which was followed in order to isolate the mitochondria, is working for these cell lines, as can be seen on the enrichment of the mitochondrial marker SLC25A5.

A direct comparison between the cell lysate and the mitochondrial fraction is not possible, as there is no marker, that would be expressed in both cellular compartments. The intensity of the bands can be compared and as such it corresponds to the expectation.

We were able to demonstrate the reduced levels of mSin1 in the mitochondrial fraction, but we were not able to determine any correlation between mSin1 and mTOR levels in the mitochondria, but we observed a possible effect of rictor on the expression of mSin1, which could be a subject to future experiments.

Supposing, that one component of mTORC2 could direct or pull other mTORC2 components to its location and therefore assemble the whole protein complex at this location means, that for determination of mTORC2's role in mitochondria, one of its components needs to be moved there. Attaching Bcl-xL to mSin1 isoforms led to mitochondrial localization of such new constructs. Transfecting the cells with the constructs, isolating their mitochondrial fraction and then analyzing them with a western blot should show, if the constructs are able to pull other mTORC2 components (mTOR) to the mitochondria, resulting in enrichment of this protein in the fraction.

Both cell lines were first transfected with two mSin1 isoforms - 1.4 and 1.5. After exchanging the medium in the cells for overnight growth, the mitochondrial fraction was isolated and the samples were analyzed with western blot.

The visualized western blot bands are pictured on Figure 48. We can see an enrichment of SLC25A5 in the mitochondrial fraction, suggesting a successful mitochondrial isolation.

mTOR levels seem to be higher in the mitochondrial fraction, which could be caused by still present cell lysate in the fraction or by successful pulling of mTOR by Bcl-xL construct. For a more complex evaluation a quantitation and normalization of the band intensities is needed.

The mSin1 levels appear to be lower in the cleared cell lysate, than in the mitochondrial fraction. The bands of the cells transfected with mSin1.5 isoform show stronger signal, than the ones transfected with mSin1.4. This could be due to the used anti-mSin1 antibody, which (as known from previous experiments) doesn't bind the mSin1.4 isoform.

Both isoforms are tagged with a GFP-tag. The incubation with anti-GFP antibody shows stronger signals in the mitochondrial fraction, where the construct containing the tag and Bcl-xL should be located. The weaker bands in the cell lysate are due to a not full-scaled isolation of mitochondria, as can be seen on bands of SLC25A5 in the cell lysate.

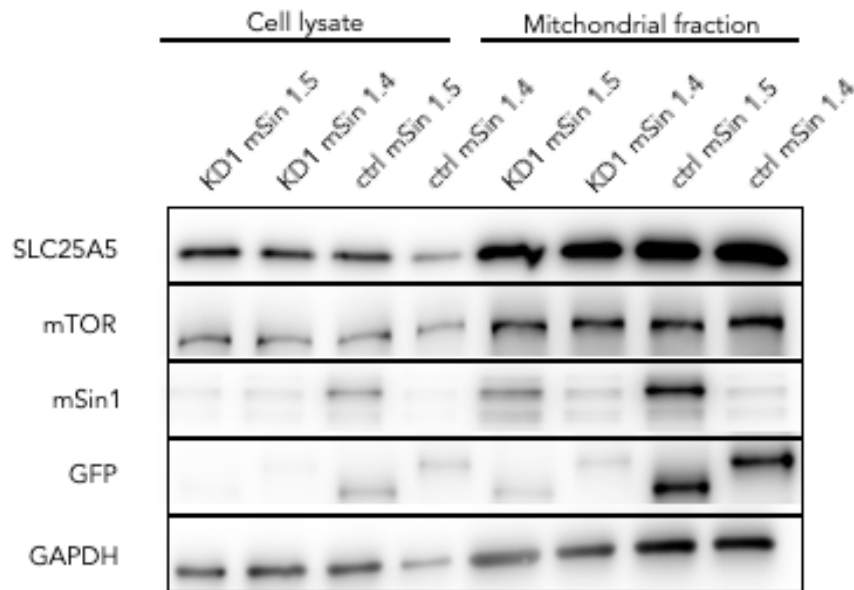


Figure 48: Western blot analysis of transfected cell lines, from which the mitochondrial fraction was isolated.

For a better look at the enrichment of SLC25A5 marker or mTORC2 components the intensities of the bands were quantified and normalized to GAPDH.

The enrichment of SLC25A5 can be also seen on Figure 49. The normalized values show an enrichment of SLC25A5 in the mitochondrial fraction for both cell lines and for both transfections. The higher values of the mitochondrial marker indicate a successful mitochondrial isolation, however as can be seen on Figure 49 the mitochondrial isolation worked better in the control cell line, where the differences in SLC25A5 levels between the cell lysate and the mitochondrial fraction are higher than it is the case of the knockdown cell line.

The mSin1 signals of isoform 4 are in general lower than the ones of isoform 5 (Figure 50). This is probably because of the lacking N-terminus of the sequence, where the epitope of the mSin1 antibody is located. This fact is proven by the even GFP signals of both isoforms. The higher expression of mSin1.5 in the control cell line is due to the stable expression of shRNA in the knockdown cell line, which silences the expression of the transgene.

The main question of this experiment was whether the mitochondrially targeted isoform 5 would be able to recruit mTOR to mitochondria. Our data do not show such recruitment. The depletion of mSin1.5 in the knockdown cell line does not reflect on mTOR levels (Figure 50).

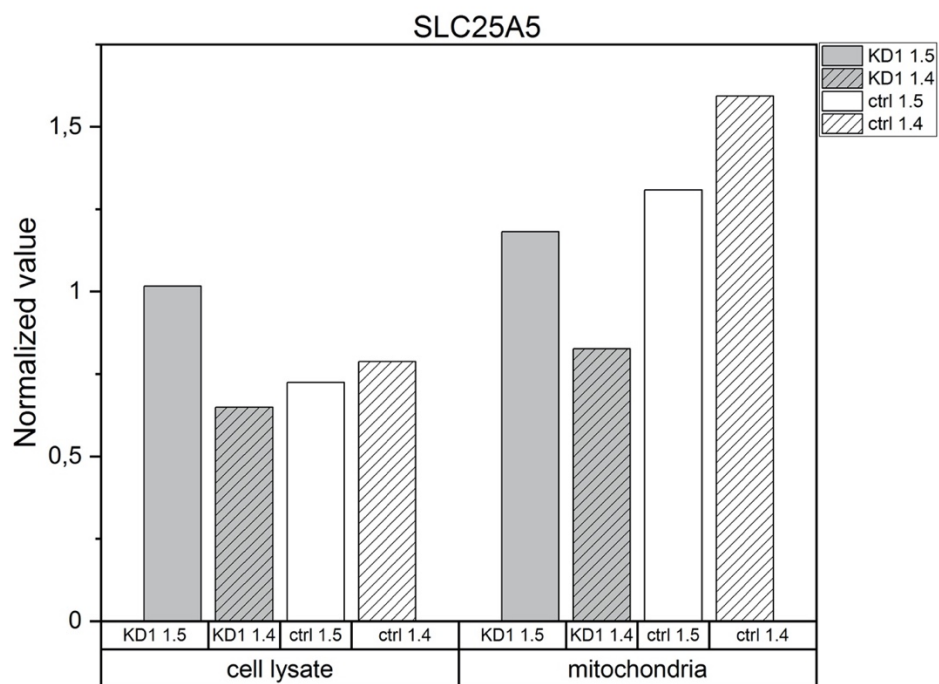


Figure 49: Normalized values of SLC25A5 of both cell lines, which were transfected with mSin1 isoform 4 or 5.

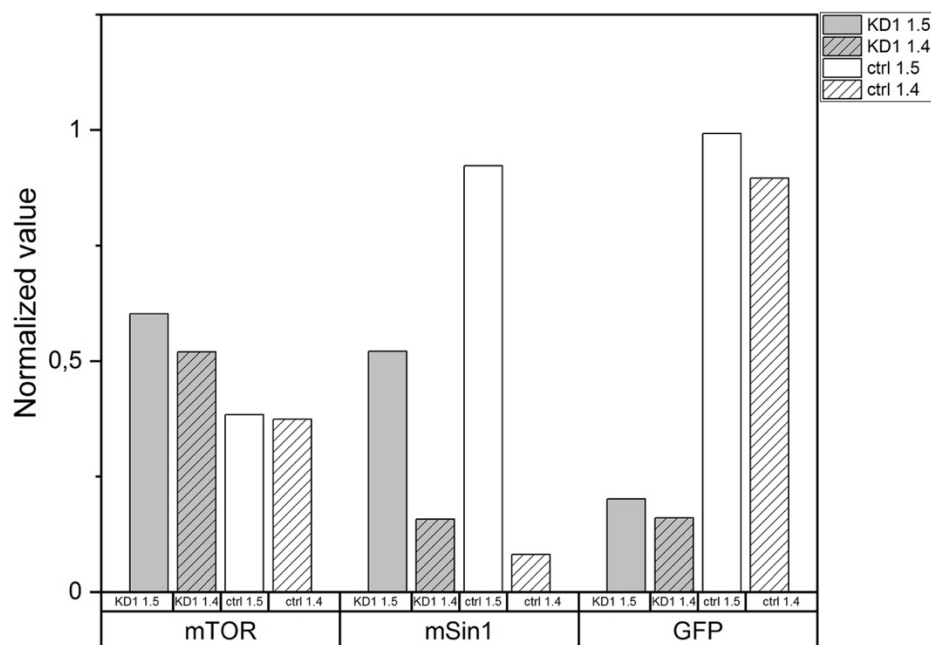


Figure 50: Normalized values of mTORC2 components in mitochondrial fraction of both cell lines transfected with isoforms 4 and 5 of mSin1.

We were not able to determine any recruiting behaviour of mSin1 towards mTOR. The experiment was however performed only once. We successfully isolated the mitochondria and transfected the cells with two different isoforms. On the other hand the isoform 4 is not able to recruit mTOR because of the lacking N-terminus as it is believed it is needed for mSin1-mTOR interaction. The isoform 5 is obviously being silenced by the shRNA.

Therefore the question if mSin1 is able to recruit mTOR (or other mTORC2 components) to mitochondria if it itself is being targeted there remains unanswered.

Conclusion

The long-term goal of this project was to study the role of mTORC2 in mitochondria. We chose the approach of creating a HeLa cell line, which expresses mSin1 (one of mTORC2 components) at a lower level (knockdown cell line). In addition we had a cell line HL-60, which knocks out the gene coding for mSin1 and therefore does not express mSin1 at all. We characterized both of these cell lines.

The investigation on the mSin1 levels in shRNA-mediated mSin1 knockdown HeLa and CRISPR-mediated mSin1 knockout HL60 cell lines resulted in reduced (HeLa) to abolished (HL60) mSin1 levels (Figure 20Figure 21). The knockdown and knockout cell lines do not have an effect on the expression of other mTORC2 component mTOR, as can be seen on Figure 22.

Next we tested the effect of reduced mTORC2 activity on Akt, more specifically on its S473 position. We observed, that mTORC2 has an effect on the phosphorylation of Akt S473. The reduction of mTORC2 activity leads to a decrease in phosphorylation of Akt on serine 473. This we showed on Figure 23, Figure 24Figure 25, where the Akt was either hyperphosphorylated with A443654 or its activity was restored with increasing serum concentration. This had little effect on the Akt S473 in the knockdown and knockout cell lines. We demonstrated, that the phosphorylation of Akt by mTORC2 on S473 occurs in PI3K-dependent manner, as PI3K inhibition by GDC-0941 resulted in reduced phosphorylation of Akt on S473.

To test if mTORC2's phosphorylation of Akt S473 affects the phosphorylation of Akt T308 we determined its levels and performed the same experiment as with Akt S473. We were not able to see a clear effect of S473 reduced phosphorylation on T308 (Figure 26) in the HL60 knockout cells. Based on pure observation of the values we could suspect a reduced T308 phosphorylation as a result of decreased S473 phosphorylation (Figure 27). However the heterogeneity of the results indicates the need of future experiments.

As Akt S473 phosphorylation contributes to the full Akt activation (along with T308) we investigated if reduced Akt S473 phosphorylation leads to lower Akt activity resulting in decreased phosphorylation of its substrate Gsk3 β . The reduction of the S473 phosphorylation didn't lead to a lower Akt activity as the phosphorylation of its substrate Gsk3 β on serine 9 was not decreased as a result of S473 lowered phosphorylation (Figure 28Figure 29).

Next we tried to determine if the Akt-pS473 reduction influences the Akt-pT308 dephosphorylation. We were however not able to observe only a minor change in the dephosphorylation behaviour or rate of Akt-pT308 (Figure 34).

Further we proceeded to the investigation of mitochondrial mSin1 and if such is able to recruit other mTORC2 components, such as mTOR, to mitochondria. For this purpose we first needed to create mSin1, that would localize itself to mitochondria. By fusing a mitochondrial membrane protein Bcl-xL to different mSin1 isoforms (2,4 and 5) and different tags (mCherry and eGFP), we were able to observe and compare the localization of these isoforms around the cell. To test if the fusion worked, samples of all isoforms were sent to sequencing. To validate that the created constructs really do localize to mitochondria, we stained mitochondria with different mitotrackers, so we could observe a possible overlapping of signals. Indeed we observed the localization of all isoforms, with isoform 2 localizing mostly to the plasma membrane and some endosomal vesicles (Figure 36), isoform 4 localizing to the plasma membrane (Figure 37) and isoform 5 localizing to the nucleus (Figure 38). Fusing the Bcl-xL protein to

mSin1 isoforms resulted indeed in the desired effect, overlapping of the mSin1-Bcl-xL signals and mitotracker, showing a clear localization of all mSin1 isoforms to mitochondria (Figure 39, Figure 40, Figure 41).

Having mitochondrially targeted mSin1, our next step was to isolate mitochondria from both cell lines and test the presence of mTORC2 components mTOR and mSin1 in HeLa and HL60 cell lines. To test if the mitochondria really accumulate in the isolated mitochondrial fraction, we analyzed the presence of SLC25A5, a mitochondrial protein. We observed a clear accumulation of mitochondrial protein in the mitochondrial fraction. (Figure 42, Figure 44) mSin1 and mTOR seem to accumulate more in the cell lysate. mTOR levels are constant, not showing almost any difference between control and knockdown cells (Figure 46, Figure 47). mSin1 on the other hand is more expressed in the control cells than in the knockdown/knockout cells, which confirms the shRNA-mediated mSin1 knockdown and CRISPR-mediated mSin1 knockout. Depletion of mSin1 does not seem to have an effect on mTOR (Figure 46, Figure 47). To test if the mSin1 constructs localizing to mitochondria are able to recruit mTOR to mitochondria as well, we transfected the cells of both cell lines with our constructs and isolated the mitochondrial fraction. The higher signals of SLC25A5 prove, that the isolated fractions contain mitochondria. The isolation worked better in the control cell line (Figure 49). Because the isoform 4 of mSin1 lacks the N-terminus, where the mSin1 antibody epitope is located, the mSin1 signal in the cells transfected with mSin1.4 is low. The shRNA against mSin1 silences the expression of mSin1.5 in the knockdown cell line, resulting in higher mSin1 levels in the corresponding control cell line. The GFP signal of both isoforms is relatively even, confirming the inability of the antibody of the mSin1 antibody to bind to the isoform 4 (Figure 50).

mTOR levels are constant and do not vary between control and knockdown cell lines transfected with different isoforms, which suggests no recruitment of mTOR by mSin1.

Outlook

However our results are quite limited. To prove if the transfected cells really do show higher levels of other mTORC2 components, other mTORC2 components, that are exclusive to mTORC2 (rictor) should be analyzed. Rictor as part of the rictor-mTOR complex, that is crucial for mTORC2 assembly should bind to isoform 5 and not to isoform 4. The same experiment could be repeated with other isoforms as well (1 and 2). The biggest difficulty to overcome in this experiment is a relatively big amount of steps (transfection, centrifugation, pipetting, purification), that can devalue the cells.

The next step after the successful transfection and analysis of the isolated material, the analysis of such transfected cells focused on mitochondrial activity (oxygen consumption rate, oxidative phosphorylation) should be performed. This should show the effects of targeted mTORC2 on mitochondrial functions.

The transfection of mSin1 knockout cells (HL60) and a similar analysis would be a great contribution and proof, that the effect is not cell line specific.

Another experiments, which would focus on the influence of mTORC2 on the Akt phosphorylation on position T308, would show if the phosphorylation of S473 on Akt does really have an effect on T308 phosphorylation or if there is a mechanism of cooperation between PDK1 and mTORC2, as our findings are not uniform in this direction. Repeating our experiments could either support or refuse this possibility, as we performed the characterization experiments, dephosphorylation and serum dependency experiments only three times. A higher number of these experiments would lead to a uniformity of the results.

As mTORC2 working mechanisms and sites of action around the cell still remain mostly unclear, it is important to undergo a more detailed research in this field.

Abstract

mTORC2's functions and mechanisms in the cell are mostly unknown. It has been successfully located to the plasma membrane and ER and MAM, so to the close proximity of mitochondria.

To examine the mTORC2's effect on and role in mitochondrial processes we characterized a mSin1 knockdown cell line. We observed reduced mSin1 levels in HeLa and HL60, which didn't have an effect on other mTORC2 component mTOR.

We show, that a uncomplete mTORC2 is not able to phosphorylate Akt on serine 473, which is therefore not fully active. This doesn't necessarily lead to differences in phosphorylation of its substrate Gsk3 β on serine 9. We didn't observe an effect of reduced Akt-pS473 on dephosphorylation of Akt on threonine. Both cell lines (control and knockdown) behave similarly in response to the increasing serum concentration, showing the fastest restoration of activity at around between 0 and 2% serum concentration.

The isolation of the mitochondrial fraction showed low levels of mTORC2 components mSin1 and mTOR in mitochondria, but no correlation between mSin1 and mTOR in control or mSin1 depleted cells.

We successfully created constructs of mSin1 isoforms 2,4 and 5, targeted to mitochondria, by fusing mitochondrial membrane protein Bcl-xL to them. This fusion indeed resulted in mitochondrial localization of these constructs, which were localized to other cellular compartments before.

The transfection of the cells with these constructs followed by the isolation of mitochondrial fraction showed an increased mSin1 presence in the mitochondrial fraction.

For the same purpose we characterized a mSin1 and mRictor knockout HL60 cell line, which led to the same observation on phosphorylation of Akt on position S473. Here the T308 phosphorylation levels remained constant or with very small changes. The mitochondrial isolation in this cell line showed constant levels of mTOR in control, mRictor and mSin1 knockout cells, confirming the observation in the mSin1 knockdown cell line. Reduced mSin1 levels in mRictor knockout cell line, when compared to the control cell line, could suggest a possible dependence of these two mTORC2 components on each other.

Zusammenfassung

Die Mechanismen und die Funktionen des mTORC2s sind bis jetzt meistens unbekannt. Es wurde erfolgreich in der Plasmamembran, ER und MAM nachgewiesen, das bedeutet in der Nähe des Mitochondriums.

Um den Effekt und die Rolle des mTORC2s in den mitochondrialen Prozessen haben wir eine mSin1 knockdown Zelllinie charakterisiert. Wir beobachteten reduzierte mSin1 Spiegel in HeLa und HL60, was keinen Einfluss auf die anderen mTORC2 Komponenten mTOR zur Folge hatte. Wir zeigen, dass ein unvollständiges mTORC2 nicht fähig Akt an der Stelle Serin 473 zu phosphorylieren, was zu einer unvollständigen Aktivierung von Akt führt. Dies führt nicht unbedingt zu Änderungen in der Phosphorylierung von Akt-Substrat Gsk3 β an Serin 9. Wir beobachteten kein Effekt des reduzierten Akt-pS473 auf die Dephosphorylierung von Akt auf der Stelle Threonin 308. Beide Zelllinien (Kontrol- und Knockdown) zeigen ähnliches Verhalten in Abhängigkeit von der steigenden Serumkonzentration, wobei sie die schnellste Wiederherstellung der Aktivität zwischen 0 und 2% Serumkonzentration zeigten.

Die Isolierung der mitochondrialen Fraktion zeigte niedrige Mengen von mTORC2 Komponenten mSin1 und mTOR im Mitochondrium, aber keine Korrelation zwischen mSin1 und mTOR sowohl in den Kontrol- und Knockdown Zellen.

Wir haben erfolgreich Konstrukte aus mSin1 Isoformen 2,4 und 5 hergestellt, die durch Anhängen des mitochondrialen Membranproteins Bcl-xL zum Mitochondrium gerichtet wurden. Dieses Anhängen führte zur Translokation dieser Konstrukte aus anderen Zellkompartimenten.

Nach der Transfektion der Zellen mit diesen Konstrukten wurde die mitochondriale Fraktion isoliert, die höhere Mengen an mSin1 im Mitochondrium zeigte.

Für den gleichen Zweck wurde eine mSin1 und mRictor knockout Zelllinie charakterisiert, die das gleiche Verhalten bezüglich der Phosphorylierung der Stelle S473 von Akt zeigte. In dieser Zelllinie blieb die Phosphorylierung von Akt an der Stelle T308 konstant. Die Isolierung der mitochondrialen Fraktion zeigte konstante Mengen an mTOR in den Kontroll-, mRictor und mSin1 knockout Zellen, was die frühere Beobachtung in der mSin1 knockdown Zelllinie bestätigt. Reduzierte mSin1 Menge in mRictor knockout Zellen im Vergleich zu den Kontrollzelle könnte die Existenz einer Abhängigkeit von diesen zwei mTORC2 Komponenten voneinander andeuten.

Materials

Antibodies

Antibody	Manufacturer	Buffer	Dilution
Anti-rabbit IgG, HRP-linked Antibody	Cell Signaling Technology	5% BSA solution	1:5000
mTOR Rabbit	Cell Signaling Technology	5% BSA solution + 0.05% NaN ₃	1:1000
mSin1 Rabbit	Cell Signaling Technology	5% BSA solution + 0.05% NaN ₃	1:1000
GAPDH Rabbit	Cell Signaling Technology	5% BSA solution + 0.05% NaN ₃	1:1000
GSK3βpS9 Rabbit	Cell Signaling Technology	5% BSA solution + 0.05% NaN ₃	1:1000
Phospho-Akt (S473) Rabbit	Cell Signaling Technology	5% BSA solution + 0.05% NaN ₃	1:1000
Phospho-Akt (T308) Rabbit	Cell Signaling Technology	5% BSA solution + 0.05% NaN ₃	1:1000

Bacteria

Bacteria	Genotype	Reference
<i>Escherichia coli</i> (<i>E.coli</i>)	DH5α	Köster et al., 2012

Cell lines

Cell line	Organism	Tissue	Cell type	Medium	Reference
HeLa	Human	Cervix	Epithelial	DMEM	Gey GO, et al. Tissue culture studies of the proliferative capacity of cervical carcinoma and normal epithelium. Cancer Res. 12: 264-265, 1952. Millius, A., & Weiner, O. D. (2009). Chemotaxis in neutrophil-like HL-60 cells. <i>Methods in molecular biology</i> (Clifton, N.J.), 571, 167–177. https://doi.org/10.1007/978-1-60761-198-1_11
HL-60	Human	Periph. blood	Promyelo blast	RPMI/HEP ES	

Chemicals

Chemical	Manufacturer
Ammonium persulfate (APS)	VWR Life Science
Bovine serum albumin (BSA)	VWR Life Science
Bromophenol blue	
Dimethyl sulfoxide (DMSO)	Sigma Aldrich
Ethanol	
Ethylendiamintetraacetat (EDTA)	
Glycine	VWR Chemicals
Glycerol	
Hydrochloric acid (HCl)	Sigma-Aldrich
Immersol 518 F/ 37°C	Zeiss
Isopropanol	Merck
Mowiol 4-88	Sigma-Aldrich
PageRuler™ Plus Prestained Protein Ladder (250-10 kDa)	Thermo Scientific
Polyethylenimine (PEI)	
Polyoxyethylene (20) sorbitan monolaurate (Tween 20)	Sigma-Aldrich
Rotiphorese Gel 30 (acrylamide mix)	Roth
Sodium azide (NaN ₃)	
Sodium chloride (NaCl)	Sigma-Aldrich
Sodium dodecyl sulfate (SDS)	Sigma-Aldrich
Tetramethylethylenediamine (TEMED)	Sigma-Aldrich
Tris(hydroxymethyl)aminomethane (Tris)	Duchefa Biochemie
β-Mercaptoethanol	Merck

Constructs

Plasmid	Resistance	Description	Reference
mSin1.2-mCherry_N1	Kanamycin	Isoform 2 of mSin1 with C-terminally fused mCherry tag	This plasmid was provided by Dr. Ivan Yudushkin, MFPL, Vienna
mSin1.4-eGFP_N1	Kanamycin	Isoform 4 of mSin1 with C-terminally fused eGFP tag	This plasmid was provided by Dr. Ivan Yudushkin, MFPL, Vienna
mSin1.5-mCherry_N1	Kanamycin	Isoform 5 of mSin1 with C-terminally fused mCherry tag	This plasmid was provided by Dr. Ivan Yudushkin, MFPL, Vienna
mSin1.2-mCherry-BclxL_N1	Kanamycin	Isoform 2 of mSin1 with C-terminally fused mCherry tag and BclxL	This plasmid was created during the practical

mSin1.4-eGFP-BclxL_N1	Kanamycin	Isoform 4 of mSin1 with C-terminally fused eGFP tag and BclxL	This plasmid was created during the practical
mSin1.5-mCherry-BclxL_N1	Kanamycin	Isoform 5 of mSin1 with C-terminally fused mCherry tag and BclxL	This plasmid was created during the practical
mSin1.5-eGFP-BclxL_N1	Kanamycin	Isoform 5 of mSin1 with C-terminally fused eGFP tag and BclxL	This plasmid was created during the practical

Consumables

Product	Manufacturer
Conical tube (15 mL, 50 mL)	Falcon
Cover glass (diameter 13 mm)	VWR Life Science
Cryogenic tubs	Thermo Scientific
Gel blotting paper (Grade GB003)	Cytiva (Formerly GE Healthcare Life Sciences)
Glass bottom microwell dishes (35 mm petri dish, 14 mm Microwell, No. 1.5 coverslipglass)	Mat Tek Corporation
Gloves	Sempercure
Parafilm	Bemis
PCR tube	VWR Life Science
Pipette tips (1000 µL, 200 µL, 20 µL)	VWR Life Science
Round bottom tube (14 mL)	Falcon
Safeseal-Tips professional (20 µL, 1000 µL)	Biozym
Serological pipets (5 mL, 10 mL, 25 mL)	VWR Life Science
Tissue culture dish	Falcon
Amersham protran 0.2 NC nitrocellulose western blotting membranes	Cytiva (Formerly GE Healthcare Life Sciences)
Microcentrifuge tube (1.5 mL, 2 mL)	VWR Life Science

Enzymes

Standard enzymes

Enzyme	Buffer	Manufacturer
Phusion DNA polymerase	5x Phusion HF reaction buffer	Thermo Scientific
T4 DNA ligase	10x T4 DNA ligase buffer	Thermo Scientific
T4 polynucleotide kinase		New England BioLabs

Restriction enzymes

Restriction enzyme	Restriction site: 5' → 3'	Manufacturer
AgeI	A [↓] CCGGT	New England BioLabs
NotI	GC [↓] GGCCGC	New England BioLabs

Inhibitors

<i>Inhibitor</i>	<i>Manufacturer</i>	<i>References</i>
A-443654	Cayman Chemical Company	Mol Cancer Ther 2005 Jun;4(6):977-86. doi: 10.1158/1535-7163.MCT-05-0005
GDC-0941	Cayman Chemical Company	J Med Chem . 2008 Sep 25;51(18):5522-32. doi: 10.1021/jm800295d
Torin1		

Instruments

<i>Instrument</i>	<i>Manufacturer</i>
Centrifuge Mikro 22R accuSpin Mirco 17	Hettich
Centrifuge rotor (Hettich) Mikro 6x120g	Fisher Scientific
Chemiluminescence imagine system (CCD camera)	Hettich
Fusion Fx	Vilber smart imagine
CO ₂ incubator MCO-20AIC	Sanyo
Electrophoresis chamber Mini-PROTEAN Tetra	BIO-RAD
Handcast System	
Freezing container Mr. Frosty Cryo	Nalgene
High precision tweezers S-Inox-H	Swiss Dumont
Ice production machine FIM	EVERmed
Incubator 9010	Binder
Laminar flow sterile cabinet	
ScanLaf - Mars Safety Class 2	Labogene
Microcentrifuge accuSpin Micro 17	Fisherbrand
NanoDrop2000	Thermo Scientific
Orbital shaker	
PMR-30	Grant Instruments
pH meter	
FiveEasy Plus FP20	Mettler Toledo
Pipetboy	Inetgra
Pipette	Eppendorf Gilson
Power supply PowerPac™ Basic Power Supply	BIO-RAD
Precision balances Pioneer PA4101	Ohaus
Shaking incubator 3031	GFL Gesellschaft Fuer Labortec
Sonicator Sonopuls UW 2070	Bandelin
Thermocycler T100	BIO-RAD
Thermomixer compact block heater	Eppendorf
Ultrapure water system Arium pro VF	Sartorius
Vortex mixer Vortex-Genie 2	Scientific Industries
Water bath	
SW23	Julabo
Western blotting system	
Mini Trans-Blot Cell	BIO-RAD

Kits

Kit	Manufacturer
Amersham™ ECL Select™ Western Blotting Detection Reagent	Cytiva (Formerly GE Healthcare Life Sciences)
GeneJET Gel Extraction Kit	Thermo Scientific
GeneJET Plasmid Miniprep Kit	Thermo Scientific

Media and serum

Liquid media

Medium	Manufacturer
Dulbecco's modified eagle's medium - high glucose (DMEM)	Sigma-Aldrich
Lysogeny broth (LB)	Sigma-Aldrich
OptiMEM	
RPMI/Hepes	

Supplementary

Serum	Manufacturer
Fetal bovine serum (FCS)	Sigma-Aldrich
L-glutamine-penicillin-streptomycin solution	Sigma-Aldrich

Solid media

Medium	Ingredients
Lysogeny broth (LB)	Sigma-Aldrich

Antibiotics

Antibiotic	Stock	Dilution
Kanamycin	50 mg/mL	1:1000

Primers

Sequencing primer

Primer	Sequence: 5' -> 3'
CMV-FW	TAA CAA CTC CGC CCC ATT
SV40PolyA-RV	CCT CTA CAA ATG TGG TAT GGC

Solutions and Buffers

Standard solutions

cOmplete, EDTA free protease inhibitor cocktail	Roche
Pierce phosphatase inhibitor mini tablets	Thermo Scientific
PageRuler™ Plus Prestained Protein Ladder (250-10 kDa)	Thermo Scientific
Preparation	
APS solution	10% 1 g APS in 10 mL mH ₂ O
BSA solution	5% 2.5 g BSA in 50 mL 1x TTBS

SDS stacking gel	5% 0.83 mL 30% acrylamide mix 0.63 mL 1.0 M Tris-HCl (pH 6.8) 0.05 mL 10% SDS 0.05 mL 10 % APS 0.005 mL TEMED 3.4 mL mH ₂ O
------------------	--

SDS separating gel	10% 6.7 mL 30% acrylamide mix 5.0 mL 1.5 M Tris-HCl (pH 8.8) 0.2 mL 10% SDS 0.2 mL 10 % APS 0.006 mL TEMED 7.9 mL mH ₂ O
--------------------	---

SDS solution	10%
Trypsin/EDTA	100 g SDS in 1000 mL mH ₂ O

Buffer

Dulbecco's phosphate buffered saline (DPBS)

Sigma-Aldrich

Phusion HF reaction buffer 5x
T4 DNA ligase buffer 10x

New England BioLabs
Thermo Scientific

Preparation

Cell lysis buffer

1.35 mL RIPA buffer
0.15 mL 10x Inhibitor mix
10x
1 tablet cOmplete, EDTA free
Protease Inhibitor Cocktail
1 tablet Pierce Phosphatase Inhibitor
Mini Tablets

Inhibitor mix

110 µL 1x TBS
890 µL mH₂O
200 mg sodium deoxycholate
0.6 mL 5 M NaCl
0.2 mL 1 M Tris pH 7.2
0.2 mL 10% SDS
0.2 mL Triton X100
16.8 mL mH₂O
10x

Radioimmunoprecipitation assay buffer (RIPA buffer)

4 g SDS
4 mL 2 β-mercaptoethanol
4.7 mL Glycerol
10 mg Bromophenol blue
12 mL 1 M Tris-HCl (pH 6.8)

SDS sample buffer

	10x
	30.3 g Tris Base
	144.4 g Glycine
SDS-PAGE running buffer	10 g SDS
	1.0 L mH ₂ O
	1x
SDS-PAGE running buffer	100 mL 10x SDS-PAGE Running Buffer
	900 mL mH ₂ O
	10x
SDS-PAGE transfer buffer	60.4 g Tris-Base (pH 7.6)
	288 g Glycine
	2.0 L mH ₂ O
	1x
SDS-PAGE transfer buffer	100 mL 10x Transfer Buffer
	900 mL mH ₂ O
	1x
TBS	100 mL 10x TBS
	900 mL mH ₂ O
	10x pH 7.6
	48.4 g Tris-Base
TBS (Tris buffered saline)	175.4 g NaCl
	add mH ₂ O to 2 L
	adjust to pH 7.6
	1 M Tris-HCl pH 6.8
Tris-HCl	30 g Tris in 250 mL mH ₂ O
	Adjust to pH 6.8 with HCl
	1.5 M Tris-HCl pH 8.8
Tris-HCl	45 g Tris in 250 mL mH ₂ O
	Adjust to pH 8.8
	1x
TTBS (TBS Tween solution)	2 mL Tween 20
	200 mL 10x TBS
	add mH ₂ O to 2.0 L

Bibliography

1. Sabers, C. J. *et al.* Isolation of a protein target of the FKBP12-rapamycin complex in mammalian cells. *J. Biol. Chem.* **270**, 815–822 (1995).
2. Vézina, C. & Kudelski, A. Rapamycin (AY-22,989), a new antifungal antibiotic. I. taxonomy of the producing streptomycete and isolation of the active principle. *J. Antibiot. (Tokyo)*. **28**, 721–726 (1975).
3. Benjamin, D., Colombi, M., Moroni, C. & Hall, M. N. Rapamycin passes the torch: A new generation of mTOR inhibitors. *Nat. Rev. Drug Discov.* **10**, 868–880 (2011).
4. Heitman, J., Movva, N. R. & Hall, M. N. Targets for cell cycle arrest by the immunosuppressant rapamycin in yeast. *Science (80-.)*. **253**, 905–909 (1991).
5. Menon, S. & Manning, B. D. Common corruption of the mTOR signaling network in human tumors. *Oncogene* **27**, S43–S51 (2008).
6. Dazert, E. & Hall, M. N. MTOR signaling in disease. *Curr. Opin. Cell Biol.* **23**, 744–755 (2011).
7. Laplante, M. & Sabatini, D. M. MTOR signaling in growth control and disease. *Cell* **149**, 274–293 (2012).
8. Hay, N. & Sonenberg, N. Upstream and downstream of mTOR. *Genes Dev.* **18**, 1926–1945 (2004).
9. Mèndez, R., Myers, M. G., White, M. F. & Rhoads, R. E. Stimulation of protein synthesis, eukaryotic translation initiation factor 4E phosphorylation, and PHAS-I phosphorylation by insulin requires insulin receptor substrate 1 and phosphatidylinositol 3-kinase. *Mol. Cell. Biol.* **16**, 2857–2864 (1996).
10. Carnero, A. & Paramio, J. M. The PTEN/PI3K/AKT Pathway in vivo, cancer mouse models. *Front. Oncol.* **4**, 1–10 (2014).
11. Scheid, M. P. & Woodgett, J. R. PKB/AKT: Functional insights from genetic models. *Nat. Rev. Mol. Cell Biol.* **2**, 760–768 (2001).
12. Sarbassov, D. D., Guertin, D. A., Ali, S. M. & Sabatini, D. M. Phosphorylation and regulation of Akt/PKB by the rictor-mTOR complex. *Science (80-.)*. **307**, 1098–1101 (2005).
13. Finlay, D. & Cantrell, D. A. Metabolism, migration and memory in cytotoxic T cells. *Nat. Rev. Immunol.* **11**, 109–117 (2011).
14. Lipton, J. O. & Sahin, M. The Neurology of mTOR. *Neuron* **84**, 275–291 (2014).
15. Brook, M. S. *et al.* Skeletal muscle homeostasis and plasticity in youth and ageing: Impact of nutrition and exercise. *Acta Physiol.* **216**, 15–41 (2016).
16. Brioché, T., Pagano, A. F., Py, G. & Chopard, A. Muscle wasting and aging: Experimental models, fatty infiltrations, and prevention. *Mol. Aspects Med.* **50**, 56–87 (2016).
17. Salto, R. *et al.* β -Hydroxy- β -methylbutyrate (HMB) promotes neurite outgrowth in Neuro2a cells. *PLoS One* **10**, 1–14 (2015).
18. Powers, R. W., Kaeberlein, M., Caldwell, S. D., Kennedy, B. K. & Fields, S. Extension of chronological life span in yeast by decreased TOR pathway signaling. *Genes Dev.* **20**, 174–184 (2006).
19. Miller, R. A. *et al.* Rapamycin-mediated lifespan increase in mice is dose and sex dependent and metabolically distinct from dietary restriction. *Aging Cell* **13**, 468–477 (2014).
20. Fok, W. C. *et al.* Mice fed rapamycin have an increase in lifespan associated

- with major changes in the liver transcriptome. *PLoS One* **9**, (2014).
21. Oldham, S. Obesity and nutrient sensing TOR pathway in flies and vertebrates: Functional conservation of genetic mechanisms. *Trends Endocrinol. Metab.* **22**, 45–52 (2011).
 22. Xu, K., Liu, P. & Wei, W. mTOR signaling in tumorigenesis. *Biochim. Biophys. Acta - Rev. Cancer* **1846**, 638–654 (2014).
 23. Guertin, D. A. & Sabatini, D. M. An expanding role for mTOR in cancer. *Trends Mol. Med.* **11**, 353–361 (2005).
 24. Pópulo, H., Lopes, J. M. & Soares, P. The mTOR signalling pathway in human cancer. *Int. J. Mol. Sci.* **13**, 1886–1918 (2012).
 25. Ehninger, D. *et al.* Reversal of learning deficits in a Tsc2^{+/-} mouse model of tuberous sclerosis. *Nat. Med.* **14**, 843–848 (2008).
 26. Ghosh, H. S., McBurney, M. & Robbins, P. D. SIRT1 negatively regulates the mammalian target of rapamycin. *PLoS One* **5**, 1–8 (2010).
 27. Julien, C. *et al.* Sirtuin 1 reduction parallels the accumulation of tau in alzheimer disease. *J. Neuropathol. Exp. Neurol.* **68**, 48–58 (2009).
 28. Querfurth, H. W. & Laferla, F. M. Alzheimer's Disease. **9**, (2010).
 29. Yang, H. *et al.* Mechanisms of mTORC1 activation by RHEB and inhibition by PRAS40. *Nature* **552**, 368–373 (2017).
 30. Peterson, T. R. *et al.* DEPTOR Is an mTOR Inhibitor Frequently Overexpressed in Multiple Myeloma Cells and Required for Their Survival. *Cell* **137**, 873–886 (2009).
 31. Averous, J. & Proud, C. G. When translation meets transformation: The mTOR story. *Oncogene* **25**, 6423–6435 (2006).
 32. Ma, X. M. & Blenis, J. Molecular mechanisms of mTOR-mediated translational control. *Nat. Rev. Mol. Cell Biol.* **10**, 307–318 (2009).
 33. Robitaille, A. M. *et al.* Quantitative phosphoproteomics reveal mTORC1 activates de novo pyrimidine synthesis. *Science (80-.).* **339**, 1320–1323 (2013).
 34. Laplante, M. & Sabatini, D. M. An Emerging Role of mTOR in Lipid Biosynthesis. *Curr. Biol.* **19**, R1046–R1052 (2009).
 35. Peterson, T. R. *et al.* mTOR complex 1 regulates lipin 1 localization to control the srebp pathway. *Cell* **146**, 408–420 (2011).
 36. Ganley, I. G. *et al.* ULK1·ATG13·FIP200 complex mediates mTOR signaling and is essential for autophagy. *J. Biol. Chem.* **284**, 12297–12305 (2009).
 37. Saito, K., Araki, Y., Kontani, K., Nishina, H. & Katada, T. Novel role of the small GTPase Rheb: Its implication in endocytic pathway independent of the activation of mammalian target of rapamycin. *J. Biochem.* **137**, 423–430 (2005).
 38. Sancak, Y. *et al.* The rag GTPases bind raptor and mediate amino acid signaling to mTORC1. *Science (80-.).* **320**, 1496–1501 (2008).
 39. Betz, C. & Hall, M. N. Where is mTOR and what is it doing there? *J. Cell Biol.* **203**, 563–574 (2013).
 40. Kim, E., Goraksha-Hicks, P., Li, L., Neufeld, T. P. & Guan, K. L. Regulation of TORC1 by Rag GTPases in nutrient response. *Nat. Cell Biol.* **10**, 935–945 (2008).
 41. Sancak, Y. *et al.* Ragulator-rag complex targets mTORC1 to the lysosomal surface and is necessary for its activation by amino acids. *Cell* **141**, 290–303 (2010).
 42. Jewell, J. L., Russell, R. C. & Guan, K. L. Amino acid signalling upstream of

- mTOR. *Nat. Rev. Mol. Cell Biol.* **14**, 133–139 (2013).
43. Ögmundsdóttir, M. H. *et al.* Proton-assisted Amino acid transporter PAT1 complexes with Rag GTPases and activates TORC1 on late endosomal and lysosomal membranes. *PLoS One* **7**, (2012).
 44. Inoki, K., Li, Y., Xu, T. & Guan, K. L. Rheb GTPase is a direct target of TSC2 GAP activity and regulates mTOR signaling. *Genes Dev.* **17**, 1829–1834 (2003).
 45. Smith, E. M., Finn, S. G., Tee, A. R., Brownei, G. J. & Proud, C. G. The tuberous sclerosis protein TSC2 is not required for the regulation of the mammalian target of rapamycin by amino acids and certain cellular stresses. *J. Biol. Chem.* **280**, 18717–18727 (2005).
 46. Martina, J. A., Chen, Y., Gucek, M. & Puertollano, R. MTORC1 functions as a transcriptional regulator of autophagy by preventing nuclear transport of TFEB. *Autophagy* **8**, 903–914 (2012).
 47. Martina, J. A. & Puertollano, R. Rag GTPases mediate amino acid-dependent recruitment of TFEB and MITF to lysosomes. *J. Cell Biol.* **200**, 475–491 (2013).
 48. Zhang, J. *et al.* A tuberous sclerosis complex signalling node at the peroxisome regulates mTORC1 and autophagy in response to ROS. *Nat. Cell Biol.* **15**, 1186–1196 (2013).
 49. Yadav, R. B. *et al.* mTOR direct interactions with Rheb-GTPase and raptor: Sub-cellular localization using fluorescence lifetime imaging. *BMC Cell Biol.* **14**, 1 (2013).
 50. Vazquez-Martin, A., Cufí, S., Oliveras-Ferraros, C. & Menendez, J. A. Raptor, a positive regulatory subunit of mTOR complex 1, is a novel phosphoprotein of the rDNA transcription machinery in nucleoli and chromosomal nucleolus organizer regions (NORs). *Cell Cycle* **10**, 3140–3152 (2011).
 51. Giguère, V. Canonical signaling and nuclear activity of mTOR—a teamwork effort to regulate metabolism and cell growth. *FEBS J.* **285**, 1572–1588 (2018).
 52. Rosner, M. & Hengstschläger, M. Cytoplasmic and nuclear distribution of the protein complexes mTORC1 and mTORC2: Rapamycin triggers dephosphorylation and delocalization of the mTORC2 components rictor and sin1. *Hum. Mol. Genet.* **17**, 2934–2948 (2008).
 53. Schieke, S. M. *et al.* The mammalian target of rapamycin (mTOR) pathway regulates mitochondrial oxygen consumption and oxidative capacity. *J. Biol. Chem.* **281**, 27643–27652 (2006).
 54. Ramanathan, A. & Schreiber, S. L. Direct control of mitochondrial function by mTOR. *Proc. Natl. Acad. Sci. U. S. A.* **106**, 22229–22232 (2009).
 55. Sarbassov, D. D. *et al.* Prolonged Rapamycin Treatment Inhibits mTORC2 Assembly and Akt/PKB. *Mol. Cell* **22**, 159–168 (2006).
 56. Bridges, D. *et al.* Phosphatidylinositol 3,5-bisphosphate plays a role in the activation and subcellular localization of mechanistic target of rapamycin 1. *Mol. Biol. Cell* **23**, 2955–2962 (2012).
 57. Saitoh, M. *et al.* Regulation of an activated S6 kinase 1 variant reveals a novel mammalian target of rapamycin phosphorylation site. *J. Biol. Chem.* **277**, 20104–20112 (2002).
 58. Peterson, R. T. & Schreiber, S. L. Translation control: Connecting mitogens and the ribosome. *Curr. Biol.* **8**, 248–250 (1998).
 59. Chiang, G. G. & Abraham, R. T. Phosphorylation of mammalian target of rapamycin (mTOR) at Ser-2448 is mediated by p70S6 kinase. *J. Biol. Chem.*

- 280**, 25485–25490 (2005).
60. Raught, B. & Gingras, A. C. eIF4E activity is regulated at multiple levels. *Int. J. Biochem. Cell Biol.* **31**, 43–57 (1999).
 61. Scaiola, A. *et al.* The 3.2-Å resolution structure of human mTORC2. *Sci. Adv.* **6**, (2020).
 62. Pearce, L. R. *et al.* Identification of Protor as a novel Rictor-binding component of mTOR complex-2. *Biochem. J.* **405**, 513–522 (2007).
 63. Boulbès, D. R., Shaiken, T. & Sarbassov, D. D. Endoplasmic reticulum is a main localization site of mTORC2. *Biochem. Biophys. Res. Commun.* **413**, 46–52 (2011).
 64. Hill, M. M., Feng, J. & Hemmings, B. A. Identification of a plasma membrane raft-associated PKB Ser473 kinase activity that is distinct from ILK and PDK1. *Curr. Biol.* **12**, 1251–1255 (2002).
 65. Partovian, C., Ju, R., Zhuang, Z. W., Martin, K. A. & Simons, M. Syndecan-4 Regulates Subcellular Localization of mTOR Complex2 and Akt Activation in a PKC α -Dependent Manner in Endothelial Cells. *Mol. Cell* **32**, 140–149 (2008).
 66. Gao, X. *et al.* PI3K/Akt signaling requires spatial compartmentalization in plasma membrane microdomains. *Proc. Natl. Acad. Sci. U. S. A.* **108**, 14509–14514 (2011).
 67. Poston, C. N., Duong, E., Cao, Y. & Bazemore-Walker, C. R. Proteomic analysis of lipid raft-enriched membranes isolated from internal organelles. *Biochem. Biophys. Res. Commun.* **415**, 355–360 (2011).
 68. Zhang, F. *et al.* mTOR complex component rictor interacts with PKC ζ and regulates cancer cell metastasis. *Cancer Res.* **70**, 9360–9370 (2010).
 69. Desai, B. N., Myers, B. R. & Schreiber, S. L. FKBP12-rapamycin-associated protein associates with mitochondria and senses osmotic stress via mitochondrial dysfunction. *Proc. Natl. Acad. Sci. U. S. A.* **99**, 4319–4324 (2002).
 70. Sarbassov, D. D. *et al.* Rictor, a Novel Binding Partner of mTOR, Defines a Rapamycin-Insensitive and Raptor-Independent Pathway that Regulates the Cytoskeleton. *Curr. Biol.* **14**, 1296–1302 (2004).
 71. Bijur, G. N. & Jope, R. S. Rapid accumulation of Akt in mitochondria following phosphatidylinositol 3-kinase activation. *J. Neurochem.* **87**, 1427–1435 (2003).
 72. Miyamoto, S., Murphy, A. N. & Brown, J. H. Akt mediates mitochondrial protection in cardiomyocytes through phosphorylation of mitochondrial hexokinase-II. *Cell Death Differ.* **15**, 521–529 (2008).
 73. Arciuch, V. G. A. *et al.* Akt1 intramitochondrial cycling is a crucial step in the redox modulation of cell cycle progression. *PLoS One* **4**, (2009).
 74. Su, C. C., Yang, J. Y., Leu, H. B., Chen, Y. & Wang, P. H. Mitochondrial Akt-regulated mitochondrial apoptosis signaling in cardiac muscle cells. *Am. J. Physiol. - Hear. Circ. Physiol.* **302**, 716–723 (2012).
 75. Engelsberg, A., Kobelt, F. & Kuhl, D. The N-terminus of the serum- and glucocorticoid-inducible kinase Sgk1 specifies mitochondrial localization and rapid turnover. *Biochem. J.* **399**, 69–76 (2006).
 76. Cordas, E., Náray-Fejes-Tóth, A. & Fejes-Tóth, G. Subcellular location of serum- and glucocorticoid-induced kinase-1 in renal and mammary epithelial cells. *Am. J. Physiol. - Cell Physiol.* **292**, 1971–1981 (2007).
 77. Hresko, R. C. & Mueckler, M. mTOR·RICTOR is the Ser473 kinase for Akt/protein kinase B in 3T3-L1 adipocytes. *J. Biol. Chem.* **280**, 40406–40416 (2005).

78. Betz, C. *et al.* MTOR complex 2-Akt signaling at mitochondria-associated endoplasmic reticulum membranes (MAM) regulates mitochondrial physiology. *Proc. Natl. Acad. Sci. U. S. A.* **110**, 12526–12534 (2013).
79. De Brito, O. M. & Scorrano, L. Mitofusin 2 tethers endoplasmic reticulum to mitochondria. *Nature* **456**, 605–610 (2008).
80. Appenzeller-Herzog, C. & Hall, M. N. Bidirectional crosstalk between endoplasmic reticulum stress and mTOR signaling. *Trends Cell Biol.* **22**, 274–282 (2012).
81. Frias, M. A. *et al.* mSin1 Is Necessary for Akt/PKB Phosphorylation, and Its Isoforms Define Three Distinct mTORC2s. *Curr. Biol.* **16**, 1865–1870 (2006).
82. Liu, P. *et al.* Ptdins(3,4,5) P3 -dependent activation of the mTORC2 kinase complex. *Cancer Discov.* **5**, 1194–11209 (2015).
83. Yang, G., Murashige, D. S., Humphrey, S. J. & James, D. E. A Positive Feedback Loop between Akt and mTORC2 via SIN1 Phosphorylation. *Cell Rep.* **12**, 937–943 (2015).
84. Holt, L. J. & Siddle, K. Grb10 and Grb14: Enigmatic regulators of insulin action - And more? *Biochem. J.* **388**, 393–406 (2005).
85. Charalambous, M. *et al.* Disruption of the imprinted Grb10 gene leads to disproportionate overgrowth by an Igf2-independent mechanism. *Proc. Natl. Acad. Sci. U. S. A.* **100**, 8292–8297 (2003).
86. Smith, F. M. *et al.* Mice with a Disruption of the Imprinted Grb10 Gene Exhibit Altered Body Composition, Glucose Homeostasis, and Insulin Signaling during Postnatal Life. *Mol. Cell. Biol.* **27**, 5871–5886 (2007).
87. Hsu, P. P. *et al.* The mTOR-regulated phosphoproteome reveals a mechanism of mTORC1-mediated inhibition of growth factor signaling. *Science* (80-.). **332**, 1317–1322 (2011).
88. Chen, J., Holguin, N., Shi, Y., Silva, M. J. & Long, F. mTORC2 signaling promotes skeletal growth and bone formation in mice. *J. Bone Miner. Res.* **30**, 369–378 (2015).
89. Jacinto, E. *et al.* SIN1/MIP1 Maintains rictor-mTOR Complex Integrity and Regulates Akt Phosphorylation and Substrate Specificity. *Cell* **127**, 125–137 (2006).
90. Yao, C. A. *et al.* Association of mSin1 with mTORC2 Ras and Akt reveals a crucial domain on mSin1 involved in Akt phosphorylation. *Oncotarget* **8**, 63392–63404 (2017).
91. Ebner, M., Sinkovics, B., Szczygieł, M., Ribeiro, D. W. & Yudushkin, I. Localization of mTORC2 activity inside cells. *J. Cell Biol.* **216**, 343–353 (2017).
92. Pan, D. & Matsuura, Y. Structures of the pleckstrin homology domain of *Saccharomyces cerevisiae* Avo1 and its human orthologue Sin1, an essential subunit of TOR complex 2. *Acta Crystallogr. Sect. F Struct. Biol. Cryst. Commun.* **68**, 386–392 (2012).
93. Yuan, Y. *et al.* Characterization of Sin1 isoforms reveals an mTOR-dependent and independent function of sin1 γ . *PLoS One* **10**, 1–16 (2015).
94. Coffey, P. J. & Woodgett, J. R. Erratum: Molecular cloning and characterisation of a novel putative protein-serine kinase related to the cAMP-dependent and protein kinase C families (Eur. J. Biochem., Volume 201, No. 2, Page 478-479). *Eur. J. Biochem.* **205**, 1217 (1992).
95. Vanhaesebroeck, B., Guillermet-Guibert, J., Graupera, M. & Bilanges, B. The emerging mechanisms of isoform-specific PI3K signalling. *Nat. Rev. Mol. Cell Biol.* **11**, 329–341 (2010).

96. Rodriguez-Viciana, P. *et al.* Phosphatidylinositol-3-OH kinase direct target of Ras. *Nature* **370**, 527–532 (1994).
97. Alessi, D. R. *et al.* Characterization of a 3-phosphoinositide-dependent protein kinase which phosphorylates and activates protein kinase B α . *Curr. Biol.* **7**, 261–269 (1997).
98. Alessi, D. R. *et al.* Mechanism of activation of protein kinase B by insulin and IGF-1. *EMBO J.* **15**, 6541–6551 (1996).
99. Facchinetti, V. *et al.* The mammalian target of rapamycin complex 2 controls folding and stability of Akt and protein kinase C. *EMBO J.* **27**, 1932–1943 (2008).
100. Ikenoue, T., Inoki, K., Yang, Q., Zhou, X. & Guan, K. L. Essential function of TORC2 in PKC and Akt turn motif phosphorylation, maturation and signalling. *EMBO J.* **27**, 1919–1931 (2008).
101. Sundaresan, N. R. *et al.* The deacetylase SIRT1 promotes membrane localization and activation of Akt and PDK1 during tumorigenesis and cardiac hypertrophy. *Sci. Signal.* **4**, (2011).
102. Manning, B. D. & Toker, A. AKT/PKB Signaling: Navigating the Network. *Cell* **169**, 381–405 (2017).
103. Cross, D. A. E., Alessi, D. R., Cohen, P., Andjelkovich, M. & Hemmings, B. A. Inhibition of glycogen synthase kinase-3 by insulin mediated by protein kinase B. *Nature* **378**, 785–789 (1995).
104. Dajani, R. *et al.* Crystal structure of glycogen synthase kinase 3 β : Structural basis for phosphate-primed substrate specificity and autoinhibition. *Cell* **105**, 721–732 (2001).
105. Kaidanovich-Beilin, O. & Woodgett, J. R. GSK-3: Functional Insights from Cell Biology and Animal Models. *Front. Mol. Neurosci.* **4**, 1–26 (2011).
106. Brunet, A. *et al.* Akt promotes cell survival by phosphorylating and inhibiting a forkhead transcription factor. *Cell* **96**, 857–868 (1999).
107. Kops, G. J. P. L. *et al.* Direct control of the forkhead transcription factor AFX by protein kinase B. *Nature* **398**, 630–634 (1999).
108. Zhang, X., Tang, N., Hadden, T. J. & Rishi, A. K. Akt, FoxO and regulation of apoptosis. *Biochim. Biophys. Acta - Mol. Cell Res.* **1813**, 1978–1986 (2011).
109. Van Der Vos, K. E. & Coffey, P. J. The extending network of FOXO transcriptional target genes. *Antioxidants Redox Signal.* **14**, 579–592 (2011).
110. Webb, A. E. & Brunet, A. FOXO transcription factors: Key regulators of cellular quality control. *Trends Biochem. Sci.* **39**, 159–169 (2014).
111. Saxton, R. A. & Sabatini, D. M. mTOR Signaling in Growth, Metabolism, and Disease. *Cell* **168**, 960–976 (2017).
112. Kovacina, K. S. *et al.* Identification of a proline-rich Akt substrate as a 14-3-3 binding partner. *J. Biol. Chem.* **278**, 10189–10194 (2003).
113. Sancak, Y. *et al.* PRAS40 Is an Insulin-Regulated Inhibitor of the mTORC1 Protein Kinase. *Mol. Cell* **25**, 903–915 (2007).
114. Haar, E. Vander, Lee, S. il, Bandhakavi, S., Griffin, T. J. & Kim, D. H. Insulin signalling to mTOR mediated by the Akt/PKB substrate PRAS40. *Nat. Cell Biol.* **9**, 316–323 (2007).
115. Han, E. K. H. *et al.* Akt inhibitor A-443654 induces rapid Akt Ser-473 phosphorylation independent of mTORC1 inhibition. *Oncogene* **26**, 5655–5661 (2007).
116. Mahajan, K. & Mahajan, N. P. PI3K-independent AKT activation in cancers: A treasure trove for novel therapeutics. *J. Cell. Physiol.* **227**, 3178–3184 (2012).

117. Ehrhardt, M., Craveiro, R. B., Holst, M. I., Pietsch, T. & Dilloo, D. The PI3K inhibitor GDC-0941 displays promising in vitro and in vivo efficacy for targeted medulloblastoma therapy. *Oncotarget* **6**, 802–813 (2015).
118. Wallin, J. J. *et al.* GDC-0941, a novel class I selective PI3K inhibitor, enhances the efficacy of docetaxel in human breast cancer models by increasing cell death In Vitro and In Vivo. *Clin. Cancer Res.* **18**, 3901–3911 (2012).
119. Boussif, O. *et al.* A versatile vector for gene and oligonucleotide transfer into cells in culture and in vivo: Polyethylenimine. *Proc. Natl. Acad. Sci. U. S. A.* **92**, 7297–7301 (1995).
120. Sonawane, N. D., Szoka, F. C. & Verkman, A. S. Chloride Accumulation and Swelling in Endosomes Enhances DNA Transfer by Polyamine-DNA Polyplexes. *J. Biol. Chem.* **278**, 44826–44831 (2003).
121. White, J. G. & Amos, W. B. Confocal microscopy comes of age. *Nature* **328**, 183–184 (1987).
122. Gallagher, S. R. *One-dimensional SDS gel electrophoresis of proteins. Current Protocols in Molecular Biology* (2012). doi:10.1002/0471142727.mb1002as97.
123. Ni, D., Xu, P. & Gallagher, S. *Immunoblotting and immunodetection. Current Protocols in Molecular Biology* vol. 2016 (2016).
124. Frezza, C., Cipolat, S. & Scorrano, L. Organelle isolation: Functional mitochondria from mouse liver, muscle and cultured fibroblasts. *Nat. Protoc.* **2**, 287–295 (2007).

Appendix

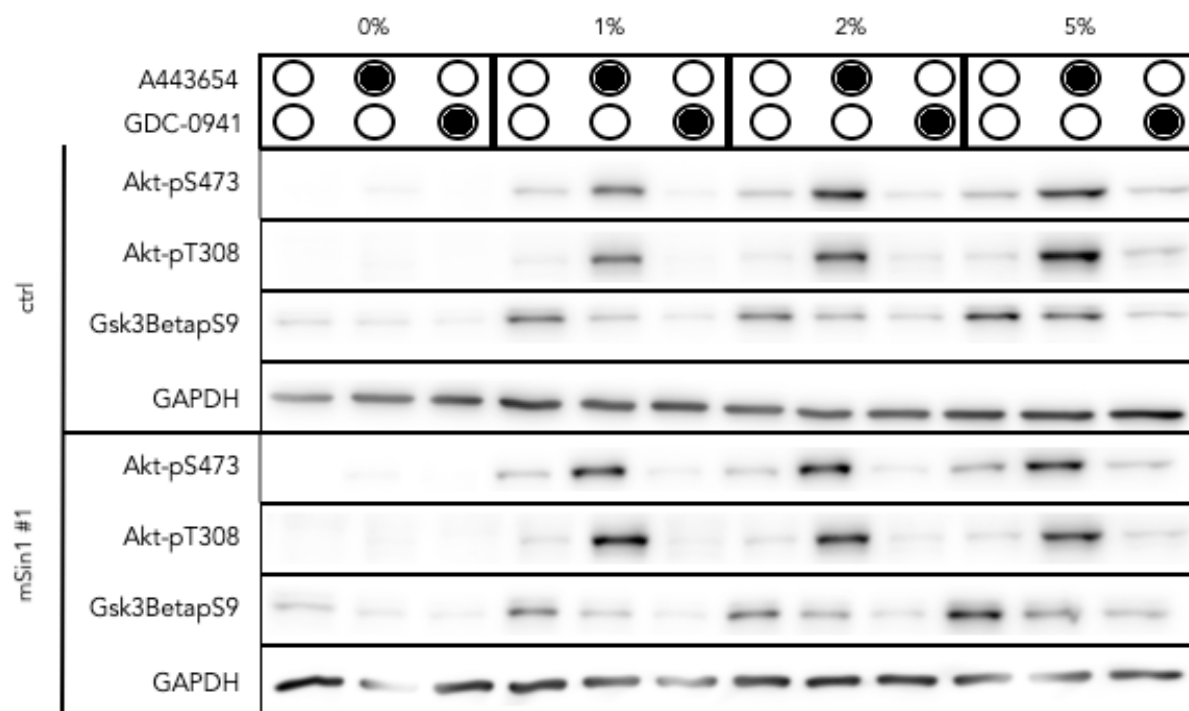


Figure 51: Visualized band of the serum concentration dependency experiment. The cells were incubated overnight with different serum concentrations and then incubated with A443654 or GDC-0941. The cells were lysed with RIPA Buffer containing an inhibitor mix, sonicated and analyzed in a western blot.